Università degli Studi di Cagliari

DOTTORATO DI RICERCA IN NEUROSCIENZE

Ciclo XXVIII

CHARACTERIZATION OF RIMONABANT EFFECTS ON G PROTEIN ACTIVITY

Settore scientifico disciplinare di afferenza
BIO/14-Farmacologia

Presentata da: Dott.ssa Alessandra Porcu

Coordinatore Dottorato: Prof. Walter Fratta

Tutor: Dott.ssa Maria Paola Castelli

Esame finale anno accademico 2014–2015

If you can't explain it simply,

you don't understand it well enough.

Albert Einstein

INDEX

General introduction

G protein-coupled receptors (GPCRs) are the largest class of cell-surface receptors, and today represent 40% of all drug targets on the pharmaceutical market. In the absence of agonists, many GPCRs have been found to exhibit spontaneous activity, which can be blocked by ligands that are referred to as inverse agonists (Milligan, 2003).

The Cannabinoid type 1 (CB1) receptor is one of the most abundant GPCRs in the central nervous system (CNS), and is coupled to $G_{i/o}$ proteins to inhibit adenylyl cyclase, activate mitogen-activated protein kinase (MAPK), inhibit voltage gated Ca^{2+} channels and activate inwardly rectifying K^+ channels (Howlett et al., 2000, Pertwee 1997). The first selective and potent CB1 receptor antagonist Rimonabant (also known SR141716A, SR) at high micromolar concentrations behaves as an inverse agonist, i.e. decreases [^{35}S]GTPγS binding in the rodent and human cerebral cortex and in Chinese hamster ovary (CHO) cells transfected with CB1 receptors (Rinaldi-Carmona et al., 1994). However, *in vitro* and *in vivo* studies performed using the CB1 receptor knockout (KO) and CHO cells not expressing CB1 receptors suggest that the inverse agonist activity of SR is CB1 receptor-independent (Pertwee et al., 2005). Several hypotheses have been postulated to explain the inverse agonism of SR, including its action on different receptors (i.e GPCR mainly coupled to $G_{i/o}$ proteins) and/or its negative modulation of the constitutive activity of CB1 receptors. Alternatively, SR might explain this "inverse agonist effect" in a receptor-independent manner by acting directly on G protein levels.

The present study aimed to determine whether the CB1 receptor-independent effects of SR are mediated via GPCRs, in particular $GABA_B$ and dopamine D2 receptors that share the same $G\alpha_{i/o}$ signaling pathways, or if SR acts directly on G protein subunits.

For this purpose, in this thesis, we investigated the molecular mechanisms of SR on G protein activity in native and recombinant systems by using different experimental approaches (i.e., GTPγS binding, Bioluminescence Resonance Energy Transfer (BRET), electrophysiological recordings). In particular, we first evaluated the effects of SR on basal and agonist-stimulated [^{35}S]GTPγS binding in systems containing CB1, $GABA_B$ and D2 receptor populations (i.e., rat membrane homogenates and CHO stable transfected with $GABA_B$ or D2 receptors), and in systems lacking CB1 and $GABA_B$ receptors (i.e., CB1- and $GABA_B$-KO mice).

Then, using the BRET approach we monitored dissociation between $G\alpha_o$ and Gβγ subunits and their conformational rearrangements before and after $GABA_B$ receptor activation. In addition, we studied the molecular interaction between the D2 receptor and $G\alpha_{i1}$ protein subunits ($G\alpha_{i1\text{-}60}$, $G\alpha_{i1\text{-}91}$ and $G\alpha_{i1\text{-}121}$), and using the same assay we detected the conformational changes between the $G\alpha_{i1}$ and Gβγ subunits. Next, we evaluated the effects of SR on adenylate cyclase activity, using BRET with the CAMYEL sensor, a recent technique developed to detect the level of cAMP in living cells. Specifically, the inhibitory effect of SR on Gi and Gs protein pathways measuring the BRET signal in cells transfected with CAMYEL and $GABA_B$, D2 or D1 receptors was investigated. Finally, whole cell voltage clamp recordings from midbrain dopamine neurons in acute rat brain slices *ex vivo* were performed to evaluate the effects of SR on baclofen and quinpirole-induced outward K^+ current both in wild type (WT) and CB1-KO mice. In addition, in order to demonstrate that SR induced the inhibition of GIRK channel activity by acting directly on G protein, we used a GPCR-free experimental setup (i.e. whole cell patch clamp experiments were performed in CHO cells transfected with GIRK1/2). The main finding of this study is that SR, at micromolar concentrations, prevents GPCR-G protein signaling through a direct interaction with the G proteins mainly with the subunits αi/o.

In the first Chapter, a brief introduction to the GPCRs, G proteins and their downstream signaling components will be firstly presented (paragraph 1). In the second paragraph of the first chapter, the Endocannabinoid System, its components such as endogenous ligands, the cannabinoid receptors and their ligands will be briefly presented. In order to introduce the main object of this thesis and better clarify the rationale of this project, the third paragraph of the same chapter will describe Rimonabant/SR, with a brief excursus of its previously reported effects in *in vitro* and *in vivo*.

In the second Chapter, the materials and methods employed to carry out this project will be described. In the third Chapter, a summary of results obtained through the *in vitro* [^{35}S]GTPγS binding assay, BRET and electrophysiological techniques will be reported. Finally, in the fourth Chapter, a detailed discussion of our results will be offered to connect them to the literature and provide some final remarks on the meanings and implications of this study.

Chapter 1. Introduction

1.1 G protein-coupled receptors

Communication between cells is one of the principal characteristics of the multicellular organism. This process is due to the existence of transmitters released from a cell, and that triggers the response after specific recognition by specialized proteins. Numerous receptors on the cell surface have been identified so far, and it is possible to classify them in three different groups.

The first group, the ionotropic receptor, is formed by ion channels, which control the permeability and the fast response of the cell, through altered ionic fluxes.

The second group, the ligand-gated receptor, is represented by ligand-activated membrane-bound tyrosine kinases that mediate cell proliferation and differentiation.

The third group gathers the G-protein-coupled receptors (GPCRs) that regulate intracellular responses involving Guanine-nucleotide-binding proteins (G-protein) and multiple membrane-bound and intracellular partners. GPCRs represent the largest and most diverse group of plasma membrane receptors essential to normal physiology and are involved in critical functions such as vision, metabolism, olfactory perception, the endocrine system, neuromuscular regulation and central nervous system (CNS) functioning.

There are more than 800 GPCRs identified in the human genome, most of them showing to have a relevant function on various diseases, including metabolic, neurodegenerative and psychiatric disorders and cancer. GPCRs are today the targets of 40% of all drugs on the pharmaceutical market, a percentage that is increasing over time.

1.1.1 Structure and classification

GPCRs consist of a single peptide containing seven hydrophobic trans-membrane (TM) regions (TM-I through VII), known as α-helices, which cross the plasma membrane, and are connected by three hydrophilic intracellular domains (IC1, IC2 and IC3) and three hydrophilic extracellular loops (E1, E2 and E3). Two cysteine residues on E1 and E2 form a disulphide bond, which is probably important for the packing and for the stabilization of a restricted number of conformations of the seven TM regions. The N-terminal is exposed to the extracellular environment while the C-terminal is intracellular (Fig. 1). Generally, the ligand recognition site involves the extracellular domains of the receptor and the pocket formed by the assembly of the seven-TM helices. Indeed, the intracellular interaction involves the C-terminal and intracellular loops with signal partners. The conformation change of the core domain generally includes the IC2 and the IC3, which are directly linked to TM-III and TM-VI (Wess J., 1998). This mechanism constitutes one of the key sites for G-protein recognition and activation. Although the structure remains similar among distinct GPCRs, they differ in the length and function of their N-terminal, C-terminal domains and intracellular loops. Sequence homologies are restricted to the transmembrane domains of closely related subtypes. Moreover, some aspects of molecular interaction are conserved throughout the superfamily, but details may be different, in particular: 1) the extracellular portion of the receptor that interacts with ligands; 2) the intracellular portion that interacts with the cytosolic proteins and 3) the portion involved in the plane of the lipid bilayer. For this reason, mammalian GPCRs are classified in three different families (Fig. 2).

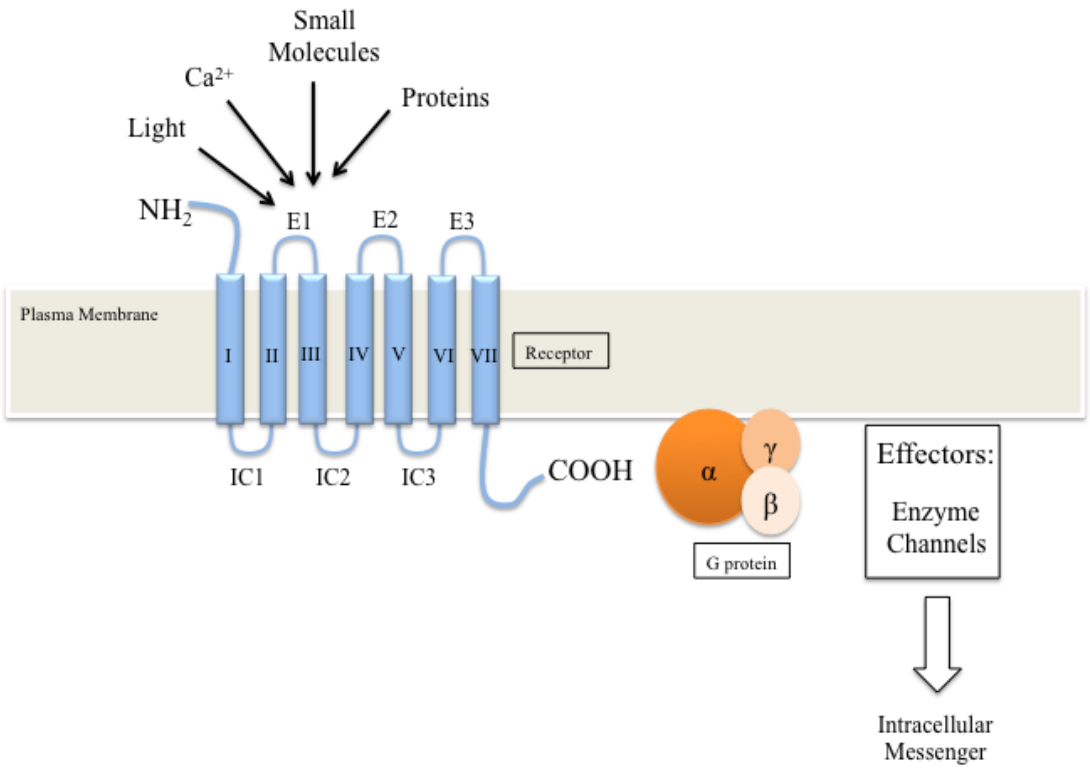

Figure 1. GPCR illustration: The central common core consisting of seven transmembrane (TM) helices (TM-I to TM VII) connected by three intracellular (IC1, IC2 and IC3) and three extracellular (E1, E2 and E3) loops.

Family 1 represents the largest group, known as the Rhodopsin-like receptor family, and includes receptors for hormones, neurotransmitters, and light receptors; all of them transduce extracellular signals through interaction with G-proteins. Some ligands typically bind to the outside surface of the plasma membrane; others can dip into the helical bundle. Three regions of these receptors have been postulated to play a critical role in the conformational change of these receptors: the bottom of the major intrahelical ligand-pocket, the connection between helix 8 and the cytosolic surface of the lipid bilayer, and the cytosolic face, that might interact with the G protein.

Family 2 contains receptors for hormones and peptides, e.g. calcitonin, glucagon, secretin and diuretic hormone. This family has a characteristic long N-terminal tail containing six conserved cysteine residues with three disulphide bonds that contribute to form a hydrophobic binding cleft for the peptide ligands. The change of the amino terminus orientation is critical for biological activation (Grace et al., 2004).

Family 3 is characterized by a very large N-terminal domain, with a Venus flytrap-like structure that plays an important role in ligand binding (White et al., 1998). The Venus flytrap domain is formed by a central β-sheet supported on both sides of the α-helices, connected by a hinge region to a central cleft. This domain is situated above a cysteine-rich domain that contains four intra-domain bonds; one of them directly links to the Venus Flytrap domain. The disulphide bonds seem to be critical for function, and increase the degree of rigidity of the receptor structure. Dimerization is a fundamental phenomenon of these receptors. The homodimeric structures are established by both covalent and no-covalent interactions; one large protein ligand can cross both protomers of the dimeric N-terminal structure. There are 22 GPCR subtypes for this family that are divided into four groups depending on the ligands: 1) metabotropic glutamate receptors, 2) calcium-sensing receptors and GPCRC6A, 3) $GABA_B$ receptors, and 4) orphan receptors (Miller et al., 2010).

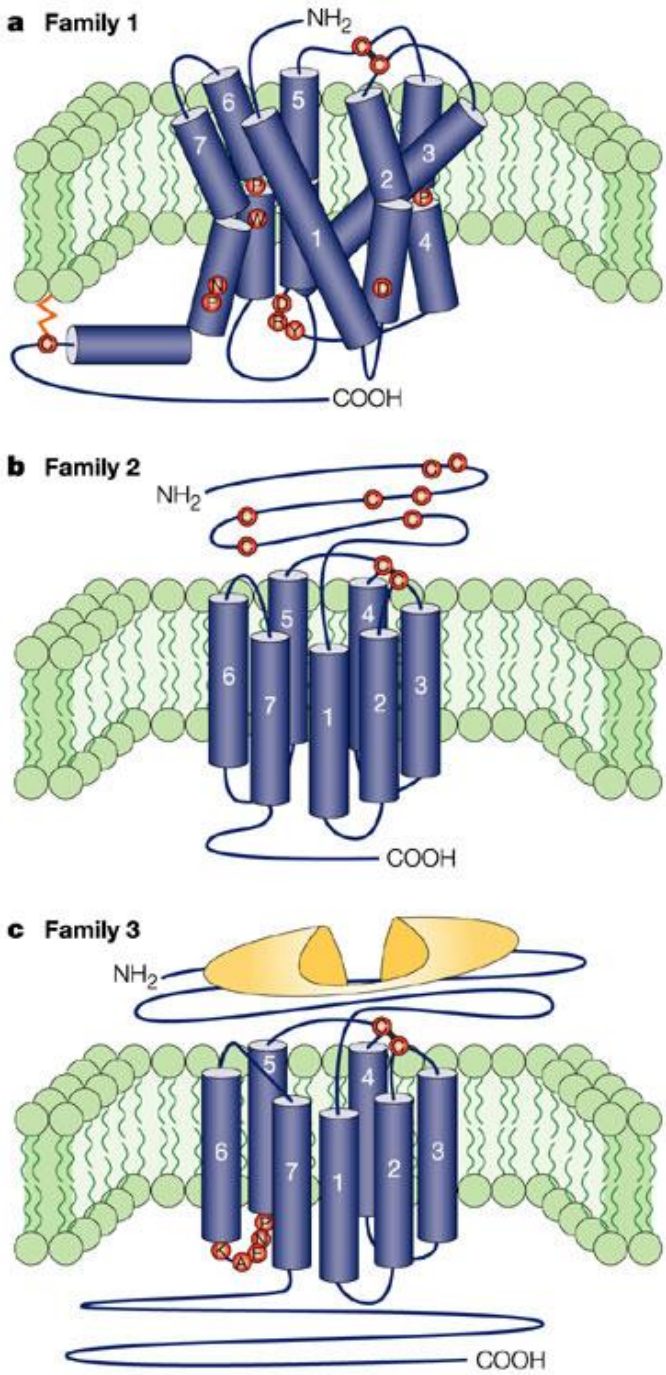

Figure 2. GPCRs classification. Three main families of GPCRs, namely Family 1 (a), Family 2 (b) and Family 3 (c), have been classified by comparing their amino-acid sequences (Clare Ellis, The state of GPCR research, *The Nature Reviews Drug Discovery*, 2004).

In summary, the structure of all these receptors is made up of seven TM helical segments that are arranged in a bundle in the lipid bilayer; and coupling with heterotrimeric G protein can induce biological effects. The interaction with different ligands requires the presence of a "ligand binding pocket" that is represented by the orthosteric natural binding pocket or the allosteric binding pocket. There are different features in these ligand-binding pockets for different GPCRs. Typically about 50-60% of residues are identical between family subtypes binding to the same ligands. Another important feature revealed by analysis of multiple crystal structures is the relative rigidity of the binding pockets (Katritch et al., 2012).

In contrast to the variety observed in the extracellular domains, multiple crystal analyses revealed high structural conservation in the IC parts. These regions are involved both in the binding to G protein and arrestin, and in downstream signal transductions through mechanisms that are supposed to be similar among GPCRs. IC domains undergo large conformational changes after receptor activation (Milligan and Kosteins, 2006). In particular, the IC3 domain displays a high variable length and sequence among GPCR families, and is believed to control receptor selectivity for different G proteins. These domains are therefore considered a potential alternative target for allosteric drugs (Katritch et al., 2012).

Allosteric sites have been identified in many GPCRs, and found to be located in direct proximity to the ligand binding-pocket, in the seven TM helical bundle for Family 2 and 3, or in the IC part of the receptor for Family 1 (May et al., 2007). Further structural analysis is needed to understand the structure and dynamics of the complexity regions implicated in the conformation and activation of receptors leading to specific selectivity for downstream effectors. GPCR function involves specific interactions with numerous binding partners.

1.1.2 G proteins

The complexity and specificity of GPCR signaling is due to the existence of the numerous closely related molecular species of their subunits. G proteins are specialized proteins that bind to the guanosine triphosphate (GTP) and guanosine diphosphate (GDP) nucleotides. Some G proteins, such as the signal proteins RAS, are small with a single subunit, while the G proteins associated with GPCRs are heterotrimeric. They consist of a α subunit and a βγ subunit complex. So far, 23 α subunits derived from 17 different genes have been identified and classified in four families and 6 β and 12 γ subunits have been described.

The α subunit contains the guanine nucleotide binding site with intrinsic GTPase activity, and a helical domain that covers the GTP in on the core of the protein. The helical domain plays a key role in directing receptor binding specificity and effector activation, this domain is also the most divergent among the Gα subunits. Analyses of the crystal structure of G protein reveal the presence of three flexible regions, (switches I, II and III) which change the conformation in GTP-bound activation, becoming more rigid. The N-terminal domain is arranged due to its interaction with the β-propeller domain of β subunits (Wall et al., 1995), playing a relevant role in the activation process through direct specific protein-protein interactions. There are different residues that are critical mediators of receptor-G protein selectivity: α2-helix, α2-β4 loop region, α4-helix and α4-β6 loop domain. This selectivity is mediated by the Gα subunit but seems to be affected also by a network of specific contacts between the G protein and the receptor.

The C-terminal of the Gα subunit was found to have an important role in the receptor-G protein interaction: for example, the adenosine diphosphate ribosylation in the last four residues by pertussis toxin leads to uncouple G_i/G_o proteins from the receptor (Van Dop et al., 1984). In addition, antibodies that can recognise C-terminal domains of the Gα subunit block

receptor-G protein signaling. The C-terminal domain possesses identical, or almost identical, residues between Gα subunits, but still exhibits differential coupling to receptors. Recently, numerous X-ray crystal structures revealed that the C-terminal binds to TM5 and to TM6 or IC3 of a GPCR (Mnpotra et al., 2014).

Gα subunits are classified into: $G\alpha_s$, with four different variants that derive from a single gene via alternative splicing of exon 3 (Milligan 2006); $G\alpha_i$, pertussis toxin-sensitive G proteins known as $G\alpha_{i1}$, $G\alpha_{i2}$ and $G\alpha_{i3}$, produced from different genes; and the $G\alpha_o$ gene that can be differentially spliced to generate $G\alpha_{o1}$ and $G\alpha_{o2}$ (Milligan et al., 2006).

Gβ and Gγ subunits together form a close heterodimer. The Gβ subunit possesses a N-terminal α-helix and a β-propeller fold formed by seven segments with a 40 amino acid sequence (WD-40 repeat).

Gγ is formed by two α-helices linked with a loop and its N-terminal participates in a coiled-coil interaction with the N-terminal α-helix of the Gβ subunit (Kimple et al., 2011).

Many studies showed that lipid modification increases membrane localization of the Gβγ heretodimer that is relevant for receptor coupling. The dimer between the Gα GDP-bound subunit and the Gβγ subunit is formed via two principal interactions: 1) a β3/α-loop and the switch II of the Gα subunit within six out of the seven WD repeats of Gβ, and 2) a contact between the side of the β-propeller of Gβ and the N-terminal helix of the Gα subunit (Kimple, 2011). These interactions play a key role in the competition between the Gβγ-subunit and Gα-GDP and for βγ effectors.

Subunit	Family	Main subtypes	Primary effector
α	α_s	$G\alpha_s$, $G\alpha_{olf}$	Adenylate cyclase ↑
	$\alpha_{i/o}$	$G\alpha_{i-1}$, $G\alpha_{i-2}$, $G\alpha_{i-3}$	Adenylate cyclase ↓
		$G\alpha_{oA}$, $G\alpha_{oB}$	K^+ channels ↑
		$G\alpha_{t1}$, $G\alpha_{t2}$	Ca^{2+} channels ↓
		$G\alpha_z$	Cyclic GMP
	$\alpha_{q/11}$	$G\alpha_q$, $G\alpha_{11}$, $G\alpha_{14}$	Phosphodiesterase ↑
		$G\alpha_{15}$, $G\alpha_{16}$	Phospholipase C ↑
	α_{12}	$G\alpha_{12}$, $G\alpha_{13}$	
β	β_{1-5}	Different assemblies of β- and γ-subunit	Adenylate cyclase ↑/↓
			K^+, Ca^{2+}, Na^+ channels
			Phospholipase ↑
			Protein kinase C ↑
			Protein kinase D ↑
			Phosphatidylinositol 3-kinase ↑
γ	γ_{1-11}		GPCR kinases ↑

Table 1. G protein subunits and their effector systems (Adapted from Hermans, 2003).

Originally, it was thought that only Gα subunits interact with effectors, enzymes or ion channels, but it is clear now that the Gβγ subunit regulates effector affinity as well.

The first identified G protein effector is the adenylate cyclase (AD) enzyme that catalyses the conversion of adenosine triphosphate (ATP) into the intracellular second messenger cyclic-adenosine 3',5'-monophosphate (cAMP). Thus, cAMP regulates the activity of the cAMP-dependent protein kinase (PKA), and cAMP-regulated guanine nucleotide exchange factors (Epac 1 and Epac 2).

This G-protein-mediated regulation of cAMP production represents one of the most relevant signal pathways able to alter cellular functions.

There are 10 different isoforms of the AD, all of them stimulated by $G\alpha_s$, and some are also regulated via the Gβγ subunit or via Ca^{2+}-calmodulin, but always in the presence of the active

$G\alpha_s$ subunit (Luttrell, 2008). The activity of AD is inhibited by the $G\alpha_i$ protein, and modulated through phosphorylation by PKA and protein kinase C (PKC).

Another effector partner of G protein is phospholipase C (PLC) that catalyses hydrolysis of the phosphatidylinositol membrane, producing two intracellular second messengers: inositol 1,4,5-trisphosphate and diacylglycerol. The first regulates the Ca^{2+} efflux from the endoplasmatic reticulum, while the latter controls the activity of some isoforms of PKC.

$G\alpha_{i12}$ and $G\alpha_{i13}$ proteins regulate cytoskeletal conformation and affect cellular growth by activating Rho family small GTPases proteins (Luttrell, 2008). These particular $G\alpha$ subunits also bind to a Regulator of G Protein signaling (RGS), thereby stimulating its guanine nucleotide exchange factor (GEF) activity. The $G\beta\gamma$ subunit is found to regulate the G protein-coupled receptor kinase, GRK2 and GRK3, which play a key role in receptor desensitization.

The $G\alpha_o$ subunit inhibits, with direct interaction, the high voltage N-type Ca^{2+} channel, whereas the $G\alpha_s$ subunit stimulates the L-type Ca^{2+} channel (Luttrell, 2008).

It is now well established that the subunit $G\beta\gamma$ inhibits some voltage-activated Ca^{2+} channels and activates the G-protein-activated rectifying K^+ channels (GIRKs or Kir3). These regulate the postsynaptic inhibitory effect of $G\alpha_{i/o}$-inactivating transmitters in neurons. This family includes four subunits, GIRK1-4: GIRK 2 or GIRK 4 homotetramery, as well as GIRK1/2, GIRK1/3, GRIK 2/3 or GIRK1/4 heterotetramery that are essential to functionality (Dascal, 2011). These subunits combine to form a classic K^+ pore-forming transmembrane domain (M1 and M2) and a large cytoplasmatic domain (N-terminal and C-terminal). The re-entrant helix, named P-loop, forms the selectivity filter (Fig. 3).

The $G\beta\gamma$ subunit binds to two or three separate segments in each GIRK subunit. This binding likely changes the conformation of the M2 segment and the proximal part of the C-terminal

that mediates open-close transition, allowing long-lasting periods of channel activity. This effect also alters the permeation and the gating on the selectivity filter (Dascal, 2001).

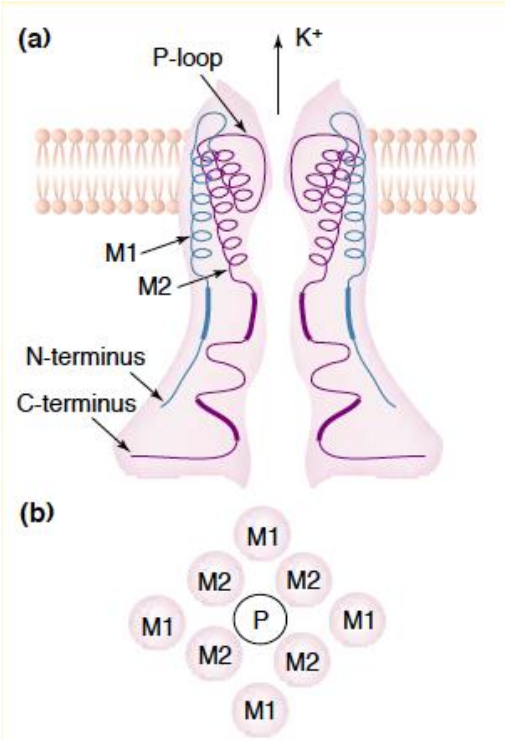

Figure 3. Representation of a GIRK channel. (a) The channel core is a transmembrane and contains two domains (M1 and M2) and a helix-P-loop that forms the selective filter. (b) Channel structure viewed from above, the four subunits surrounding the central pore **(**Dascal, 2001).

In contrast to the simple paradigm that a single receptor interacts with a particular G protein, or with multiple G proteins belonging to the same family, it is now accepted that many GPCRs can simultaneously couple distinct unrelated G proteins, leading to another mechanism for activation of multiple intracellular effectors by a single receptor (Hermans, 2003).

Several studies have shown that G protein subunit expression is controlled dynamically and

that GPCR activity could play a role in this regulation. Receptor-mediated selective regulation of the G protein could contribute to increase specificity of signal transduction between receptors that share a multiplicity of G proteins.

Moreover, there are varieties of intracellular proteins that can control the activity of different partners of the G protein signal cascade. The family of RGS, for example, is able to increase the GTPase activity of Gα subunits, showing specificity for either $G_{q/11}$ or G_s protein types.

1.1.3 Mechanism of signal transduction

The conformational change from the inactive to the active state of a receptor is necessary for G protein activation. The mechanism of GPCR activation involves the disruption of intramolecular relation and the formation of new interactions. Specific movements of TM helices are essential for G protein activation. For example, the introduction of a disulphide cross-linking into TM3 and TM6 blocks G protein activation via cytoplasmatic loops. The magnitude of movement of TM6 is higher than those of TM3 and TM7, resulting in a greater exposition of the inner face of TM2, TM3, TM6 and TM7 (Karnik et al., 2003).

There is some evidence to suggest specificity in receptor-mediated conformational changes with the G proteins. Perhaps, the most apparent connection is the α5-helix that links to the C-terminal of the Gα subunit to the nucleotide binding pocket at the β6/α5 loop; mutations in this region are found to have effects on nucleotide exchange and to modulate receptor coupling (Oldham and Hamm, 2008).

Using different techniques, it was found that a receptor induces perturbation in the α5 helix of G protein and this might be transmitted to the nucleotide-binding pocket via α1-helix and β2 and β3 strands.

The loop that connects the β6 strand and the α5-helix contains the guanine-ring-binding motif:

mutations in this residue enhance spontaneous GDP release (Oldham and Hamm, 2008).

Moreover the α3-β5 loop was reported to be important for interaction between the receptor and the $G\alpha_s$ subunits, while the N-terminal of both $G\alpha_o$ and $G\alpha_i$ subunits might have a role for GDP affinity interacting with β2 and β3 strands. Switches I, II and the phosphate-binding loop have an important interaction with GDP.

G protein is considered in its "off state" when it binds to GDP and when the Gαβγ subunits form a heterotrimer, and in its "on state" when it binds to GTP. Receptor activation induces conformational change in the G protein, leading to GDP releasing from the Gαβγ heterotrimer (Fig. 4).

Two models have been suggested to explain how the receptor induces conformational changes on Gαβγ subunits allowing GDP release. The first model, proposes that by using the N-terminal of the Gα subunit as a lever arm, the receptor pulls the Gβγ dimer away from the Gα subunit. GDP release occurs when Switches I and II are preyed away from the nucleotide binding pocket.

In the second model, it is proposed that the receptor uses the N-terminal of the Gα subunit to force the Gβγ dimer into the Gα subunit, leading the Gγ subunit to bind to the Gα-helical domain. GDP release might occur when this interaction causes a gap between the helical and the GTPase domain of the Gα subunit.

This step is rate-limiting in G protein activation, and consequently it allows the activation of downstream signaling effectors. Since there is direct evidence of specific receptor-mediated conformational changes in G proteins, previous studies have found that interdomain interactions cause nucleotide exchange, although this also depends on Gα subunit involvement. For example, in $G\alpha_s$ and $G\alpha_{i1}$ subunits these interactions can be disrupted leading to an increase in the rate of basal activity or a decreased rate of receptor-catalysed

exchange (Warner et al., 1998). The increased rate on basal exchange might lead to the opening of the interdomain fissure, which reduces GDP affinity. A reduced rate of catalysed exchange may explain how the receptor transmits a conformational change across the domain interface. Crystallography studies have revealed a movement of the GTPase domain and the helical regions relative to each other in order to release GDP (Ceruso et al., 2004).

The displacement of GDP is followed by the binding of GTP that is more abundant in the cells, and causes a strong rearrangement in the Switch regions, leading to dissociation of Gα-GTP and the Gβγ dimer. In this way, both complexes can interact and regulate effector systems. The Gα subunit has an intrinsic GTPase activity, and hydrolyses the terminal phosphate of GTP to restore GDP on the nucleotide-binding pocket. This binding allows the reassociation of the Gαβγ hetorotrimer and to the arrest of the cycle (Milligan and Kosteins, 2006).

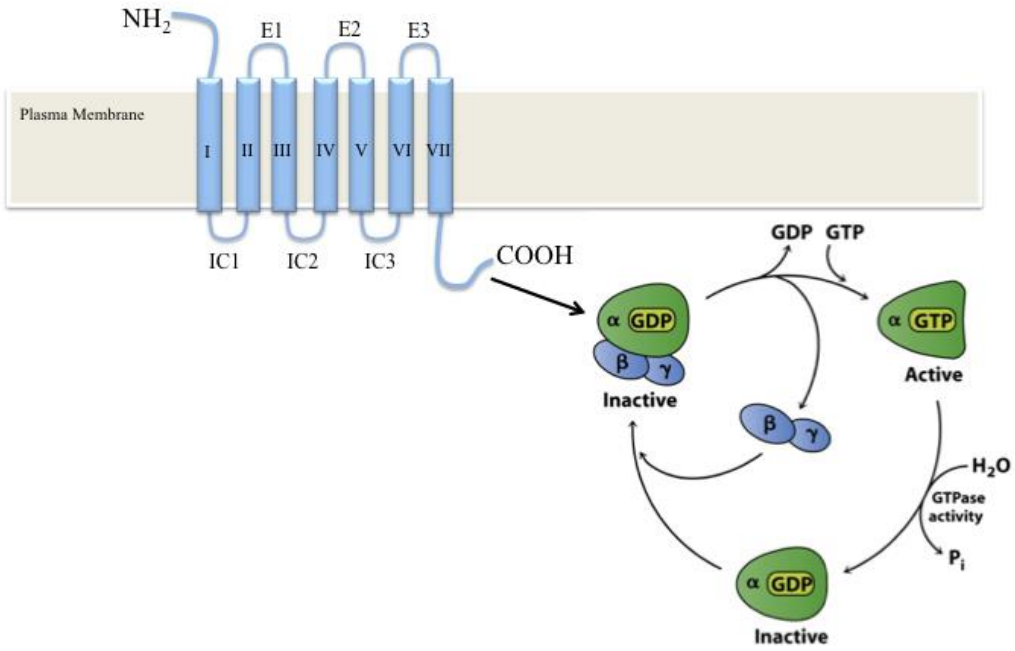

Figure 4. The G protein cycle. Conversion of a G protein heterotrimer from a GDP-bound to a GTP-bound state, promoted by interaction with the receptor.

1.1.4 Properties of GPCR heteromers

Constitutive activity is the ability of a GPCR to adopt an active conformation in the absence of an agonist. In 1982 and 1984 Koski and Cerione provided the first evidence for constitutive activity for the δ opioid receptor and β_2-adrenoceptor. So far, more than 40% of all GPCRs have been found to exhibit constitutive activity (Seifert and Wenzel, 2002).

To better understand this concept, the two-state model was proposed, assuming that GPCR exists in equilibrium between an inactive (**R**) state and an active (**R***) state. In the **R** state, the receptor is uncoupled from G protein, whereas in the **R*** state, it can couple and activate G protein. As previously described, modifications of TM3 and TM6 lead to a conformational switch from **R** to **R***. This particular mechanism is highly conserved among GPCRs (Bockaert and Pin, 1999). Importantly, the transition from **R** to **R*** can occur spontaneously, and independently from an agonist.

This constitutive activity increases G protein basal activity and the activation of effector systems, in comparison with the absence of GPCR. Full agonists maximally stabilize the **R*** state and shift the equilibrium towards **R***. Accordingly, agonists efficiently increase the basal GDP/GTP exchange rate of G proteins and increase effector system activity. Partial agonists are less efficient than full agonists at stabilising the **R*** state leading to a less efficient GDP/GTP exchange compared with full agonists.

In contrast to full agonists, full inverse agonists maximally stabilize the **R** state and reduce basal GDP/GTP exchange, thereby blocking the effects of agonists. For this reason, several inverse agonists were originally classified as antagonists.

On the contrary, a neutral antagonist, does not alter the equilibrium between **R** and **R*** and does not change basal G protein activity, yet blocks both the inhibitory effects of inverse agonists and the stimulatory effects of agonists (Wenzel and Seifert, 2002).

Moreover, the equilibrium position between **R** and **R*** is different for several receptors which might explain the various levels of basal activity for different GPCRs.

The classical view of receptor activation was overtaken by the discovery of the ternary complex model. This model proposes that the receptor interacts with its cognate G protein independently from the presence of the ligand, and that an active receptor complex can be formed only when all three components are associated, forming the ternary complex **AR*G**. However, this model limited the existence of the receptor in its inactive state (agonist free) and active state (agonist bound). The extended ternary complex model provided a mechanism that considers the spontaneous formation of an active-state receptor independently from the presence of the agonist, and the possibility that the receptor binds to the G protein in its active state (**R*G**) or inactive state (**RG**), leading to alterations in the affinity between receptor and G protein (Fig. 5).

A Ternary complex model

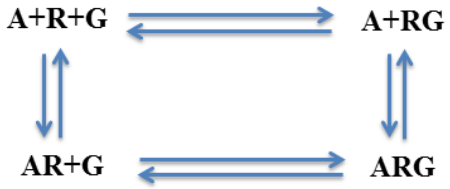

B Extended ternary complex model

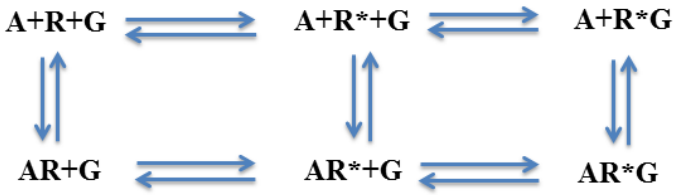

Figure 5. Evolution of the ternary complex. (A) Receptor ligand interaction model with the G protein bound to the activated receptor. (B) Evolved model to explain ligand independent G protein activation. **A**: agonist, **R**: inactivated receptor, **R***: activated receptor, **G**: G protein (Greasley and Clapham, 2006).

Several studies suggest that the interaction between the receptor and the G protein occurs before the activation process. An alternative hypothesis proposes that G protein might pre-assemble with the inactive receptor. Previously, studies have found that the β_2-receptor can be associated with $G\alpha_s$ subunits or $G\beta\gamma$ independently from its activation suggesting the existence of a preassembled signaling complex (Duc et al., 2015).

Bouaboula et al. (1997) have demonstrated that a cannabinoid receptor inverse agonist could block the constitutive activity of the receptor by sequestering the Gα subunit in its GDP-bound form, blocking Cannabinoid receptor type 1 (CB1) signaling a downstream cascade.

The ability of ligands to decrease or increase the separation of G protein subunits, which induce an inhibition or activation of cellular effectors, is one representation of ligand efficacy (Kenakin, 2002).

In this context, it is important to evaluate whether there are therapeutic differences in the clinical use of drugs having negative efficacy versus neutral blockers. Indeed, the basal activity of GPCRs plays a role in the physiological system and molecules that have negative efficacy might be used for many conditions.

Classically, the drug discovery process selects and optimizes compounds that interact selectively with a specific receptor, but previous studies have shown that critical conditions, such as cancer or pain, are to ascribe to the concomitant activation of many different GPCRs. For this reason, understanding the mechanism underlying the negative efficacy of drugs on basal activity, may lead to novel therapeutic strategies, since the simultaneous blockade of the

various GPCRs involved could be relevant in these pathologies.

During the process of activation and deactivation, G protein subunits interact with different reaction partners: the binding sites of these interactions could be considered as relevant targets for synthetic ligands.

Over the last two decades, new theories have been developed to explain how a ligand can induce or stabilize different receptor conformations, resulting in activation of distinct effectors (Fig. 6). Heteromerization, i.e. association of different GPCR types, today represents a potential new mechanism that can explain the different regulation of GPCR signaling and their specificity (Rozenfeld and Devi, 2011).

Many studies have reported that the heteromerization of receptors alters G protein activity and interaction. For example, association between the μ opioid receptor (MOR) and the δ opioid receptor (DOR) decreases MOR activity in response to an agonist (Gomes et al., 2000), while association with the CB1 receptor does not affect its activity (Rios et al., 2006). Other evidence indicates that heteromerization can cause a switch in G protein coupling. Despite MOR and DOR coupling to the $G\alpha_i$ subunit when they are expressed individually, their heteromerization changes the coupling from $G\alpha_i$ to $G\alpha_z$ (Hasbi et al., 2007). Previously, studies on D1 and D2 receptors have shown that heteromerization between these two receptors leads to a switch from $G_{\alpha s/olf}$ (for D1) and $G\alpha_i$ (for D2) to a $G\alpha_{q/11}$ (So et al., 2007).

Together, these findings suggest the possibility that heteromerization might influence diversification of receptor properties, which could contribute to the regulation of receptor function *in vivo* (Rozenfeld and Devi, 2011).

Lastly, mutations that cause constitutive activation of G protein α subunits have been found in different human diseases. Most of these mutations alter the G protein coupling efficiency or induce agonist-independent signaling activity. The possible influence of these mutations on

the interaction with different G proteins remains to be explored (Hermans, 2003).

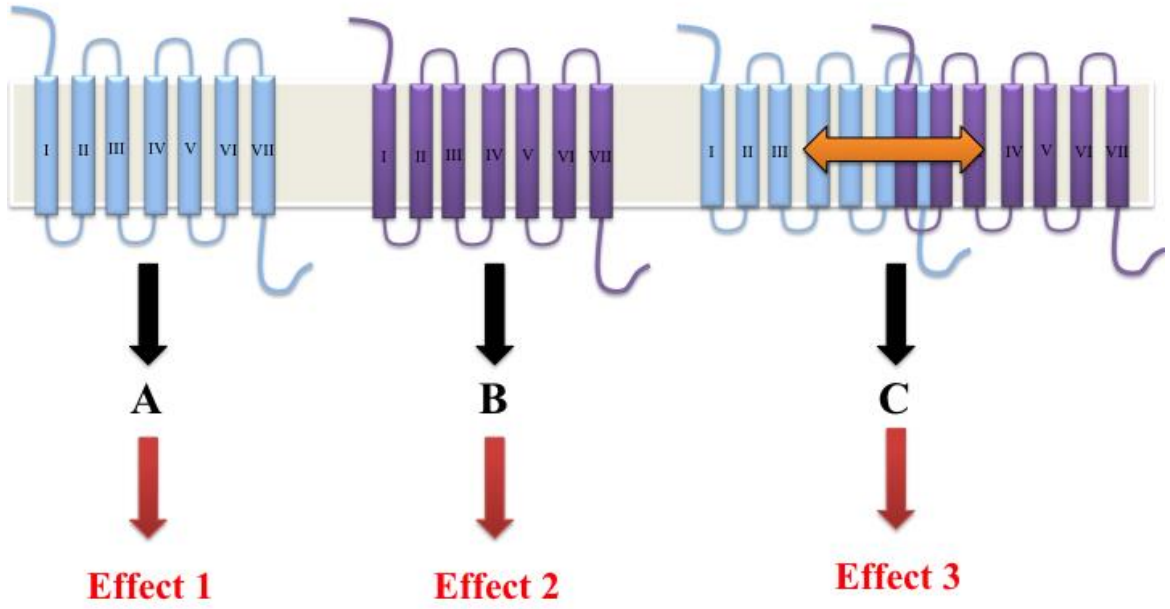

Figure 6. Functional interactions of GPCRs. Activation of two different GPCRs induces two independent signaling pathways A and B, resulting in two independent effects, 1 and 2. Interaction of GPCRs results in the activation of the heteromer-specific signaling pathway C responsible for downstream effect 3.

1.1.5 The role of GPCRs in the pathophysiology of human diseases

GPCRs play an important role in modulating tissue and cell physiology and homeostasis and their signal pathways are associated with various pathological processes such as neuronal degeneration, cancer, cardiovascular and immune system disease.

Moreover, GPCRs are potential targets for treating several pathophysiological disorders including obesity and metabolic syndromes. These pathological conditions are extremely complex and multifactorial, but there is evidence that neuropeptides binding to GPCRs can

regulate appetite and have effects on its pathophysiology. In addition neuropeptides regulate energy homeostasis through feeding behaviour and food intake, representing a promising target for treating obesity (Kimple et al., 2011).

Several members of GPCRs are found to have roles in pancreatic function and glucose homeostasis and in type-2 diabetes (Kimple et al., 2011).

The pathophysiology of heart diseases is characterized by the chronic activation of different GPCR signaling systems. So far, only a small fraction of these receptors, such as the angiotensin, endothelin, adrenergic and adenosine receptors have been characterized as potential drug targets for cardiac therapy (Heng, 2013).

Different functions of GPCRs have been evaluated in the pathophysiology of cancer and today they are being investigated as potential drug treatment targets, due to their involvement in the uncontrolled growth and proliferation of cancerous cells, metastasis, angiogenesis, differentiation pathways and alteration of the normal apoptotic pathway, and cross-talk with other non-GPCRs (Heng, 2013).

The physiology of some neurodegenerative diseases such as Alzheimer's, Parkinson's and Huntington's, involves the main GPCRs expressed on CNS. First of all, muscarinic acetylcholine receptors (M1 and M3), metabotropic glutamate receptors (mGlu1-4) and serotonin (5-HT) receptors are implicated in the formation of amyloid plaques through the modulation of α-,β-,γ-secretase involved in the neurodegeneration of Alzheimer's disease.

The major groups of GPCRs' target for Parkinson's disease are the dopaminergic receptors and metabotropic glutamate receptors. The selective loss of dopaminergic neurons suggest that dopamine receptor stimulation might provide some symptomatic relief for this disease as well as the stimulation of mGlu-4 signaling that enhances neurotransmission in the basal ganglia (Kim et al., 2010).

Dyskinesic symptoms are due to an imbalance between striatal dopaminergic and cholinergic activity. For this reason, another strategy may be to inhibit muscarinic acetylcholine receptor signaling as an alternative therapy. Parkinson disease is also characterized by loss of serotoninergic activity, and therefore the 5-HT 1A, 1B, 2A and 2C subtypes are potentially promising drug targets.

Glutamate receptors mediating excitotoxicity are the major players in the pathogenesis of Huntington's disease. Also, the CB1 receptors represent a promising target. Depletion of Endocannabinoid signaling is another biomedical hallmark of this pathology and stimulation of CB1 receptors could have beneficial therapeutic effects (More and Choi, 2015).

1.2 The Endocannabinoid System

The discovery, in 1990 and 1993, of a specific membrane receptor of marijuana's psychoactive component, (-)-Δ^9-tethrahydrocannabinol (THC), led to the discovery of an endogenous signaling system, known today as the "Endocannabinoid System" (ECS).

In mammalian tissue there are two types of cannabinoid receptors: CB1, found predominantly in the central nervous system and less in the peripheral nerve terminals and cannabinoid receptor type 2 (CB2), localized primarily on immune cells (Howlett et al., 2004). Both CB1 and CB2 receptors are coupled to the $G_{i/o}$ subtype of G-proteins, and when activated by agonists they inhibit the activity of adenylyl cyclase, activate mitogen-activated protein (MAPK) kinase and inhibit the function of voltage gated Ca^{2+} channels. Only CB1 receptors have been found to modulate the activity of K^+ channels (Katona and Freud, 2012).

The ECS consists of endogenous ligands, named endocannabinoids (EC) that target the CB1 and CB2 receptors, and of enzymes and processes responsible for their biosynthesis, metabolism, cellular uptake and inactivation (Katona and Freund, 2012).

The EC, present in the brain and peripheral tissues, are derivatives (amides, esters and ethers) of a long-chain polyunsaturated fatty acid, mainly arachidonic acid, capable of binding and functionally activating the cannabinoid receptors (Di Marzo et al., 2004). To date, several EC have been identified, see Fig. 7 (Pertwee, 2015).

The most studied EC so far are anandamide (N-arachinodil-ethanolamine, AEA), 2-arachinoyl-glycerol (2-AG), 2-arachidonyl-glyceryl ether (noladin, 2-AGE), O-arachidonoyl-ethanolamine (virhodamine) and N-arachidonoyl-dopamine (NADA) (Fig 7).

Due to their hydrophobic structure, their main cell signaling actions are limited to paracrine (cell-to-cell) or autocrine (same cell) signaling, rather than systemic effects, mediating

retrograde signaling that may lead to the inhibition of neurotransmitter release (Svinzeska et al., 2008).

They present unique characteristics since they:

- present a lipid structure that makes them lipophilic
- are hydrophobic with limited mobility in an aqueous environment
- are deputed to local cell-signaling (paracrine or autocrine)
- are formed from the internal lipid constituents of the cellular membrane
- are synthesized and released "on demand" and not stored in resting cells
- have a very short half-life
- undergo degradation by Fatty Acid Amide Hydrolase (FAAH)

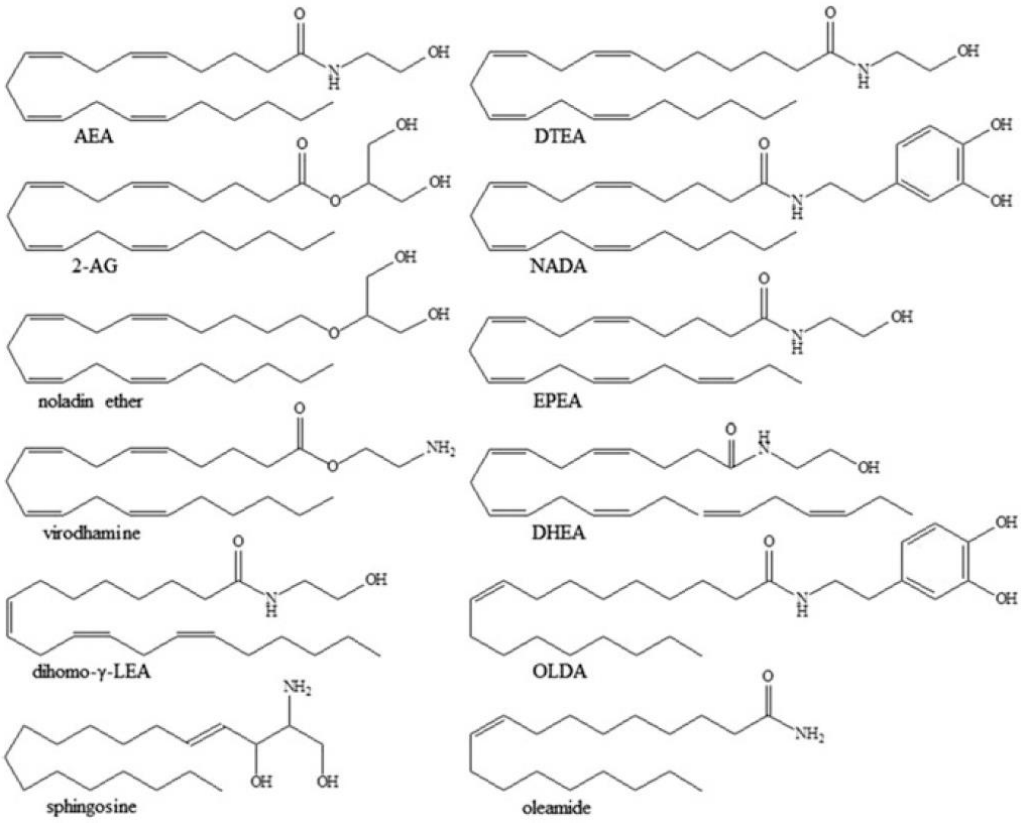

Figure 7. Chemical structures of Endocannabinoids and Cannabinoids (Pertwee, 2015).

The activity of EC is controlled by their endogenous levels, and therefore by a balance between biosynthetic and degradative mechanisms.

The level of 2-AG in no-stimulated tissues and cells is usually much higher than other EC and it acts on both cannabinoid receptors. 2-AG is at the crossroad of several metabolic pathways and is an important precursor of arachidonic acid and/or degradation product of arachidonic acid and of phopho-, di- and triglycerides. In previous studies several stimuli have been found to lead to the formation of 2-AG in neuronal and non-neuronal cells (Sugiura et al., 2002).

It was postulated that EC are not stored in pre-formed vesicles, yet they are synthesized and released "on demand". However, more recent views have imposed a reconsideration of this "dogma", because AEA can be stored in adiposomes and is bound to intracellular transporters (Maccarrone et al., 2010).

Once released into the extracellular space by a putative endocannabinoid transporter, EC are cleared away from their extracellular targets. This process is driven by controllable and selective mechanisms such as by the membrane transport protein or intracellular enzymatic process. Degradation by FAAH and monoacylglycerol lipase (MAGL) which cleave anandamide and 2-AG, respectively, into arachidonic acid and ethanolamine, and arachidonic acid and glycerol, leads to the diffusion of these compounds from the extracellular milieu into the extracellular space (Glaser et al., 2003).

EC act primarily at CB1 and CB2 receptors, AEA, NADA and 2-AGE are more selective for CB1, while virodhamide seems to have more affinity for CB2 (Mukhopadhyay et al., 2002).

It is now well established that AEA and 2-AG do not interact only with these receptors, they exhibit instead a degree of promiscuity that applies also to the less-studied arachidonic acid-derived endocannabinoids (Di Marzo and De Petrocellis, 2012).

A receptor with a different distribution to CB1 receptors and sensitive to AEA has been discovered in several brain areas of CB1 knock out (KO) mice. This receptor, named Transient Receptor Potential Vanilloid 1 Receptor (TRPV1), has been described in vascular endothelial cells where it controls the local vasodilatation but not in systemic effects induced by AEA. Furthermore, some plasma membrane channels involved in Ca^{2+} and K^{+} homeostasis also appear to be targeted by micromolar concentrations of AEA (Di Marzo et al., 2002).

The ECS regulates a variety of physiological processes and plays an important role in the control of mood, which makes it critical for the pathogenesis of several psychiatric disorders.

The first psychoactive compound of *Cannabis sativa*, THC was identified and characterized in 1964. Since its discovery, additional active compounds have been identified, but THC is still one of the most widely used illicit drugs, since it promotes relaxation and euphoria. It influences the CNS in a complex manner, and its chronic use may promote dysphoria, depressive mood and increased anxiety. Numerous selective and non-selective agonists and antagonists of CB1 receptors have been developed and used as tools to elucidate the role of the ECS. Few of them have advanced to clinical trials for treatment of pain, obesity, neurodegenerative disorders, inflammation and nicotine and alcohol addiction.

1.2.1 Cannabinoid receptors

The characterization and distribution of CB1 receptors in the CNS plays a key role in understanding the pharmacological effects of specific agonists and antagonists of these receptors.

CB1 and CB2 receptors belong to the superfamily of receptors that couple to G proteins, with seven hydrophobic transmembrane domains connected by extracellular and intracellular

loops, an N-terminal extracellular domain and a C-terminal domain which binds to the G protein complex (Bramblett et al., 1995).

The CB1 receptor has been cloned from rat, mouse and human tissues and exhibits a 97-99% amino acid sequence identity across species. It is one of the most abundant GPCR in the CNS, but it has also recently been found in cardiovascular tissue, the reproductive system and in the gastrointestinal tract (Croci et al., 1998; Sazbo et al., 2001).

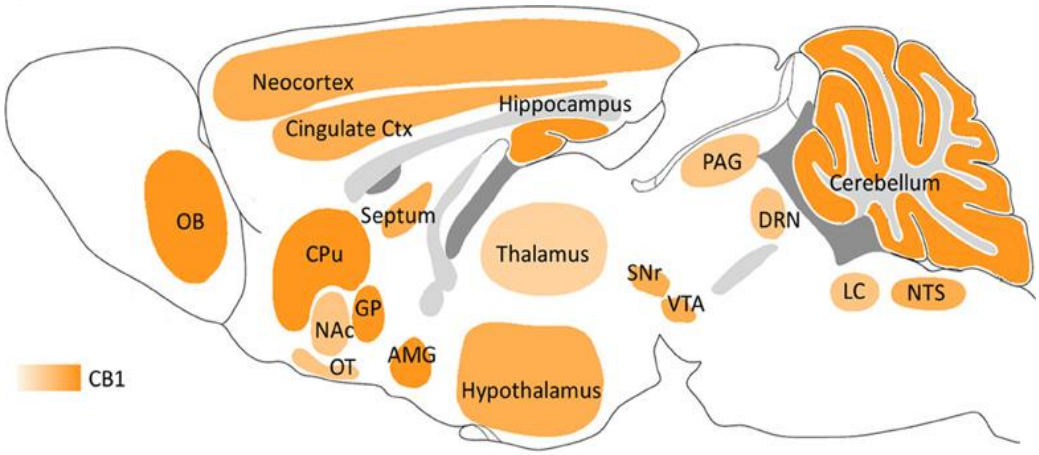

Figure 8. Schematic representation of CB1 receptor distribution in the rat brain (Flores et al., *Frontiers in Neuroscience*, 2013).

The CB1 receptor is coupled to $G_{i/o}$ proteins to inhibit adenylyl cyclase, activate MAPK, inhibit voltage gated Ca^{2+} channels and activate inwardly rectifying K^{+} channels (Howlett et al., 2000; Pertwee, 1997). It was found mainly at the terminals of central and peripheral neurons, where they usually mediate inhibition of the release of a range of different excitatory

and inhibitory neurotransmitters (For a review see Howlett et al., 2002; Pertwee and Ross, 2002; Szabo and Schlicker, 2005).

CB1 receptors have also been found on postsynaptic structures and in some astrocytes, microglia (Rodriguez et al., 2001; Stella 2010; Bosier et al., 2013), and oligodendrocytes and these cells are also able to synthetize and degrade EC (Walter et al., 2002; Stella 2009). Lastly, a recent controversial study (Benard et al., 2012; Hebert-Chatelain et al., 2014; Morozov et al., 2013) reported that CB1 receptors are associated with mitochondria in astrocytes, where they may play a role in energy balance and synaptic plasticity.

The CB1 receptor has a wide and characteristic distribution in the CNS: it is particularly enriched in the cortex, hippocampus, amygdala, basal ganglia outflow tracts, and cerebellum, this distribution being linked to the most prominent behavioral effects of cannabinoids (Mackie, 2005).

As shown in Fig. 8, high density of CB1 receptors in the hippocampus is associated with disruptive effects of cannabinoids on memory and cognition (Herknham et al., 1990). High concentration on basal ganglia could be related to the role of EC in the fine-tuning of motor control. Previous studies have shown that CB1 receptor expression and binding is decreased in neurodegenerative diseases, such as Parkinson's and Huntington's (Glass et al., 1997).

High density of CB1 receptors on the rat cerebellum may have a role in the immobility, catalepsy and ataxia observed after acute administration of THC and other cannabinoids in *in vivo* experiments (Fonseca et al., 1998). In contrast, a low density of CB1 receptors in the human cerebellum is linked to effects on motor function after THC use (Herknham et al., 1990).

Others brain regions present a moderate density of CB1 receptors, such as the medial hypothalamus, basal amygdala and solitary nucleus.

Stimulation of CB1 receptors on the hypothalamus interferes with the level and action of neuropeptides regulating energetic homeostasis, food intake, and lipogenesis in peripheral tissues and increases leptin release from the adipose tissue (Cota et al., 2003).

Stimulation of CB1 receptors in the nucleus accumbens increases the dopaminergic reward pathway and influences the motivation to eat and to take drugs of abuse. (Parsons and Hurd, 2015)

A high density of CB1 receptor on the periaqueductal grey and dorsal horn of the spinal cord is related to their involvement in pain modulation (Maldonado et al., 2006).

Stimulation of CB1 receptors by THC and other cannabinoid receptor agonists involves beneficial effects such as analgesia, attenuation of nausea and vomiting in cancer chemotherapy, reduction of intraocular pressure, appetite stimulation, relief from muscle spasm and spasticity in multiple sclerosis (Pertwee et al., 2000). Unfortunately, there are numerous side effects associated with these therapeutic effects, including alterations in cognition and memory, sedation, dysphoria/euphoria and panic (Howlett et al., 2002).

The CB2 receptors have been found predominantly in peripheral cells and immune cells (i.e. leucocytes) spleen and tonsils. They have also been identified in the gastrointestinal system and in numerous other cell types, including pulmonary endothelial cells (Zoratti et al., 2003), adipocytes (Roche et al., 2006), osteocytes, osteoclasts and osteoblasts (Ofek et al., 2006). Indeed, it has been reported that 2-AG affects meiosis in spermatogonia via CB2 and a number of other aspects of reproductive function (Maccarrone, 2008; Grimaldi et al., 2009).

CB2 receptors have also been found in the CNS, in both microglial and neuronal cells (Ameri, 1999; Gong et al., 2006; Atwood and Mackie, 2010) and when activated can modulate immune cell migration and cytokines release within the brain. The neuronal presence of CB2 receptors on neurons was a matter of debate for a long time, due to low levels of CB2

compared to CB1 receptors, the presence of CB2 in microglia and endothelial cells, and nonspecific antibodies.

Indeed, recent considerable functional and anatomical evidence suggests that the CB2 receptor is expressed in the CNS mainly in activated microglia and very likely in some neurons (Atwood and Mackie, 2010).

In line with these notions, the CB2 receptor is implicated in the control of the proliferation, differentiation and survival of neuronal and non-neuronal cells. There are conflicting studies that show both apoptosis and inhibition of tumour growth in host cells after CB2 receptor stimulation (Romero et al., 2002; Guzman 2003). Recently, several studies have reported that this receptor is also involved in brain neuroinflammation and neurodegenerative diseases, including Alzheimer's disease, Huntington's chorea, amyotrophic lateral sclerosis and others. Interestingly, in experimental models of these disorders, the activation of CB2 receptors has been related to a delayed progression of neurodegenerative events, in particular, those related to the toxic influence of microglial cells on neuronal homeostasis (Fernandez-Ruiz et al., 2008).

1.2.2 Classification of Cannabinoid receptor ligands

The discovery and characterization of CB1 and CB2 receptors were followed by the development of different molecules, which can be subdivided into two classes: agonists and antagonists/inverse agonists.

Cannabinoid receptor agonists are classified according to their chemical structures into:

1. "Classical" Cannabinoids: this group consists of ABC-tricyclic dibenzopyran derivatives that are either natural compounds obtained from *Cannabis sativa*, or synthetic analogs (Fig. 9). The most investigated of this group are Δ^9-THC, Δ^8-THC

and HU-210 (11-hydroxy-Δ^8-THC-dimethy-pentyl), all inducing cannabimimetic responses *in vivo* and *in vitro*.

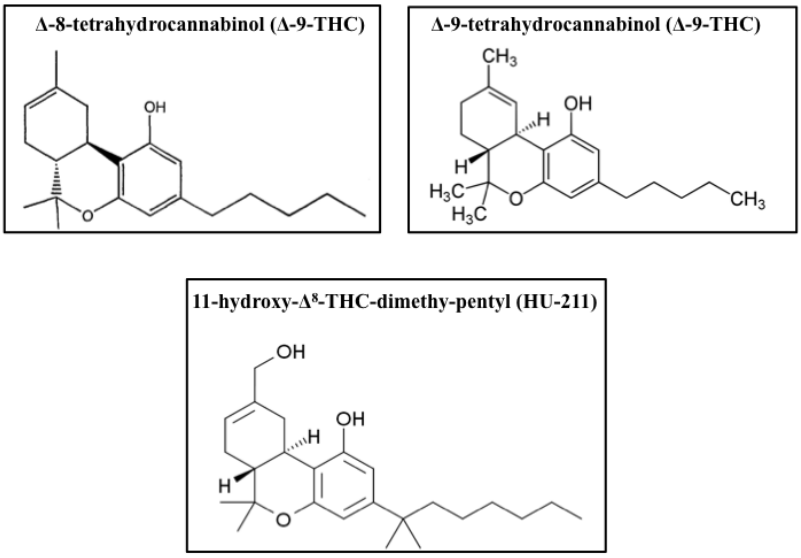

Figure 9. Chemical structures of ABC-tricyclic dibenzopyran derivatives.

2. "Non-classical" cannabinoids: during the course of studies of the structure-activity relationship to obtain an analgesic effect, researchers at Pfizer synthesized new analogues without the dihydropyran ring of THC (Fig. 10). These compounds were CP47497 and its bicyclic derivative, CP55940 that is still the agonist most used for radioligand binding assays. It binds to CB1 and CB2 receptors with similar affinity and displays high affinity in vivo with more potency than Δ^9-THC.

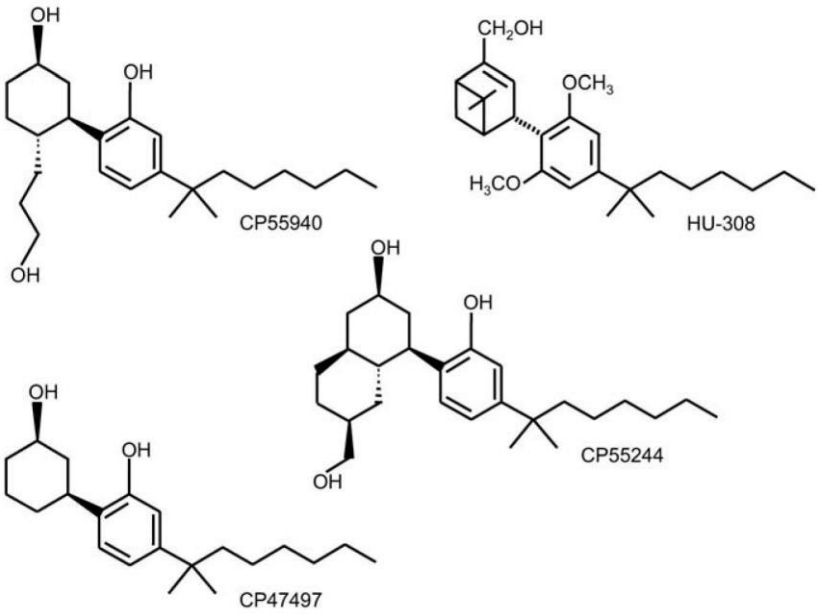

Figure 10. Chemical structures of "non-classical" cannabinoids.

3. Aminoalkylindoles: this class results from the modification of a series of non-steroidal anti-inflammatory compounds. R-(+)-WIN55212 is the most commonly used and studied, and displays affinity for both CB1 and CB2 receptors, with moderate selectivity in the CB2 receptor. *In vivo*, it produces the same pharmacological effects of THC (Howlett et al., 2002).
4. Eicosanoids: consist of prostaglandins (PG), thromboxanes (TX), leukotrienes (LT) and lipoxins (LX). They produce a wide range of biological effects on inflammatory responses, on the intensity and duration of pain and fever, and on reproductive function. They also play important roles in inhibiting gastric acid secretion, regulating blood pressure through vasodilation or constriction, and inhibiting or activating platelet aggregation and thrombosis. The principal eicosanoids of biological significance to humans are a group of molecules derived from the C_{20} fatty acid, arachidonic acid (Szefel et al., 2015).

CB1 receptor agonists *in vivo* assays show the so-called "mouse tetrad", which reveals their ability to produce hypokinesia, hypothermia, catalepsy and antinociception. There are no standard *in vivo* bioassays for CB2 receptor agonists. Repeated administration of CB1 receptor agonists can cause tolerance possibly due to receptor internalization and or to alterations in cAMP and PKA activity (Sim-Selley, 2003).

In *in vitro* bioassays these agonists are commonly used to measure the effect on signal pathways that involve CB1 and CB2 receptor activation. For example, stimulation of binding to G proteins of the hydrolysis-resistant GTP analogue [^{35}S]GTPγS decreases cyclic AMP production and has an effect on the intracellular concentration of Ca^{2+} and K^{+} (Pertwee 2006).

The cannabinoid receptor antagonists/inverse agonists are classified as follows (see Fig. 11):

1. Diarylpyrazoles: the prototypic compounds of this series are the Sanofi molecules SR1417161A (SR) and SR144528. Both prevent or reverse effects mediated by CB1 and CB2 receptors, respectively. However, there are many studies that showed the ability of SR141716A to produce opposite effects as compared to those produced by cannabinoid agonists. They can behave as inverse agonists and reduce the constitutive activity of signal transduction pathways (Howlett et al., 2002). Two analogues of SR, AM251 and AM281 have been found to produce inverse cannabinoid mimetic effects in CB1 receptor bioassay systems. AM251 suppressed rat food intake and food-reinforced behavior, it inhibited the basal G protein activity in rat cerebellar membranes and it enhanced the electrically-evoked glutamate release from rat cerebellar neurons (Pertwee et al., 2005). AM281 increased mouse locomotor activity,

and it inhibited the basal [^{35}S]GTPγS binding to primary cultures of rat cerebellar granule cells (Pertwee et al., 2005).

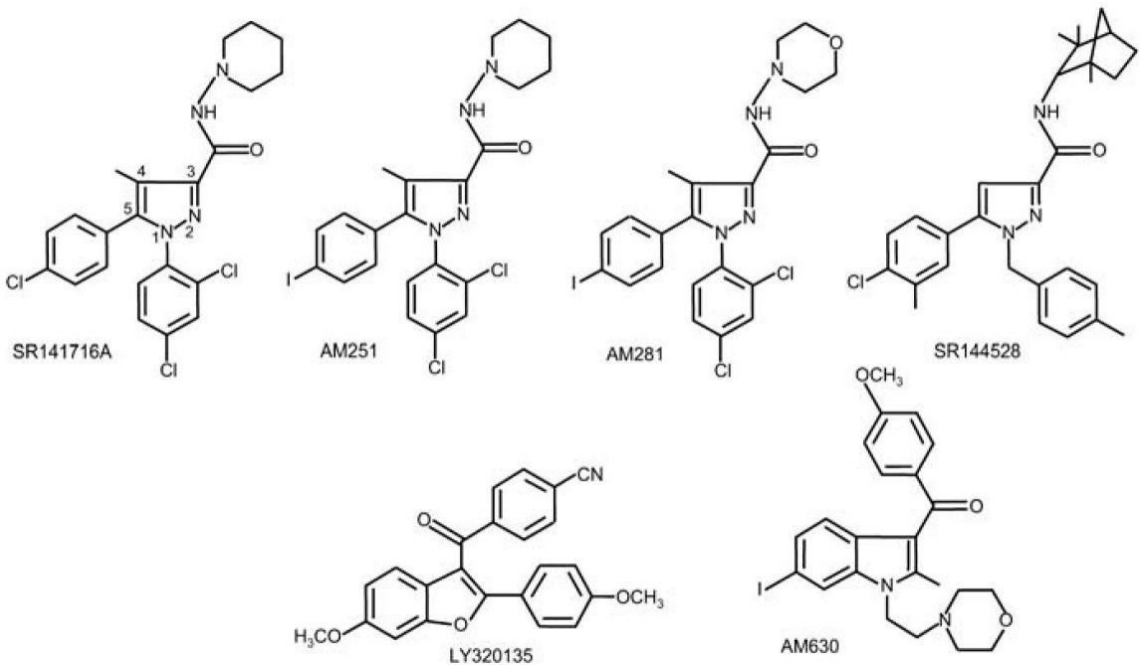

Figure 11. Chemical structures of cannabinoid receptor antagonist/inverse agonists.

2. Other compounds: the most used of the benzofuran series is LY320135, developed by Eli Lilly, found to have much higher affinity for the CB1 receptor than CB2 receptors, the AM630 is selective for CB2 (Howlett et al., 2002).

All the aforementioned diarylpyrazoles produce inverse cannabinoid mimetic effects in at least one bioassay system. For example, the *in vivo* inverse effects of these compounds in rats or mice include hyperalgesia in models of inflammatory and neuropathic pain, the stimulation of intestinal motility and food intake (Pertwee et al., 2005).

In vitro, the inverse agonist effects include increase in acetylcholine, noradrenaline and aminobutyric acid release in hippocampal slices, and inhibition of [^{35}S]GTPγS binding in membrane preparations (Pertwee et al., 2005).

Cannabinoid receptor ligands as well as agents that might modify cannabinoid transport, metabolism and activity of the ECS might be used as potential hypnotics, analgesics, antiemetic, antihypertensive and immunomodulatory drugs, anti-inflammatory, antiepileptic and drugs, but also for treating glaucoma, spasticity, eating disorders and alcohol withdrawal (Svíženská et al., 2008).

There is evidence that not all inverse cannabinoid mimetic effects are produced through a single mechanism. This project is aimed to understand the mechanism of the inverse agonist of SR.

1.2.3 CB1 receptor cross-talk with other endogenous systems

The broad distribution of CB1 receptors in the CNS underlines their modulatory role in several neurotransmitter systems.

Metabotropic $GABA_B$ and CB1 receptors have been found to display similar pharmacological effects and localization in different brain regions. The $GABA_B$ receptor belongs to Family C of the GPCRs and its distribution reflects its pharmacological relevance. At a presynaptic level it is present on inhibitory and excitatory terminals where it suppresses neurotransmitter release by inhibiting the voltage-sensitive Ca^{2+}-channel and by modulating synaptic vesicles. At a postsynaptic level, $GABA_B$ receptors induce a slow inhibition through activation of K^+ channels, which hyperpolarizes the membrane and avoids the current propagation (Bettler and Tiao, 2006).

By regulating neurotransmission, $GABA_B$ receptors are an important therapeutic target in the treatment of psychiatric disorders, epilepsy, drug addiction and pain (Pinard et al., 2010). Both CB1 and $GABA_B$ receptors play a relevant role in pathways involved in cognition, learning, memory and anxiety. Previous studies reported functional interaction between CB1 and $GABA_B$ receptors. In the cerebellum both receptors are localized on granule cells and share a common adenylyl cyclase catalytic unit (Cinar et al., 2008). In contrast, in the rat hippocampal synapses they are coupled to $G_{\alpha o1}$, $G_{\alpha i2}$ and $G_{\alpha i3}$ but not $G_{\alpha i1}$. One possible explanation for the cross-talk between CB1 and $GABA_B$ receptors is the competition for a G protein common pool. Recently, it was found that CB1 receptors can sequester $G_{i/o}$ proteins and prevent α_2-adrenergic and somatostatin receptor signaling. It was also demonstrated that sequestration is specific to the pertussis toxin-sensitive $G_{i/o}$ proteins (Vàsquez and Lewis, 1999).

The ECS is involved in memory, learning and reward and overlaps with the dopaminergic system. There is evidence of a functional interaction between these two systems, in particular between D2 and CB1 receptors. D2 receptors belong to GPCR Family 1 and are involved in numerous signal transduction pathways, such as the inhibition of adenylate cyclase activity, inwardly rectifying K^+ and Ca^{2+} channels, and mitogen-activated protein kinases (Vanhauwe et al., 1999). With *in situ* hybridization assays and immunocytochemistry techniques the co-localization of the CB1 and D2 receptor in rat caudate putamen and nucleus accumbens was demonstrated. Moreover, CB1/D2 co-expression has been found in dendrite, neuronal cell bodies and in terminal regions (Pickel, 2006). Using FRET experiments, Marcellino et al. (2008) have also shown that CB1/D2 receptors form a heterodimeric complex.

In addition, at the cellular level Glass and Felder (1997) have demonstrated that co-activation of CB1 and D2 receptors decreases the inhibition of cAMP, suggesting that an interaction

between CB1 and D2 receptors allows a switch in G-protein coupled from $G\alpha_i$ to $G\alpha_s$. Similarly, a chronic activation of D2 receptors appears to change CB1 coupling to Gs proteins.

In vitro studies showed direct interactions between μ-receptors and CB1 receptors, with a co-localization and formation of functional heterodimers. Using cells transfected with both receptors, it was found that WIN produced a non-competitive antagonist of morphine-induced G protein activity, while a CB1 inverse agonist increased agonist stimulation of the μ-receptor (Canals and Milligan, 2008).

The functional cross-talk between the ECS and others has been suggested to be involved in numerous brain disorders. For this reason, characterization of the domains involved in the heteromerization between CB1 receptors and different GPCRs might be relevant to determine how these interactions can contribute to the pathophysiology of brain diseases.

1.3 Rimonabant

Rimonabant, also known as SR141716A or SR (trade name Acomplia), was the first selective central CB1 receptor antagonist, developed by Sanofi-Aventis, indicated for the treatment of obesity. Obesity is one of the most relevant eating disorders in industrialised countries and is defined as abnormal or excessive fat accumulation (body mass index, BMI >30 kg/m^2) that may impair health and longevity. CB1 receptors are believed to play a role in controlling food consumption. Based on the promise that cannabinoid receptor agonists stimulate appetite, it resulted that a block of cannabinoid receptors in the brain might reduce the appetite. Compounds with potential inhibitory activity against this receptor were thus screened and SR emerged from this screening process as the most promising compound.

The beneficial effects of SR were confirmed in a series of clinical studies, including pivotal phase III trials that involved over 6,000 obese subjects in both the US and Europe (Verty et al., 2009).

Two-year data from the phase III multicentre Rimonabant In Obesity (RIO) trial, which compared this drug at doses of 5 mg and 20 mg to a placebo with respect to weight reduction and prevention of weight gain, showed that the positive results seen after a year's treatment were sustained over the full two-year trial period. SR was found to induce effective lipolysis, reduce hepatomegaly, and to improve dyslipidemia by reducing triglycerides, free fatty acids, and total cholesterol levels and by increasing the HDL/LDL ratio.

On 21 June 2006, the European Commission approved the sale of SR in all 25 member states of the European Union.

In the United States SR was submitted to the Food and Drug Administration (FDA) for approval. However, SR safety data indicated an increased risk for suicidal ideation in patients at the highest dose of 20 mg. The FDA Committee expressed concerns about the increased

risk of psychiatric and neurological adverse events.

In October 2008, the European Medicines Agency's Committee for Medicinal Products for Human Use stated that the risks of SR outweighed its beneficial effects. The Agency then recommended suspension of the product from the UK market, and Sanofi removed the drug from the market.

As reported in par 1.2.2, SR was the first selective and orally active CB1 receptor antagonist (Rinaldi-Carmona et al., 1994), which blocks agonist-induced activation of cannabinoid CB1 receptors in a competitive manner and binds with significantly greater affinity to cannabinoid CB1 than cannabinoid CB2 receptors. The possibility that SR also acts as an "inverse agonist", inhibiting CB1 receptor-constitutive activity, was suggested by Compton et al. (1996), who showed that the *in vivo* injection of high doses (3 mg) of SR stimulated motor activity. Since then, inverse cannabinoid mimetic effects of SR have been observed in experiments performed both *in vivo* and *in vitro* (Pertwee, 2005).

The following paragraphs report selected examples concerning the *in vivo* and *in vitro* antagonist as well as agonist inverse effects of SR mediated by CB1- and not CB1-receptors and/or by its interaction with other receptors.

1.3.1 *In vivo* studies

The first *in vivo* studies on SR have shown that it antagonizes discriminative stimulus properties, the hypothermic, motor and antinociceptive effects of cannabinoids in rodents and non-human primates (Compton et al., 1996, Wyley et al. 1995, Nakamura-Palacios et al., 1999). Specifically, intravenous injection of SR in mice inhibited THC-induced hypothermia, hypoactivity and antinociception with doses <3 mg/kg. It also antagonized the hypothermic

effects of CP55940 and of WIN in rodents, an effect observed for 18h after oral administration (Mansbach et al., 1996; Rinaldi-Carmona et al., 1994). However, SR was found to not antagonize the hypothermia and analgesia produced by administration of AEA (Welch et al., 1998). SR also blocked the hypomotility induced by THC, CP55940 and WIN, and when given by intracerebrovascular administration blocked catalepsy Lichtman and Martin, 1996).

SR also reverted the thermal- and chemical-antinociceptive effects of THC, as well as the effects of WIN in mice (Compton et al., 1996; Rinaldi-Carmona 1994) and both THC and WIN in rhesus monkeys (Vivian et al., 1997). Moreover, SR antagonized the "pop corn" effect in mice, the barrel rotations in rats induced by WIN (Souilhac et al, 1995) and turning behaviour produced by unilateral intrastriatal injections of cannabinoid agonists (Vivian et al, 1997). In addition, SR blocked the hypotension and bradycardia induced by THC, CP55940 and WIN in rats and guinea pigs and precipitated a withdrawal syndrome in rats made tolerant to THC. Finally, other studies have shown that SR antagonized the cannabinoid-induced effect on learning and memory. In particular, SR produced a rightward shift in the cannabinoid dose-effect curves for response rate in a repeated acquisition procedure. This effect was not observed with doses of SR >1 mg/kg, suggesting that other actions of SR may disrupt its antagonist effects of CB1 receptors on learning (Nakamura-Palacios et al., 1999). SR blocks the hypotension and bradycardia induced by THC, CP55940 and WIN in rats and guinea pigs and precipitates a withdrawal syndrome in rats made tolerant to THC (Rubino et al., 1998).

Despite all these findings, several studies have shown that there are *in vivo* actions of SR that cannot be explained by antagonism on CB1 receptors. In particular, high doses of SR (10 mg/kg, i.p.) disrupted learning memory in rats previously treated with THC. In contrast, in a

range of doses between 0.03-3 mg/kg, SR improved social short-term memory in adult and aged rodents (Terranova et al., 1996).

SR has been found to have effects on food intake, with doses from 0.03 mg/kg to 3 mg/kg reducing spontaneous sucrose intake in food-restricted rats. It was also shown to reduce sucrose drinking in food-restricted rats after one week of habituation in a dose dependent-manner (Arnone et al., 1997). Recently, Ward et al. (2009) have shown that SR decreased sweet-tasting liquid food intake in a dose-dependent manner in both male and female wild-type and knock-out mice.

Finally, behavioural studies have displayed that SR also exerts opposite *in vivo* effects to CB1 receptor agonists, since it produces hyperalgesia (Richardson et al., 1997; Pertwee et al., 2000), a decrease in food consumption (Colombo et al., 1998; De Vry et al., 2004; Verty et al., 2004) and an improvement in memory (Lichtman et al., 2002; Terranova et al., 1996).

Experiments performed with CB1-KO mice support the hypothesis that SR produces at least some of its inverse agonist by binding to CB1 receptors. Thus, SR enhances an electrically evoked release of noradrenaline in vasa deferentia and reduces food intake from WT mice, but not in CB1R KO. On the contrary, there are also reports showing that reduced food intake and increased severity of induced colitis, effects opposite to those produced by CB1R agonists, are observed both in SR-treated CB1-KO and in SR-treated WT mice (Di Marzo et al., 2001; Massa et al., 2004). Furthermore, SR at high doses produced significant anxiolytic effects in CB1- KO mice.

1.3.2 *In vitro* studies

As mentioned, SR competitively blocked the specific binding of the CB1 radioligand agonist [^{3}H]CP55,940 to CB1 and CB2 receptors, with a nanomolar affinity for CB1 receptors in human and rat brains, and a micromolar affinity for the CB2 receptor. In competitive studies, unlabelled SR was found to have IC_{50}>1 μM for several other receptors such as: adenosine A_1 and A_2, α_1, α_2, β_1 and β_2 adrenoceptors, histamine H1, H2 and H3, serotonin $5HT_{1A}$, $5HT_2$ and $5HT_3$ (Rinaldi-Carmona, 1994). In functional assays with isolated tissue preparations, SR antagonized the effects induced by cannabinoids; for instance in guinea pig isolated ileal muscle-myenteric preparations, as well as in mouse isolated vas deferens and urinary bladder preparations, SR reverted the cannabinoid agonist inhibition of the twitch response evoked by electrical stimulation (Pertwee et al., 1997; Rinaldi-Carmona, 1996). Further, it antagonized WIN-mediated inhibition of the depolarization-induced release of dopamine and norepinephrine from guinea pig hippocampal slices (Schlicker et al., 1996). SR reverted the WIN-mediated inhibition of adenylyl cyclase activity in synaptosome preparations from the rat brain (Nakamura-Palacios et al., 1999). In all these assays, SR behaved as a competitive antagonist with affinities in the nanomolar range that are consistent with its ability to interact with the CB1 receptor.

In contrast Landsman et al. (1997) showed that SR is a rather inverse agonist in membrane prepared from Chinese hamster ovary (CHO) transfected with human CB1 receptor, as assessed by the [^{35}S]GTPγS binding assay. Inverse agonist effects of SR were characterized using ligand-modulated [^{35}S]GTPγS binding, a methodology performed to investigate drug actions directly on G protein. Specifically, SR inhibited [^{35}S]GTPγS binding in CB1 transfected cell lines (MacLennan et al., 1998; Breivogel et al., 2001), in neuronal cells, and in the rat and mouse brain (Breivogel et al., 2004; Bouaboula et al., 1997; Sim-Selley et al.,

2001). Accordingly, SR produces a decrease in MAPK activity and an increase in evoked neurotransmitter release (Gifford et al., 2000; Breivogel et al., 2004; Schlicker et al., 2001) in basal cyclic AMP (cAMP) and forskolin stimulated cAMP production in the heterologous expression system, neuronal cell lines and rat or human brain membranes (Bouaboula et al., 1997; Felder et al., 1998; Mato et al., 2002; Meschler et al., 2000). Moreover, Pan et al. (1998) showed that SR increased N-type Ca^{2+} currents in superior cervical ganglion neurons by inhibiting the tonically active state of CB1 receptors.

In addition, when tested alone at concentration >1 μM SR decreased [^{35}S]GTPγS basal binding in membrane from CB1-WT and CB1-KO mice, and this effect was not blocked by the CB1 receptor neutral antagonist (O-2050), suggesting that the inverse agonist effects of SR are CB1 receptor independent (Cinar and Szucs, 2009).

Recently, Erdozain et al. (2012) found that SR at concentrations of > 1 μM acted as inverse agonists in the *post-mortem* human brain, demonstrating that this effect is not mediated by the CB1 receptor. SR inhibited basal [^{35}S]GTPγS binding to human cortical membranes in a concentration-dependent manner and, in the presence of 1 μM, did not modify the inhibitory curve of SR. Moreover, the neutral CB1 receptor antagonist, O-2050, at 10 μM and 100 μM fails to affect the inhibition produced by SR on basal [^{35}S]GTPγS binding. These data support the hypothesis that the inverse agonist effect of SR is not CB1 receptor-mediated. In order to exclude that SR might bind to a site distinct from the ortosteric agonist-binding site, or that its effects might be due to an allosteric modulation, the effect of Org27569, an allosteric modulator of the CB1 receptor was tested. This compound did not modify the inhibition of the basal G protein signaling produced by SR excluding the possibility that the SR effects are mediated by an interaction with a CB1 allosteric site.

1.3.3 Effects of SR on other receptors

Savinainen et al. (2003), using the [^{35}S]GTPγS binding assay, demonstrated that SR inhibited G protein activity in brain membranes prepared for the A1 receptor.

In 2004, another study on a rat Parkinson's model, showed that after the infusion of SR into denervated striatum nerves, ipsilateral rotation in hemiparkinsonian rats was reduced, leading to an improvement in motor performance (Pinna et al., 2014). The results suggest that SR had opposite effects on D1 and D2 receptor function, leading to a positive modulation of motor processes induced by D1 receptor stimulation, but to a reduction of D2 dopamine receptor function.

Accordingly, Alonso et al. (1999) reported that SR reduced D2 receptor function in rat striatum. Crunelle et al. (2013) found that chronic administration of SR (1–3 mg/kg/day) dose-dependently increased D2 receptor availability in the dorsal and ventral striatum. Since the latter region regulates food intake, the effects of SR observed in this study might be related to increasing D2 receptor availability.

In addition, acute treatment with SR reduced dopamine released in the nucleus accumbens after food and drug administration (Melis et al., 2007). The effects of SR on the striatal dopaminergic system need further investigation.

Indeed, a recent *in vitro* study showed that the constitutive activity of CB1 receptors negatively regulates the function of co-expressed μ-opioid receptors (Canals and Milligan, 2008).

Accordingly, strong evidence that SR might act on receptors other than the CB1 receptors was provided by Cinar et al. (2009). They found that SR completely inhibited and decreased G protein activation induced by the μ-receptor agonist Tyr-D-Ala-Gly-(NMe)Phe-Gly-ol Tyr-D-Ala-Gly-(NMe)Phe-Gly-ol (DAMGO) in the cortex of CB1-WT and CB1-KO mice, and in

CHO expressing μ-opioid receptors (Cinar and Szucs, 2009). These authors confirmed the hypothesis that the inverse agonist effect of SR was not CB1 receptor-independent and possibly even non-receptor-mediated. Another study reports that SR bound to the μ-receptor with a significant affinity and antagonized the ability of morphine to inhibit the activity of adenylyl cyclase in CHO cells stable transfected with μ-receptors. Interestingly, 10 μM of SR inhibited G protein basal activity in CHO-WT cells that are devoid of μ-receptors (~20% on the [^{35}S]GTPγS basal binding). Moreover a pre-treatment of SR attenuated morphine analgesia in B6/SJL mice and in C57BL/6J mice. Altogether, these results demonstrate that SR might act on different GPCRs with a multitude of effects in *in vivo* testing (Seely et al., 2012).

Finally, a very recent study showed that in competition binding experiments, SR at a low micromolar range in CHO cells transfected with rat kappa opioid receptor (CHO-rKOR), inhibited KOR agonist [^{3}H]U69593 binding and specifically reduced KOR basal activity at lower micromolar concentrations in [^{35}S]GTPgS binding assays. The decrease of G protein basal activity induced by SR was higher at 10 μM compared with 1 μM, but interestingly only the effect induced by the lower dose of SR was reverted by nor-BNI (the κ-receptor antagonist). Thus the inverse agonistic effect of Rimonabant at 10 μM concentrations is not KOR related (Zador et al., 2015).

1.4 Aim of the study

Several possible mechanisms, such as modulation of the constitutive activity of the CB1 receptor, antagonism at CB1 receptors of endogenously released endocannabinoids, and CB1 receptor-independent mechanisms, either through another receptor or by a receptor-independent mechanism have been proposed to explain SR induced inverse agonist effects. In addition, recent findings have led to the hypothesis that SR might directly inhibit G protein activity by a non-receptor-mediated mechanism.

Based on these premises, the present study aimed to determine whether the CB1 receptor-independent effects of SR are mediated via GPCRs, in particular $GABA_B$ and dopamine D2 receptors, that share the same Gαi/o signaling pathways, or if SR acts directly on G protein.

Hence this project was carried out in different phases in order to characterize:

1. Effects of SR on G-protein activity using the [^{35}S]GTPγS binding assay in native and recombinant systems containing CB1, $GABA_B$ and D2 receptor populations (rat and mouse membrane homogenates) and in CHO stable transfected with $GABA_B$ receptors, D2 receptors and in CHO non-transfected cells; and the effects of SR on G protein activity in systems lacking CB1 and $GABA_B$ receptors (CB1 and $GABA_B$-knockout mice).

2. Effects of SR on G-protein heterodimerization and subunit rearrangement using the BRET assay in recombinant systems.

3. Effects of SR on G-protein effectors using different techniques such as BRET to monitor adenylyl cyclase activity, and electrophysiological recordings in both native and recombinant systems.

Chapter 2. Materials and Methods

2.1 Chemicals

5'-O-(3-[^{35}S]thiotriphospate) ([^{35}S]GTPS) (1250 Ci/mmol) was purchased from PerkinElmer Life , GABA, GDP, guanosine 5′-*O*-(3-thiotriphosphate) (GTPγS), were obtained from Sigma /RBI (Natick, MA). R(-)baclofen, CGP54626, quinpirole, L-Sulpiride, WIN55,212-2 (WIN), AM251 were purchased from Tocris Bioscience (Ellisville, MO). [^{35}S]GTPγS (125 Ci/mmol), and [^{3}H]CGP54626 (85 Ci/mM) were obtained from PerkinElmer Life and American Radiolabeled Chemicals Inc. (St. Louis, MO), respectively. SR1417161A (SR) was a generous gift from Sanofi-Aventis.

2.2 Animals

Male Sprague-Dawley rats and DBA mice (Charles River Laboratories, Calco, Italy), weighing 200 to 250 and 17 to 20 g, respectively, were used. Rats and mice were housed 4 and 20/cage, respectively, in standard plastic cages with wood chip bedding, at temperature of 22 ± 2 °C and 60% humidity and under a 12 h light/dark cycle (lights on from 7.00 a.m.). Tap water and standard laboratory rodent chow (Mucedola, Settimo Milanese, Italy) were provided ad libitum in the home cage.

Mutant mice with the CB1 receptor gene deleted (CB1-KO) were obtained and genotyped as previously described (Marsicano et al., 2002), while $GABA_{B(1)}$-KO (*$GABA_{B(1)}$-/-*) mice were generated on inbred Balb/c strain background (Schuler et al., 2001).

The animals were housed in a temperature- and light-controlled room. Lighting was ensured in a 12-h cycle, and food and water were available ad libitum.

2.3 Tissue preparation

Male rats (250 g) were sacrificed by decapitation, their brains rapidly removed and cerebral cortices and striata were dissected on ice. Cortical tissues were homogenized using a glass-teflon homogenizer (Glass-Col, Terre Haute, IN) in 15 volumes (v/w) of ice-cold 0.32 M Sucrose and 1 mM EDTA. The homogenate was centrifuged at 1000 x *g* for 10 min, then the supernatant was collected and re-centrifuged at 20000 x *g* for 20 min. The pellet was re-suspended in 20 volumes (v/w) of ice-cold distilled water, homogenized using a Polytron homogenizer, and centrifuged at 8000 x *g* for 20 min. The last centrifugation of supernatant together with the buffy layer was performed at 45000 x *g* for 40 min, then the supernatant was discarded and the final pellet was frozen and stored at -80°C for at least 24 h before use.

For striata, tissues were homogenized in 20 volumes of buffer (50 mM Tris-HCl, 3 mM $MgCl_2$ and 1 mM EGTA, pH 7.4). The homogenate was centrifuged twice at 48,000 x g at 4°C for 10 minutes, resuspended in homogenization buffer and frozen at -80°C until use.

The Bradford (1976) protein assay was used for protein determination using bovine serum albumin as a standard according to the supplier protocol (Bio-Rad, Milan, Italy)

2.4 [^{35}S]GTPγS binding assay in rat and mice membranes

On the day of experiment, for $GABA_B$-stimulated [^{35}S]GTPγS binding, rat cortex membranes were thawed at 4°C and suspended in 20 volumes (v/w) of Krebs-Henseleit buffer (143 mM NaCl, 50 mM Tris-HCl, 5.9 mM KCl, 1.2 mM $MgSO_4$ and 2.5 mM $CaCl_2$, pH 7.4), homogenized, incubated at RT for 10 min an then centrifuged for 10 min at 40000 x *g* at 4°C. This step was repeated for three times. Afterward membranes were incubated in ice-cold water for 1h on ice, and then centrifuged for 20 min at 18000 x *g* at 4°C to obtain the final

pellet. The final pellet was re-suspended in assay buffer, containing 50 mM Tris-HCl buffer, pH 7.7; 10 mM $MgCl_2$; 1.8 mM CaCl; 100 mM NaCl; 30 µM guanosine 5'-diphosphate, to a final concentration of 20 µg of protein. Membrane homogenates and drugs were pre-incubated in PerkinElmer PicoPlates 96 (300 µl volume) for 30 min at 30°C. The main incubation was subsequently started by the addition of [^{35}S]GTPγS to a final concentration of 0.2 nM. After 40-min incubation at 30°C, the samples were filtered using a PerkinElmer UniFilter-GF/B, washed twice with 300 µl of buffer, and dried for 1 h at 30°C.

For CB1-stimulated [^{35}S]GTPγS binding, cortical membranes (10-15 µg of proteins) were incubated in assay buffer (50 mM Tris-HCl, 3 mM $MgCl_2$, 0.2 mM EGTA and 100 mM NaCl, BSA 0.1%, pH 7.4) at 30°C for 1 h with 30 µM GDP and 0.05 nM [^{35}S]GTPγS in a final volume of 1 ml. After incubation, the samples were filtered using a PerkinElmer UniFilter-GF/B, washed twice with 1 ml of buffer and dried for 1 h at 30°C.

For D2-stimulated [^{35}S]GTPγS binding, striatal membranes (20 µg of proteins) were pre incubated in assay buffer (20 mM K-HEPES, 7 mM $MgCl_2$, 1 mM EDTA, 1mM DTT and 100 mM NaCl, pH 7.6) at RT for 30 min with 300 µM GDP. The main incubation was subsequently started by the addition of [^{35}S]GTPγS to a final concentration of 0.1 nM in a volume of 300 µl. After 60 min of incubation at 35 °C, the samples were filtered using a PerkinElmer UniFilter-GF/B, washed twice with 1 ml of buffer (20 mM K-HEPES and 100 mM NaCl, pH 7.6), and dried for 1 h at 30°C.

The radioactivity on the filters was counted in a liquid microplate scintillation counter (TopCount NXT; PerkinElmer Life and Analytical Sciences) using 50 µl of scintillation fluid (Microscint 20; PerkinElmer Life and Analytical Sciences). Basal binding was assessed in the absence of agonist and in the presence of GDP, and nonspecific binding was measured in the presence of 10 µM unlabeled GTPγS. The stimulation by agonist was defined as a percentage

increase above basal levels (i.e., [disintegrations per minute (agonist) – disintegrations per minute (no agonist)/(disintegrations per minute (no agonist)] x 100). Data are reported as means S.E.M. of three to six experiments, performed in triplicate. Nonlinear regression analysis of concentration-response data was performed using Prism 2.0 software (GraphPad Prism) to calculate E_{max} and EC_{50} values.

2.5 [^{3}H]CGP54626 binding assay

[^{3}H]CGP54626 binding were performed as previously described (Castelli et al., 2012). Briefly, binding was carried out using 50 μg of membrane proteins, 2 nM [^{3}H]CGP54626 in a volume of 1 ml at 22–24°C for 30 min. Nonspecific binding was estimated in the presence of 10 μM unlabeled CGP54626. Free ligand was separated from bound ligand by rapid filtration through Whatmann GF/B glass filters using a Brandel 30-samples harvester (Brandel Inc., Gaithersburg, MD). Filters were then rinsed twice with ice-cold Krebs-Henseleit buffer. Filter-bound radioactivity was counted in a liquid scintillation counter (Tri-carb 1600; PerkinElmer Life and Analytical Sciences) using 3 ml of scintillation fluid (Ultima Gold MV; PerkinElmer Life and Analytical Sciences). [^{3}H]CGP54626 displacement curves were determined using increasing concentrations (from 1 nM to 0.5 mM) of SR and increasing concentrations (from 0.1 nM to 0.1 μM) of the unlabeled CGP54626.

The calculation of IC_{50} was performed by nonlinear curve fitting of the concentration-effect curves using GraphPad Prism (GraphPad Software Inc., San Diego, CA). The F test was used to determine the best approximation of a nonlinear curve fitting to one or two site model ($P < 0.05$).

2.6 Cell culture, transfection and membrane preparation for [^{35}S]GTPγS binding assay

Culture and maintenance of CHO-K1 cells stably expressing human $GABA_{B(1b,)}$ and rat (CHO-$GABA_{B2}$) was performed as described (Urwyler et al., 2001) and maintained in DMEM supplemented with 500 μM L-glutamine (Sigma), 40 mg/ml L-proline (Sigma), 0.5 mg/ml genecitin , 0.25 mg/ml zeocine, (Invitrogen) and 10% FBS in a humidified atmosphere of 5% CO_2 at 37 °C.

Preparation of membranes from CHO-$GABA_B$ for [^{35}S]GTPγS binding assay was performed as previously described (Urwyler et al., 2001). Briefly, CHO-$GABA_{B2}$ cells were grown to 80-90 % confluency in 145-cm Petri dishes. Then, the culture dishes were washed twice with ice-cold PBS, 10 mM HEPES buffer, pH 7.4 was added to the plates and cells were scraped off. Crude membranes from several dishes were collected and centrifuged at 4°C for 20 min at 15000 x g. The pellet was re-suspended in 10 ml HEPES buffer and homogenized using a glass- glass homogenizer (10 strokes). Afterward, the suspension was centrifuged (18000 x *g*, 30 min, 4° C), and the pellet was re-suspended in a small volume of buffer and homogenized again (20 strokes). Aliquots were frozen in liquid nitrogen and stored at -80 °C until use.

CHO-K1 cells stably expressing D2 receptors were prepared using Lipofectamine 2000 (Invitrogen) as described (Newman-Tancredi et al., 1999). Briefly, CHO-K1 cells were cultured to 80% confluence ($3x10^6$ cells in 100-mm dishes) and incubated for 6 h with 30 μg of pcDNA3.1 (Zeo) plasmid containing the cDNA encoding for the human D2-long receptor (gently gift from O Civelli, Dept. of Pharmacology, University of California, USA) and 60 μl of Lipofectamine reagent in serum-free Opti-MEM. Selection antibiotic (0.3 mg/ml zeocin) was added to the cell culture medium 48 h after transfection, and surviving colonies were picked 14 days after beginning selection. To confirm D2-long expression, competition and

saturation binding experiments using [^{3}H]YM09151-2, the specific D2 receptor antagonist, were performed as previously described (Vanhauwe et al., 1999). The clone expressing the highest level of specific D2-long receptors was selected, designated as CHO-D2 cells, maintained in DMEM containing 300 µg/ml zeocin and used throughout the study.

For membranes preparation for GTPγS binding, CHO-D2 cells were grown in a 145-cm Petri dishes. At 90% confluence, 5 mM sodium butyrate was added to increase the receptor expression level and the cells were further incubated for 24 h (Vanhauwe et al., 1999). Then, medium was removed, the culture dishes were washed once with 5 ml of ice-cold PBS and stored at -80°C until use. Cells on Petri dishes were thawed, cells were harvested using 5 ml of 10 mM Tris-HCl (pH 7.4), 1 mM EDTA, 1 mM 4-(2-amino- ethyl)benzene-sulfonyl-fluoride hydrochloride and homogenized with a dual homogenizer (motor-driven Teflon pestle and conical glass tube). Then homogenate was centrifuged (10 min at 1000 x *g* at 4°C), and the resulting pellet was re-suspended and centrifuged again (10 min at 1300 x *g* at 4°C). Both supernatants were pooled and centrifuged at 50000 x g for 1h at 4°C. The resulting pellet was re-suspended in 50 mM TrisHCl (pH 7.4), containing 10% glycerol and stored in aliquots at -80°C until use.

2.7 [^{35}S]GTPγS binding assay in CHO, CHO-GABA$_B$ and CHO-D2 cell membranes

On the day of the experiment, the frozen membranes were thawed and then centrifuged for 10 min at 12000 x *g* and 4°C. The pellet was resuspended in 1 ml of ice-cold distilled water and incubated for 1 h on ice. After a further centrifugation as before, the final pellet was re-suspended in the appropriate amount of assay buffer.

For CHO-GABA$_B$ stimulated [^{35}S]GTPγS binding, membranes (20 µg of proteins) were incubated in assay buffer (50 mM Tris-HCl, 10 mM $MgCl_2$, 0.2 mM EGTA and 100 mM

NaCl, 2 mM $CaCl_2$, pH 7.7) at 22-24°C for 1 h with 30 µM GDP and 0.2 nM [^{35}S]GTPγS in a volume of 0.3 ml. After incubation, the samples were filtered using a PerkinElmer UniFilter-GF/C, washed twice with 1 ml of buffer and dried for 1 h at 50°C (Urwyler et al., 2001).

For CHO-D2 and CHO non transfected stimulated [^{35}S]GTPγS binding, membranes (10 µg of proteins) were pre-incubated in assay buffer (50 mM K-HEPES, 10 mM $MgCl_2$, 100 mM NaCl, 0.1% BSA, pH 7.4) for 30 min at 30°C with 10 µM of GDP. The main incubation was subsequently started by the addition of [^{35}S]GTPγS to a final concentration of 0.1 nM. After 90 min incubation at 30°C, the samples were filtered using a PerkinElmer UniFilter-GF/B, washed twice with 300 µl of buffer 50 mM HEPES, pH 7.4, and dried for 1 h at 30°C. The radioactivity on the filters was counted in a liquid microplate scintillation counter (TopCount NXT; PerkinElmer Life and Analytical Sciences) using 50 µl of scintillation fluid (Microscint 20; PerkinElmer Life and Analytical Sciences).

2.8 Bioluminescence resonance energy transfer (BRET) measurements

Human Embryonic Kidney 293T (HEK293T) cells or CHO-$GABA_B$ cells were growing in 10-cm culture dishes at 37°C, 5% CO_2, in DMEM supplemented with 10% FBS. Transient transfections of different constructs were carried out using Lipofectamine 2000 (Invitrogen), according with manufacturer's instruction. 48 or 24 hours after transfection, cells were washed twice with PBS, incubated in the presence or absence of SR (different concentrations), for 1 h before substrate addition in a 96-well microplate (Corning Incorporated-Costar).

BRET1 between Renilla luciferase (Rluc) and Venus or Yellow Fluorescent Protein (YFP) was measured after the addition of the Rluc substrate Coelenterazine h (NanoLight Technologies) with a final concentration of 5 µM. BRET1 readings were collected (except in

kinetics experiments; see below) at the appropriate wavelengths using Infinite® F500 microplate reader (Tecan). The BRET1 signal was calculated as the ratio of the light emitted by YFP or Venus (530–570 nm) over the light emitted by Rluc (370–470 nm). BRET1 signal values were corrected by subtracting the background signal detected when Rluc-tagged construct was expressed alone from the signal detected in cells coexpressing both Rluc- and Venus- or YFP-tagged constructs (Net BRET). Data were analyzed using Microsoft Excel and plot using GraphPad PRISM. Statistical significance was assessed using one-way analysis of variance (ANOVA) followed by Bonferroni's test where appropriate.

2.9 BRET in CHO $GABA_B$ transfected with $G\alpha_o$-Rluc and $G\gamma_2$-Venus

CHO cells stably expressing $GABA_{B1}$ and $GABA_{B2}$ were transfected with plasmids encoding $G\alpha_o$-Rluc, Venus-$G\gamma_2$, FLAG-$G\beta_2$ (gift from Pin J.P., Institute de Génomique Fonctionnelle, Montpellier) and were seeded into 96- well microplates. 24 h after transfection, cells were washed with PBS and the measurement was initiated using Tecan after 10 minutes of incubation of 5 μM Coelenterazine h. 10 μM GABA was injected after 29 cycles of reading, and CGP54626 was injected after 99 cycles. Luminescence and fluorescence signals were detected sequentially with an integration time of 200 ms. The BRET ratio was calculated as the ratio of light emitted by Venus-$G\gamma_2$ (530-570 nm) over light emitted by $G\alpha_o$-Rluc (370-470 nm) and corrected by subtracting ratios obtained with the Rluc fusion protein alone. The results were expressed in mBRET units (BRET x 1000). The curves were fitted using GraphPad Prism 5.0 ("Plateau followed by one-phase decay"). ΔBRET was calculated as the difference between the basal and the plateau of BRET signal.

2.10 BRET in HEK293 transfected with $G\alpha_i$-Venus and D2-Rluc

HEK293T were transfected with D2-Rluc (gift from Kern A., The Scripps Research Institute Florida, USA) and $G\alpha_{i\text{-}60}$Venus or $G\alpha_{i\text{-}91}$Venus or $G\alpha_{i\text{-}121}$Venus (gift from Lambert N., Georgie Regents University Augusta, USA) and were seeded into 96- well microplates.
48 h after transfection, cells were washed with PBS and the measurement was initiated using Tecan after 10 minutes of incubation of 5 μM Coelenterazine h. 100 μM Quinpirole was injected after 29 cycles of reading. Luminescence and fluorescence signals were detected sequentially with an integration time of 200 ms. The BRET ratio was calculated as the ratio of light emitted by Venus-Gαi (530-570 nm) over light emitted by D2-Rluc (370-470 nm) and corrected by subtracting ratios obtained with the Rluc fusion protein alone. The results were expressed in mBRET (BRET x 1000).

2.11 BRET in HEK293 transfected with $G\alpha_i$-Venus and $G\beta_1$-Rluc or $G\gamma_2$-Rluc

HEK293T were transfected with $G\alpha_{i\text{-}60}$Venus, $G\alpha_{i\text{-}91}$Venus or $G\alpha_{i\text{-}121}$Venus and $G\beta_1$-Rluc or $G\gamma_2$-Rluc (gift from Jacquier V., University of Basel, Switzerland) and were seeded into 96-well microplates. 24 h after transfection, cells were washed with PBS and the measurement was initiated on Tecan after 10 minutes of incubation of 5 μM Coelenterazine h. Luminescence and fluorescence signals were detected sequentially with an integration time of 200 ms. The BRET ratio was calculated as the ratio of light emitted by Venus-$G\alpha_i$ (530-570 nm) over light emitted by $G\beta_1$-Rluc or $G\gamma_2$-Rluc (370-470 nm) and corrected by subtracting ratios obtained with the Rluc fusion protein alone. The results were expressed in mBRET (BRET x 1000).

2.12 BRET in HEK293 with CAMYEL sensor

HEK293T were transfected with Myc-$GABA_{B1a}$, Myc-$GABA_{B2}$ or D2-HA and CAMYEL (purchased from American Type Culture Collection, Manassa, VA, USA) and were seeded into 96- well microplates and were seeded into 96- well microplates. 24 h after transfection, cells were washed with PBS and the measurement was initiated using Tecan after 10 minutes of incubation of 5 μM Coelenterazine h.

0.5 μM Forskolin was injected after 19 cycles of reading, GABA 100 μM or quinpirole 10 μM were injected after 99 cycles. Luminescence and fluorescence signals were detected sequentially with an integration time of 200 ms. The BRET ratio was calculated as the ratio of light emitted by YFP (530-570 nm) over light emitted by Rluc (370-470 nm) and corrected by subtracting ratios obtained with the ratio of light emitted by YFP (530-570 nm) over light emitted by Rluc (370-470 nm) measured on HEK293T transfected with CAMYEL only. The curves were fitted using GraphPad Prism 5.0 ("Plateau followed by one-phase association"). The amplitude-weighted mean time constant (tau CAMYEL activity) was obtained by fitting BRET recovery phase to a double exponential function. ΔBRET was calculated as the difference between the basal and the plateau of BRET signal.

2.13 Whole cell voltage clamp recordings from dopamine neurons

Whole cell patch clamp recordings from VTA DA cells were as described previously (Melis et al., 2006). Briefly, male Sprague Dawley rats (Harlan Nossan, San Pietro al Natisone, Italy) or CB1-KO and littermate wild-type (WT) control mice were anesthetized with halothane and killed. Recordings were made from horizontal slices superfused with artificial cerebrospinal fluid (ACSF, 37° C) saturated with 95% O2 and 5% CO2 containing (in mM): 126 NaCl, 1.6 KCl, 1.2 NaH2PO4, 1.2 MgCl2, 2.4 CaCl2, 18 NaHCO3, and 11 glucose. Evoked field

potential recordings were as described previously (23). All the drugs were dissolved in DMSO. The final concentration of DMSO was < 0.01 %. Statistical significance was assessed using one- or two-way analysis of variance (ANOVA) for repeated measures followed either by Dunnett's or t test (with Welch's correction), where appropriate.

2.14 Whole cell patch clamp recordings from CHO cells

CHO cells expressing $GABA_{B1}$ and $GABA_{B2}$ were transiently transfected with Kir3.1/3.2 plasmids encoding using Lipofectamine 2000 (Invitrogen), according with manufacturer's instruction. 24 hours after transfection experiments on CHO cells were performed at room temperature as previously described (Schwenk et al., 2010). During recording CHO cells were continuously superfused with an extracellular solution composed of (in mM): 145 NaCl, 2.5 KCl, 1 $MgCl_2$, 2 $CaCl_2$, 10 HEPES, 25 Glucose; pH 7.3, 323 mOsm. Patch pipettes had resistances between 3-4 MΩ when filled with intracellular solution composed of (in mM) 107.5 potassium gluconate, 32.5 KCl, 10 HEPES, 5 EGTA, 4 MgATP, 0.6 $Li_4GTP\gamma S$, 10 Tris phosphocreatine; pH 7.2, 297 mOsm. Series resistance (< 5 MΩ) was compensated by 80%. Kir3 responses induced by GTPγS were recorded with an Axopatch 200B patch-clamp amplifier (Molecular Devices, USA); filtering and sampling frequencies were set to 1 kHz and 5 kHz, respectively. Data analyses were done with pClamp 10 (Molecular Devices, USA). Data are given as mean ± SD. Statistical significance was assessed using t-test. SR was dissolved in intracellular solution at a final concentration of 10 μM. Before the recording, CHO cells were preincubated in the extracellular solution with or without the drug for 45 minutes at room temperature (22 - 24°C).

Chapter 3. Results

3.1 Effect of SR on G-protein activity in native and recombinant systems

3.1.1 SR inhibits G-protein basal activity in rat cortical and striatal membranes

As shown in Fig. 12, SR dose-dependently, and significantly reduced the basal activity of [^{35}S]GTPγS with a potency of 3.9 ± 0.45 μM (IC_{50}), reaching maximal inhibition (Imax, approximately 48%) at 100 μM in the rat cortical membranes (A). In striatal membranes, non-linear regression analysis of SR concentration-response curves showed that maximal inhibition of basal [^{35}S]GTPγS activity was 60% and half-maximal inhibition was obtained at 3.67 ± 0.5 μM (B).

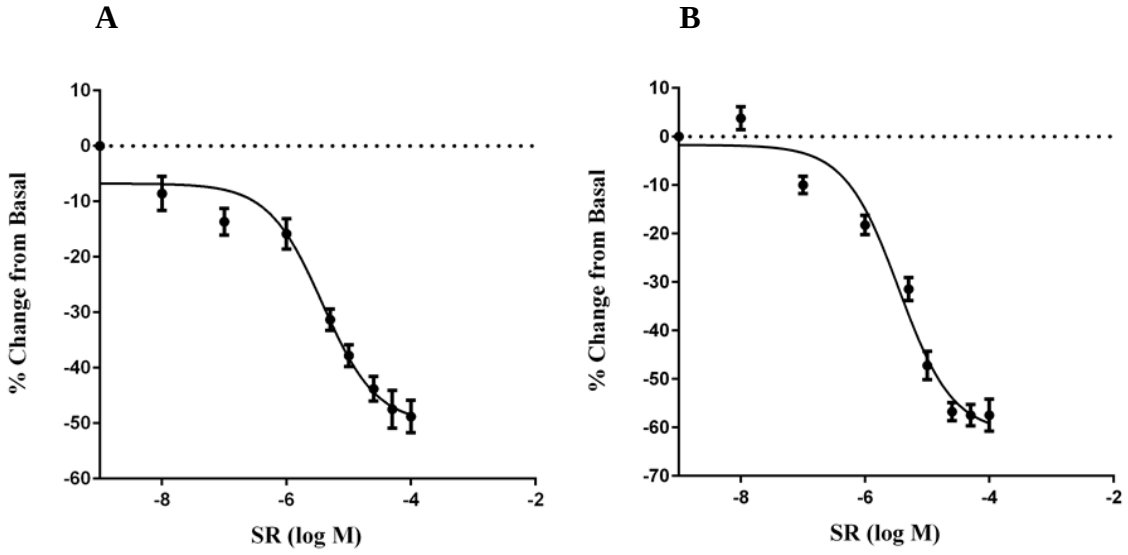

Figure 12. Effect of SR on basal [^{35}S]GTPγS binding in rat cortical membranes (A) and striatal membranes. (B) Tissue membranes were incubated with increasing concentrations of SR as described in the Materials and Methods Section. Data are mean ± SEM values of at least three independent experiments performed in triplicate, expressed as percent change from basal activity, binding in the absence of ligands being defined as 0. SR: SR141716A.

3.1.2 SR inhibits G-protein basal activity in cortical membranes of CB1-KO and WT mice

To determine whether the effect of SR on basal [^{35}S]GTPγS binding was mediated by CB1 receptors, a range of concentrations of SR was used in membrane prepared from tissue cortex of WT and CB1-KO mice. As shown in Fig. 13A, SR produced a concentration-dependent and saturable inhibition of [^{35}S]GTPγS binding in the cortex of WT mice with an IC_{50} of 12.56 ± 2.12 μM, and an Imax of 38% on basal activity. A similar concentration of SR, 12.66 ± 2.12 μM, was required for half-maximal inhibition of [^{35}S]GTPγS binding in cortex of CB1-KO mice, as illustrated in Fig. 13B. These results demonstrated that the inhibitory effect of SR on basal [^{35}S]GTPγS binding in the mouse cortex is CB1 receptor-independent.

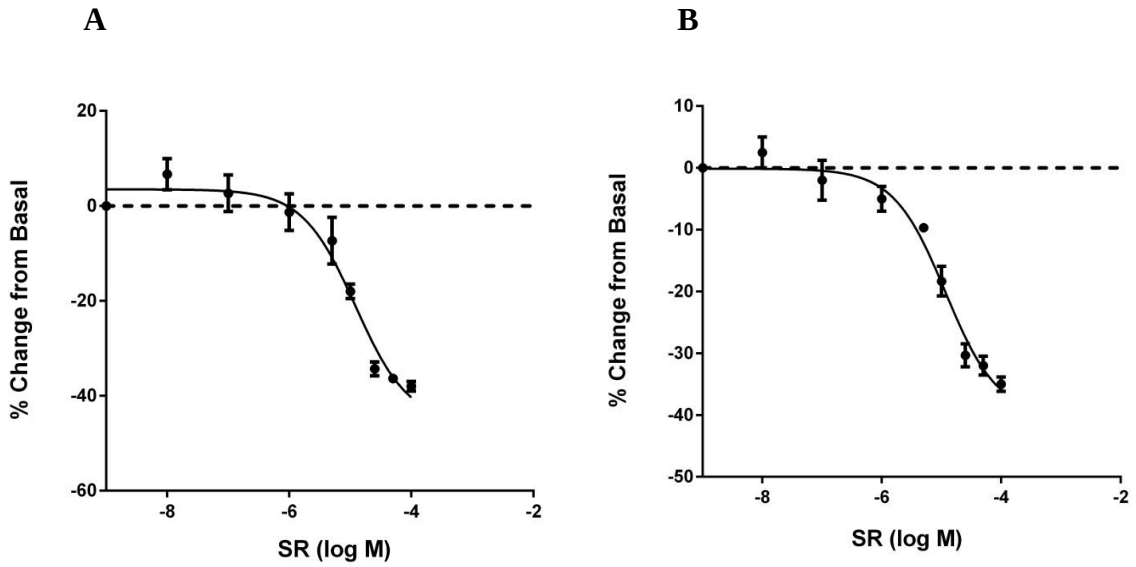

Figure 13. Effect of SR on basal [^{35}S]GTPγS binding in cortical membranes of WT (A) and CB1-KO mice (B). Tissue membranes were incubated with 0.05 nM [^{35}S]GTPγS and 30 μM of GDP and increasing concentrations of SR as described in the Materials and Methods Section. Data are mean ± SEM values of at least three independent experiments performed in triplicate, expressed as percent change from basal activity, binding in the absence of ligands being defined as 0. CB1-KO CB1 knockout mice; SR: SR141716A.

3.1.3 SR inhibits basal G-protein activation in cortical membrane of $GABA_B$-KO and WT mice

To determine whether the effects of SR on basal [^{35}S]GTPγS binding were mediated by other GPCRs mostly coupled to the inhibitory subunit $G_{i/o}$ (i.e. $GABA_B$ receptors), SR concentration-response curves were performed in rat cortical membranes of $GABA_B$-KO mice and their WT counterparts. SR reduced the basal activity of [^{35}S]GTPγS binding with a potency of 4.3 ± 1.2 μM, achieving maximal inhibition (approximately 48%) at 100 μM in WT mice cortical membranes (Fig. 14A). In $GABA_B$-KO mice, non-linear regression analysis of SR concentration-response curve showed that maximal inhibition of basal [^{35}S]GTPγS activity was 45% and half-maximal inhibition was obtained at 3.9 ± 0.8 μM, as shown in Fig. 14B. Thus, the inhibitory effect of SR on basal [^{35}S]GTPγS binding was independent from $GABA_B$ receptors as it was observed both in WT and $GABA_B$-KO mice.

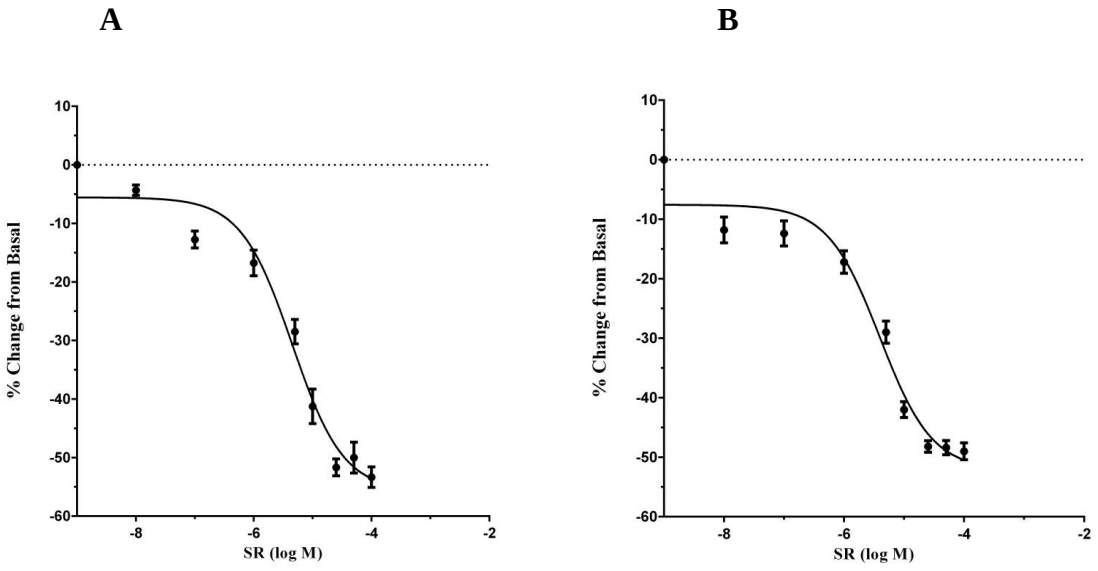

Figure 14. Effect of SR on basal [^{35}S]GTPγS binding in cortical membranes of wild-type (WT) and GABA$_B$-KO mice. Effect of SR141716A on basal GTPγS binding in WT (A) and in GABA$_B$-KO (B) mice cortical membranes. Proteins were incubated with 0.1 nM [^{35}S]GTPγS and 30 μM of GDP and varying concentrations of SR as described in the Materials and Methods Section. Data are mean ± SEM values of at least three independent experiments performed in triplicate, expressed as percent change from basal activity, binding in the absence of ligands being defined as 0. GABA$_B$-KO: GABA$_B$ knockout mice; SR: SR141716A.

3.1.4 SR inhibits G protein basal activity in CHO-GABA$_B$, CHO-D2 and in parental CHO-K1 cells

Rat and mouse tissue membrane preparations contained a heterogeneous mixture of receptors, where receptor-receptor interactions (hetero-oligomerization, cross-talk, etc.) might occur. To exclude this possibility, we examined the mechanism of action of SR by using membrane preparations from CHO-K1 cells stable transfected either with GABA$_B$ receptors or D2 receptors, thereby containing a homogeneous population of receptors (GABA$_B$ or D$_2$).

SR in a concentration-dependent manner significantly reduced the basal activity of [^{35}S]GTPγS with a potency of 8.9 ± 1.1 μM, achieving maximal inhibition (approximately 28%) at 100 μM in CHO GABA$_B$ membranes (Fig. 15A), and a potency of 9.7 ± 4.6 μM in CHO-D2 membranes and at 100 μM a maximal inhibition of 15% (Fig. 15B).

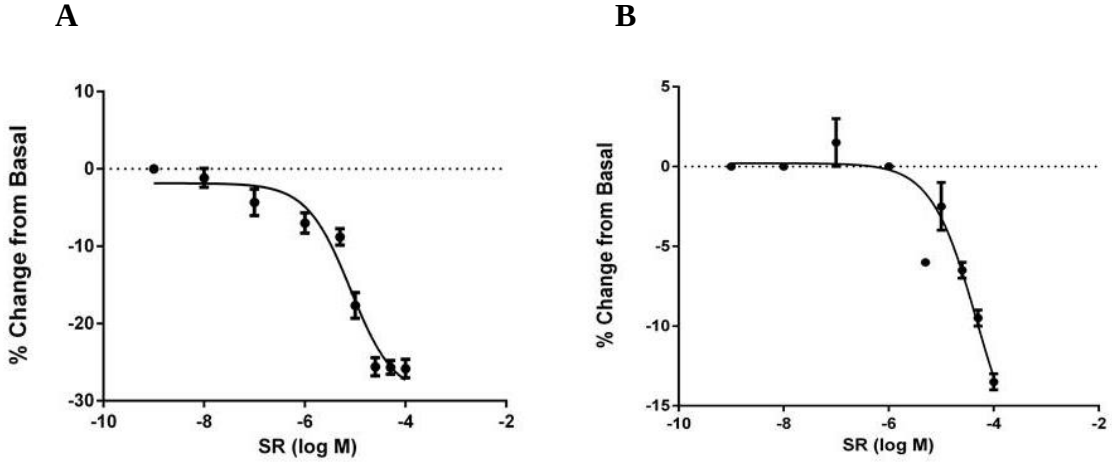

Figure 15. Effect of SR on basal [^{35}S]GTPγS binding in CHO-GABA$_B$ (A) and CHO-D2 membranes (B). SR inhibited basal GTPγS binding in CHO-GABA$_B$ (A) and CHO-D2 membranes (B). Tissue membranes were incubated as described in the Materials and Methods section. Data are mean ± SEM values of at least three independent experiments performed in triplicate, expressed as percent change from basal activity, binding in the absence of ligands being defined as 0. SR: SR141716A.

Finally, to evaluate the effects of SR on G protein activity in a system devoid of receptors we investigated the effect of SR on [^{35}S]GTPγS basal activity in not transfected parental CHO-K1 cell membranes. According to our results in native systems, in parental CHO-K1 cells increasing concentrations of SR reduced the basal activity of [^{35}S]GTPγS with a potency of 5.1± 1.3 μM, reaching maximal inhibition (approximately 25%) at 100 μM (Fig. 16).

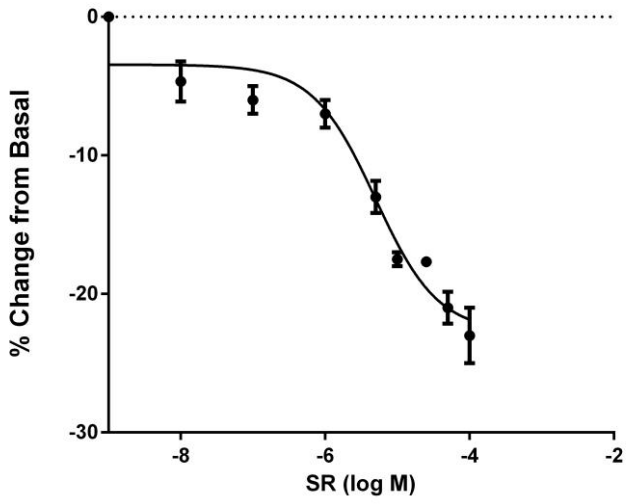

Figure 16. Inhibition of basal G protein by SR using [^{35}S]GTPγS binding assay in parental CHO-K1 cells. SR dose-dependently, saturable, and significantly reduced the basal activity of [^{35}S]GTPγS in a concentration dependent manner in parental CHO-K1 cells. Data are mean ± SEM values of at least three independent experiments performed in triplicate, expressed as percent change from basal activity, binding in the absence of ligands being defined as 0. SR: SR141716A.

3.1.5 Effects of SR on CB1 receptor G protein activity in [^{35}S]GTPγS binding assay

Consistently with a CB1 receptor agonist profile, WIN at 10 μM stimulated the binding of [^{35}S]GTPγS in rat cortical membranes up to 164% of the basal activity. This effect was mediated via CB1 receptors, since it was blocked by co-application of 0.1 μM of AM251 (a CB1 receptor antagonist-inverse agonist).

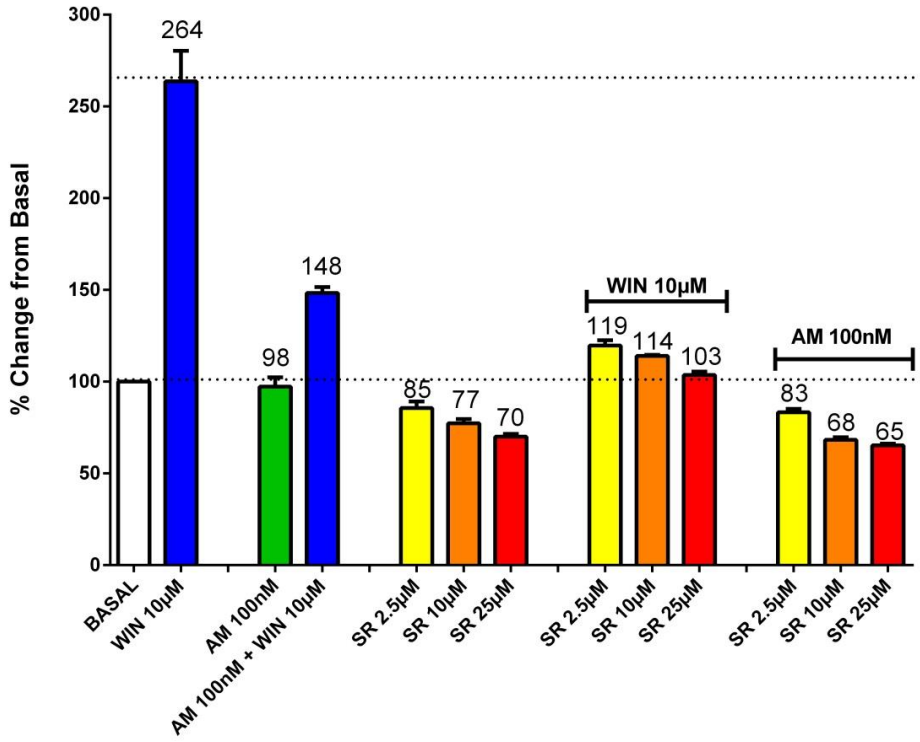

Figure 17. Effects of SR on [^{35}S]GTPγS binding in native CB1 receptors. SR at 2.5, 10 and 25 μM was tested alone or in combination with WIN, a CB1 receptor agonist, or its respective competitive/inverse antagonist AM251, utilizing 0.05 nM [^{35}S]GTPγS and 30 μM of GDP in rat cortical membranes. Data are mean ± SEM of at least four independent experiments performed in triplicate, and expressed as percentage of basal activity, binding in the absence of ligands being defined as 100%. Horizontal dotted lines indicate baseline values and the degree of stimulation with agonist alone, respectively. Numbers above the columns represent the percentage of stimulation or inhibition of [^{35}S]GTPγS binding relative to basal activity. AM: AM251, SR, SR141716A; WIN, WIN55212-2.

SR by itself at 2.5 μM, 10 μM and 25 μM, decreased the G protein basal activity (-15%, -23%, -30%, respectively) and this effect was not reversed by 0.1 μM of AM251 (-17%, -32%, 35%). SR in a concentration-dependent manner antagonized the G protein stimulation induced by WIN 10 μM; at a concentration of 25 μM, it completely blocked the activity of G protein, thus acting as a CB1 receptor antagonist (Fig. 17).

3.1.6 Effects of SR on $GABA_B$ and D2 receptors G protein activity in [^{35}S]GTPγS binding assay

To evaluate whether SR inhibits G protein activity acting on different GPCRs, we performed [^{35}S]GTPγS binding assay in different tissue preparations containing various receptor populations, i.e. cortical, striatal rat membrane homogenates.

As expected, baclofen at 10 μM stimulated [^{35}S]GTPγS binding to rat cortical membranes up to 43% of the basal activity. This effect was mediated via $GABA_B$ receptors, since it was blocked by CGP54626, a competitive antagonist of the $GABA_B$ receptor. SR itself at 2.5, 10 and 25 μM, significantly decreased the G protein basal activity (-12%, -26%, -36%, respectively) and its inhibitory effect was not blocked by 30 μM of CGP54626. Unexpectedly SR (10 and 25 μM) also antagonized the baclofen-induced activation of G proteins (Fig. 18A).

As shown in Fig. 18B, quinpirole at 1 mM stimulated the binding of [^{35}S]GTPγS to striatal membranes up to 20% of the basal activity, this effect being completely blocked by the D2 receptor competitive antagonist L-sulpiride (10 μM). SR alone (2.5 μM, 10 μM and 25 μM) and in combination with 10 μM of L-sulpiride, decreased the G protein basal activity in a concentration-dependent manner (-24%, -35%, -46%, respectively).

Finally, at the highest concentration tested SR completely antagonized G-protein stimulation induced by quinpirole.

A

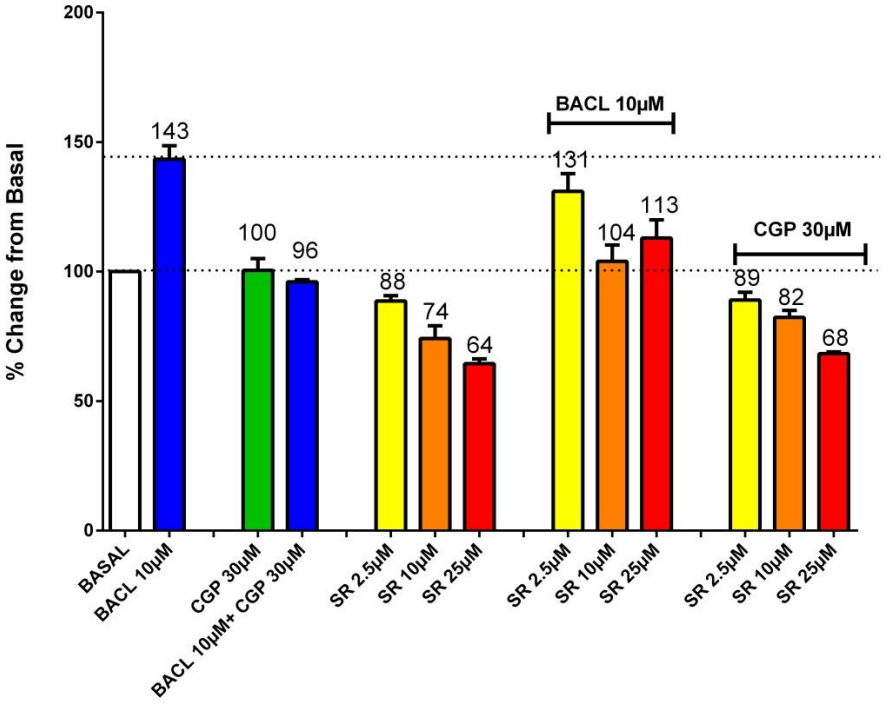
% Change from Basal
200
150
100
50
0
143
100
96
88
74
64
131
104
113
89
82
68
BACL 10µM
CGP 30µM
BASAL
BACL 10µM
CGP 30µM
BACL 10µM+ CGP 30µM
SR 2.5µM
SR 10µM
SR 25µM
SR 2.5µM
SR 10µM
SR 25µM
SR 2.5µM
SR 10µM
SR 25µM

B

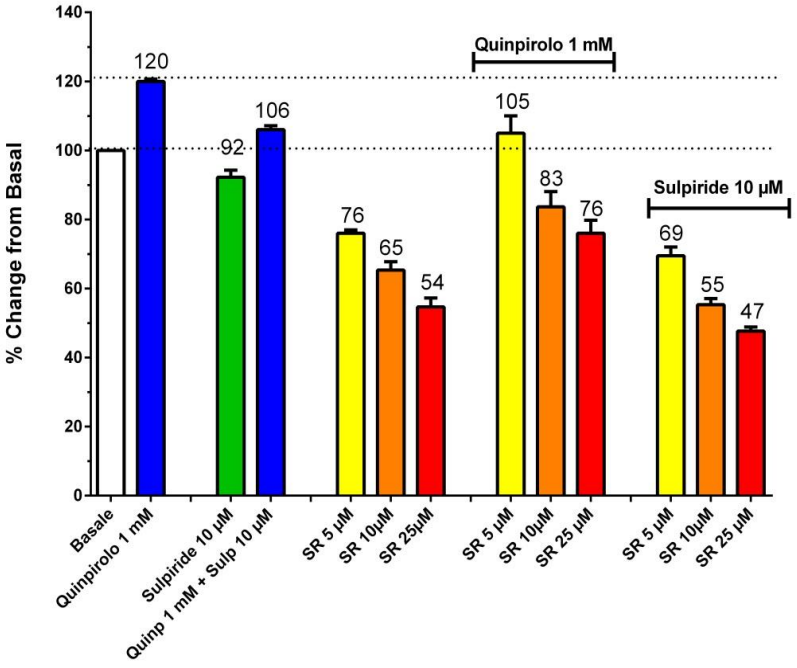
% Change from Basal
140
120
100
80
60
40
20
0
120
92
106
76
65
54
105
83
76
69
55
47
Quinpirolo 1 mM
Sulpiride 10 µM
Basale
Quinpirolo 1 mM
Sulpiride 10 µM
Quinp 1 mM + Sulp 10 µM
SR 5 µM
SR 10µM
SR 25µM
SR 5 µM
SR 10µM
SR 25 µM
SR 5 µM
SR 10µM
SR 25 µM

Figure 18. Effects of SR on [^{35}S]GTPγS binding in native $GABA_B$ (A) and D2 (B) receptors. SR was tested alone or in combination with baclofen or quinpirole, respectively $GABA_B$ and D2 receptor agonists, or their respective competitive antagonists, CGP54626 and L-sulpiride, utilizing 0.2 nM [^{35}S]GTPγS and 30 μM of GDP in rat cortical membranes (A), and 0.1 nM [^{35}S]GTPγS and 300 μM of GDP in striatal membranes (B). Horizontal dotted lines indicate baseline values and the degree of stimulation with agonist alone. Data are mean ± SEM of at least three independent experiments performed in triplicate, and expressed as percentage of basal activity, binding in the absence of ligands being defined as 100%. The numbers above the columns represent the percentage of stimulation or inhibition of GTPγS binding relative to basal activity. BACL: baclofen; CGP: CGP54626; SR: SR141716A; Quinp: quinpirole; Sulp:Sulpiride.

3.1.7 SR inhibits agonist-stimulated [^{35}S]GTPγS binding in rat cortical and striatal membranes

The [^{35}S]GTPγS assay measures the level of G protein activation after agonist stimulation allowing to determine pharmacological ligand parameters such as potency and efficacy. Baclofen concentration-response curves were performed in the absence and in the presence of different fixed concentration of SR (0.1 μM, 1 μM and 5 μM). As shown in Fig. 19A, baclofen stimulated [^{35}S]GTPγS binding in a concentration-dependent manner with an EC_{50} value of 10.26 ± 1.2 μM and a maximal stimulation of 188.3 ± 10.4%. Increasing the fixed concentrations of SR induced a rightward shift of the baclofen concentration-response curve with a concomitant significant decrease of maximal stimulation induced by baclofen. Thus, in the presence of 5 μM of SR, the EC_{50} for baclofen increased by 2-fold (23.08 ± 4.3 μM) and the Emax was 157.8 ± 6.7% over basal value (-17% versus Emax of baclofen).

SR induced a more strong effect on quinpirole-stimulated [^{35}S]GTPγS binding in striatal membranes. As shown in Fig. 19B, SR (1 μM and 5 μM) significantly shifted to right the stimulation curve induced by quinpirole. The EC_{50} for quinpirole increased by approximately 18 and 24 fold in the presence of SR at 1 μM and SR 5 μM, respectively. Moreover, the

maximal efficacy induced by quinpirole in the presence of 1 µM and 5 µM of SR was significantly ($p<0.0001$) reduced (122 ± 2.6% and 108 ± 2.6% over basal value).

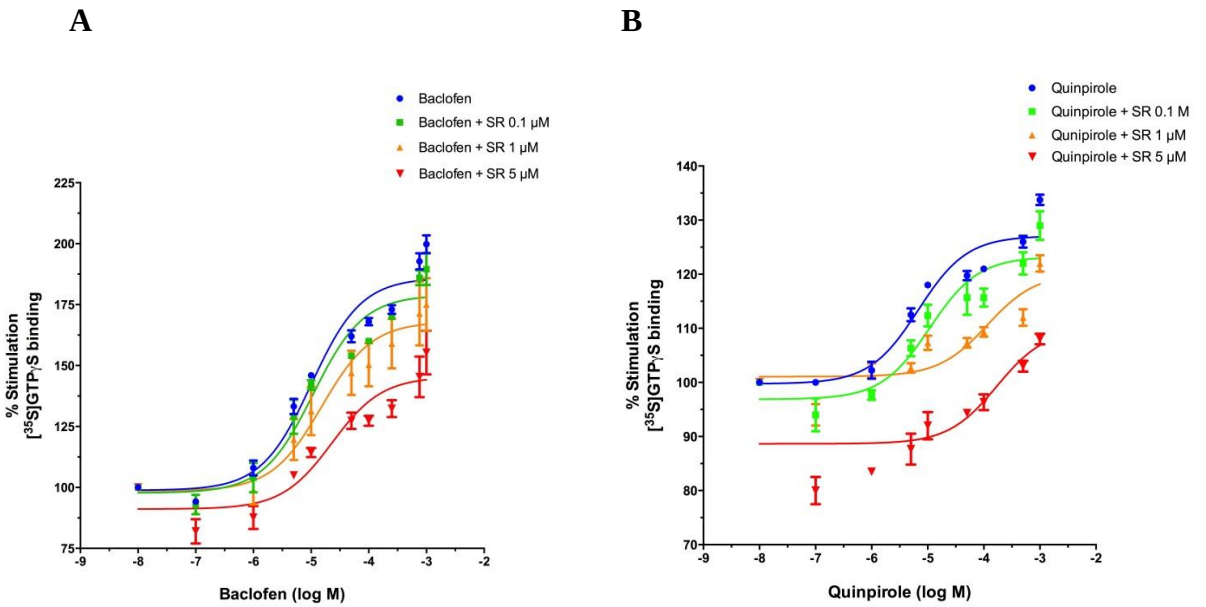

Figure 19. Effect of SR on agonist-stimulated [^{35}S]GTPγS binding to rat cortical (A) and striatal (B) membranes. Concentration-response curves for baclofen (A) and quinpirole (B) in the [^{35}S]GTPγS binding assay, in the absence (●) and presence of SR (■: 0.1 µM; ▲: 1 µM; ▼ 5 µM). (A) EC_{50} and Emax, baclofen: 10.26 ± 1.2 µM and 188.3 ± 10.4%; baclofen + SR 0.1 µM: 14.96 ± 4.1 and 183.7 ± 6.9%; baclofen + SR 1 µM: 19.5 ± 3.3 and 156.3 ± 8.9 ; baclofen + SR 5 µM: 23.08 ± 1.2 and 152.8 ± 5.7 ; (B) EC_{50} and Emax, quinpirole: 6.96 ± 1.07 µM and 134.1 ± 0.7% ; quinpirole + SR 0.1 µM: 10.86 ± 2.4 µM and 129 ± 4.2%; quinpirole + SR 24 ± 8.6 µM and 122.4 ± 3.8%, quinpirole + SR 5 µM 70 ± 2.7 µM and 108.3 ± 1.0%. Data are from a typical experiment performed in triplicates, expressed as percent stimulation over basal activity, binding in the absence of ligands being defined as 100%. SR:SR141716A.

Moreover, increasing concentrations of SR in the presence of fixed concentrations of baclofen decreased its agonistic effect with IC_{50} values in the micromolar range. Specifically, in the presence of a submaximal (10 µM) (Fig. 20A) or a saturating concentration (100 µM) of

baclofen (Fig. 20B), SR inhibited baclofen-stimulated GTPγS binding with an IC_{50} of 11.6 ± 1.60 μM and of 11.50 ± 1.70 μM, reaching a maximal inhibition of 58 ± 2.32% and 62 ± 0.3%, respectively.

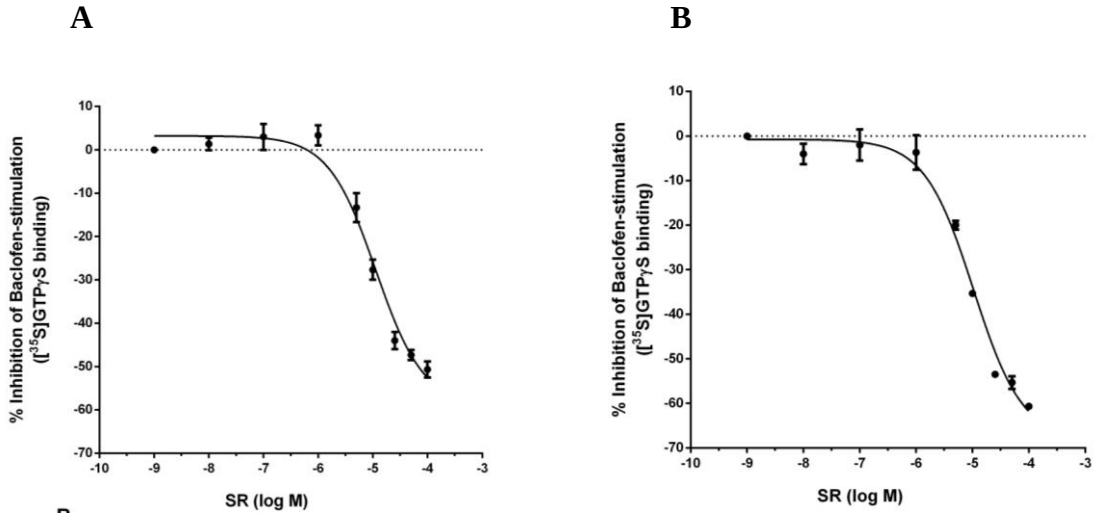

Figure 20. Effects of SR on baclofen-induced [^{35}S]GTPγS binding in membranes from rat cortex. The inhibiting effect of SR was measured at two fixed concentrations of baclofen, 10 μM (A) and 100 μM (B). Horizontal dotted lines indicate the levels of stimulation obtained by either a submaximal (10 μM) or a saturating concentration (100 μM) of baclofen alone. Data are from a typical experiment performed in triplicates, expressed as percent inhibition of either 10 or 100 μM baclofen-stimulated [^{35}S]GTPγS binding, being defined as 0%.

3.1.8 SR inhibits baclofen-stimulated [^{35}S]GTPγS binding in CB1-KO mice

To further evaluate whether CB1 receptors mediate the effect of SR on baclofen-stimulated G protein activation, baclofen concentration-response curves were performed in CB1-KO mice cortical membranes. As shown in Fig. 21, baclofen stimulated [^{35}S]GTPγS binding in a concentration-dependent manner with an EC_{50} value of 6.0 ± 1.78 μM and an Emax of 143.7 ± 1.66%. In the presence of a fixed concentration of SR (5 μM) the agonistic potency of

baclofen was reduced by 2 fold (EC_{50}: 9.98 ± 0.58 µM) and the efficacy decreased by approximately 15-20% with an Emax of 121.3 ± 1.2%, suggesting that the inhibitory effect of SR on G-protein activation was likely CB1 receptor–independent.

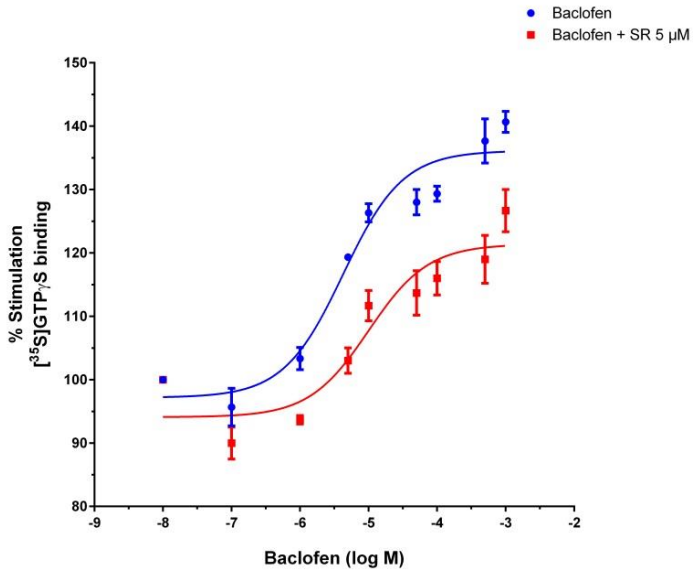

Figure 21. Effect of SR on baclofen-stimulated G protein activity in cortical membranes of CB1-KO mice. [^{35}S]GTPγS binding assay was performed as described in the Materials and Methods section, utilizing 0.2 nM [^{35}S]GTPγS and 30 µM of GDP and increasing concentrations of baclofen in the presence or absence of 5 µM SR. Data are mean ± SEM values of at least three independent experiments performed in triplicate, expressed as percent change from basal activity, binding in the absence of ligands being defined as 100. CB1-KO: CB1 knockout mice; SR: SR141716A.

3.1.9 Effect of SR on [^{3}H]CGP54626 binding in rat cortical membranes

SR up to a concentration of 1 mM failed to modify [^{3}H]CGP54626 binding, whereas CGP54626 caused complete inhibition of the specific binding of the competitive antagonist of the $GABA_B$ receptor [^{3}H]CGP54626 with an IC_{50} of 3.0 ± 0.09 nM (Fig. 22). These data demonstrated that SR did not bind to the orthosteric binding site of the $GABA_B$ receptors.

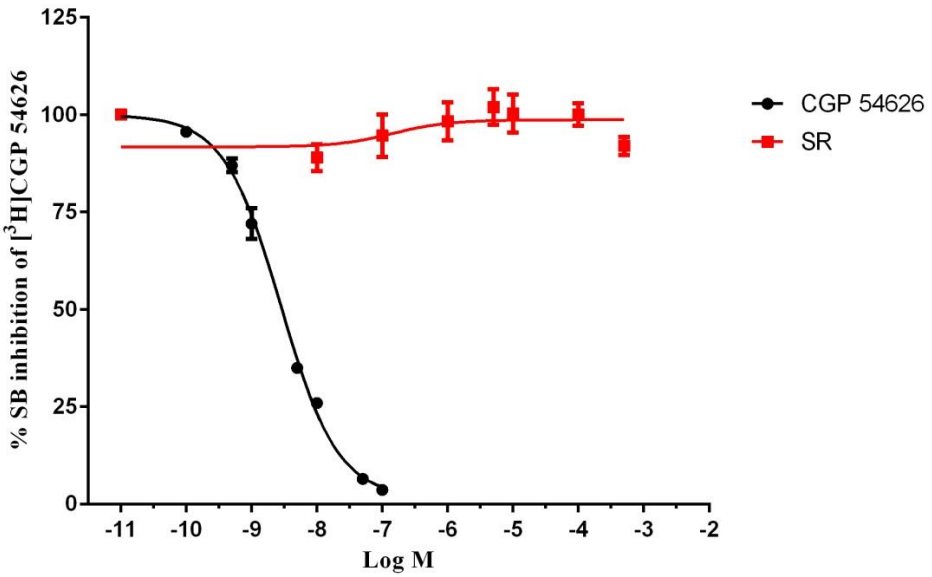

Figure 22. Displacement curves of **[^{3}H]CGP54626** by SR and CGP5462 in rat cortical membranes. Binding experiments were performed as described in the Materials and Methods section. Cortical rat membranes were incubated in the presence of 3 nM of [^{3}H] CGP54626 (85 Ci/mM) with serial dilutions ranging from 10-11 to 10-4 M of the unlabelled compounds. Data represent a typical experiment out of three independent experiments, expressed as percentage of specific binding (SB). The calculation of IC_{50} was performed by non-linear curve fitting of the concentration-effect curves using Graphpad Prism Program. The F-test was used to determine the best approximation of a non-linear curve fitting to one or two site model ($p<0.05$). SR: SR141716A.

3.2 Effect of SR on G protein subunits rearrangements

3.2.1 SR stabilizes the constitutive state of G protein in CHO-$GABA_B$ expressing $G\alpha_o$-Rluc and $G\gamma_2$-Venus

To understand SR molecular mechanism on G protein inhibition, BRET approach was used to monitor dissociation between $G\alpha_o$ and $G\beta\gamma$ subunits and their conformational rearrangements before and after $GABA_B$ receptors activation.

BRET signal was measured before receptor stimulation, to observe the effect of SR on G protein basal activity. As shown in Fig. 23, SR increased significantly the basal BRET signal measured between $G\alpha_o$-Rluc and $G\gamma_2$-Venus subunits, in a concentration dependent manner. These data suggested that SR stabilizes the constitutive formation of the $G\alpha\beta\gamma$ trimer, independently from receptor activation.

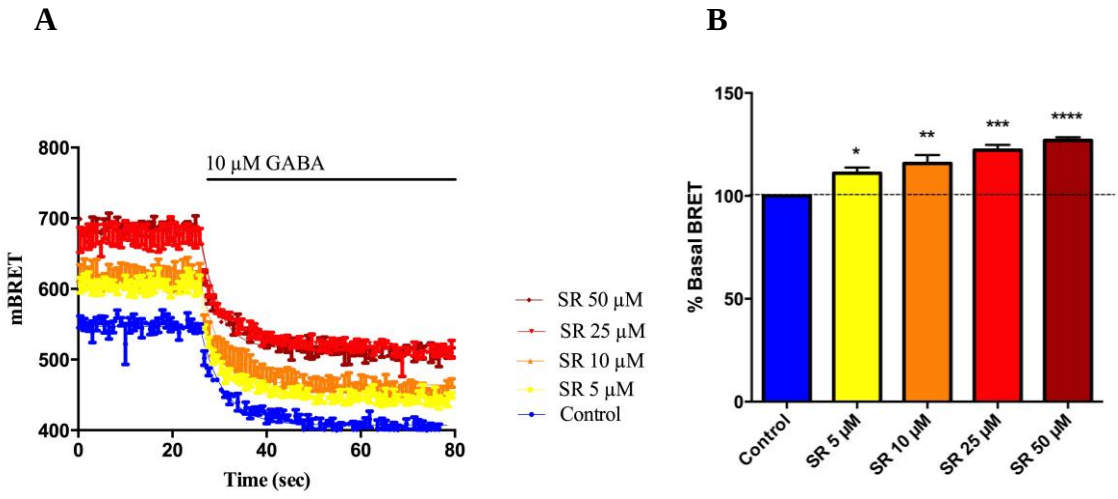

Figure 23. Modulation of basal BRET by SR in CHO cells expressing $GABA_B$ receptor and Gαo-Rluc, Flag-Gβ2 and Gγ2-Venus. (A) SR-induced changes in the basal BRET signal before GABA application, indicating its effect on G protein basal activity. The curves were fitted with Plateau followed by one-phase decay equation using Prism GraphPad software. (B) Bar graph of the change in basal BRET ratio determined in

experiments as in (A). Data are presented as a mean ± SEM of 6 experiments. *p<0.05, **p<0.01, ***p<0.001,****p<0.0001 vs Control, Bonferroni test. SR: SR141716A.

In order to evaluate the effect of SR on G protein dissociation following $GABA_B$ receptor activation, ΔBRET was calculated as the difference between the basal and the plateau of BRET signal, indicating the amount of $GABA_B$-mediated G protein dissociation.

During $GABA_B$ receptor activation by 10 µM of GABA, SR induced a significant decrease (at 25 µM and 50 µM) in ΔBRET, as shown in Fig. 24. The effect of SR on the agonist-induced change in BRET between $G\alpha_o$-Rluc and $G\gamma_2$-Venus was concentration-dependent. Taken together, these results indicated that SR stabilizes the G protein trimeric state and inhibited the molecular rearrangement between $G\alpha_o$ and $G\beta\gamma$ subunits when the $GABA_B$ receptor is activated.

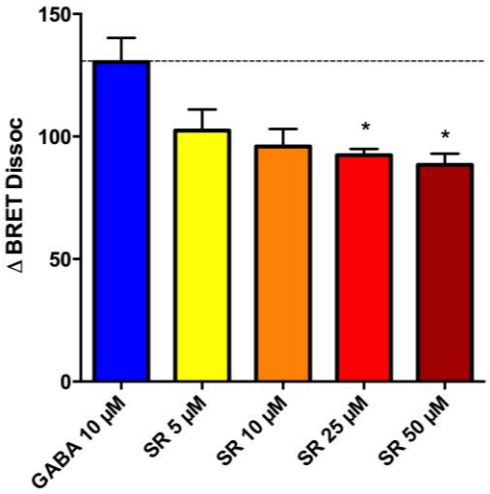

Figure 24. Modulation of signal BRET by SR in CHO cells expressing $GABA_B$ receptor and $G_{\alpha o}$-Rluc, Flag-$G\beta_2$ and $G\gamma_2$-Venus. Bar graph of the change in BRET ratio determined in experiments showed that SR decreased the BRET ratio during G protein activation, indicating a rearragement of Gαo-Rluc and Gγ-Venus. Data are presented as a mean ± SEM of 6 experiments. *p<0.05 vs GABA, Bonferroni test. SR: SR141716A.

3.2.2 SR induces a rearrangement between the D2 receptor and the G protein

In order to investigate more in depth the effects of SR on the molecular interaction between the D2 receptor and the G protein, different constructs were created for $G\alpha_{i1}$, with Venus tag inserted in connecting loops on opposite ends of the helical domains (Fig. 25). One Venus was inserted in the loop connecting helices A and B ($G\alpha_{i1\text{-}91}$); the second was inserted in the loop connecting helices B and C ($G\alpha_{i1\text{-}121}$). Previous studies have shown that these tags do not have any effect on biochemical and catalytic properties of these fusion proteins (Gales et al., 2006). The third Venus was introduced in the linker 1 region connecting the helical and GTPase domains of $G\alpha_{i1}$ subunit ($G\alpha_{i1\text{-}60}$).

To monitor conformational change between $G\alpha_{i1}$ and D2 receptor, Rluc was fused to receptor C-terminal (Fig. 25). These positions were chosen based on the $G\alpha\beta\gamma$ complex crystal structure and were already used in several studies (Gales et al., 2006, Ayoub et al., 2009), showing correct expression and efficient coupling with different receptors.

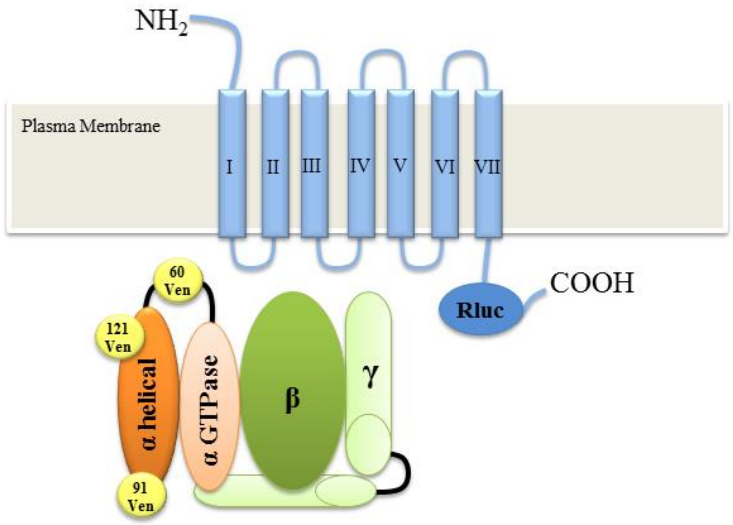

Figure 25. Schematic representation of G protein and receptor BRET fusion proteins. Rluc probe in D2 receptor is shown in blue and Venus probes on G α_{i1} subunits are shown in yellow.

Basal BRET signal was detected between the D2 receptor (D2-Rluc) and each of $G\alpha_{i1}$-Venus protein subunits ($G\alpha_{i1\text{-}60}$, $G\alpha_{i1\text{-}91}$ and $G\alpha_{i1\text{-}121}$), after 1h incubation of SR.

As shown in Fig. 26, SR increased BRET signal between D2-Rluc and $G\alpha_{i1\text{-}91}$-Venus and between D2-Rluc and $G\alpha_{i1\text{-}121}$-Venus. However, no effect was observed between D2-Rluc and $G\alpha_{i1\text{-}60}$-Venus in the presence of SR (25 μM). This lack of changes in the BRET signal did not result from disruption of fusion protein activity, since quinpirole application induced G protein dissociation detected for all of three different constructs, confirming their functionality. Moreover, differences in the basal BRET signal between all of three fusion proteins were not due to the difference in the expression level quantified by fluorescence measurements.

Using this model, the changes in the basal BRET signal observed with SR might reflect a rearrangement on constitutive receptor-$G\alpha\beta\gamma$ complex, which is consistent with the increase in basal BRET observed between $G\alpha_o$-Rluc and $G\gamma_2$-Venus.

Together, the SR-promoted BRET changes support the hypothesis that the Gα subunit might be the direct target of this compound.

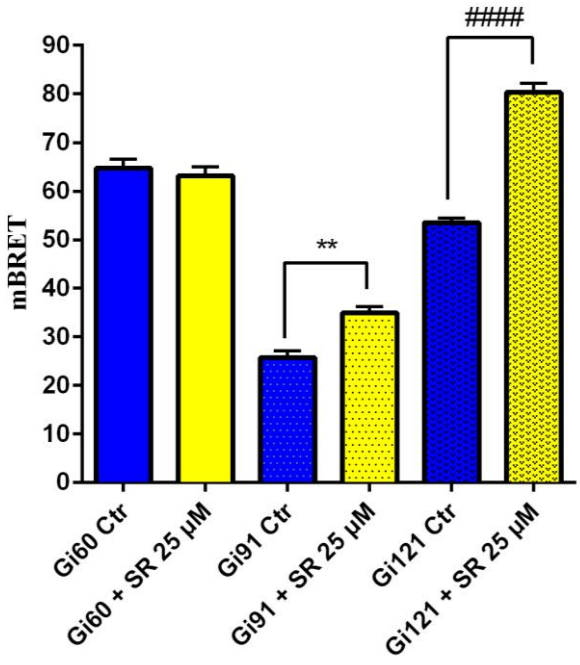

Figure 26. Effect of SR on $G\alpha_{i1}$ subunit and D2 receptor rearrangement. Differences in BRET signals observed between specified $G\alpha_{i1}$ subunits and D2 receptor, in the presence and absence of 25 µM of SR. Data are presented as a mean ± SEM of 5 experiments. **p<0.01 vs Gi91 Ctr, ####p<0.0001 vs Gi121 Ctr, Bonferroni test.

3.3.2 SR induces a conformational change on G protein subunits independently from the receptor

To investigate whether SR can induce BRET changes between G protein subunits independently from the receptor, other constructs were used. The Rluc tag was inserted in the C-terminal of Gβ and Gγ subunits (Fig. 27). The introduction of these new tags in Gβγ dimer has been shown not to affect its functional properties (Gales et al., 2006).

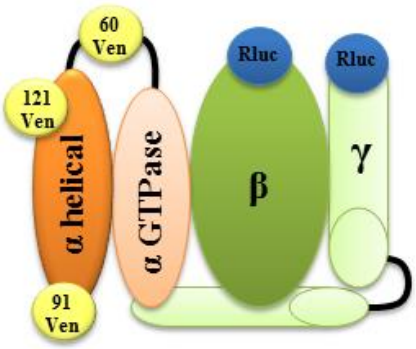

Figure 27. Schematic representation of the different tags on the G protein subunits. Rluc probes in Gβ and in Gγ C-terminal are shown in blue and Venus probes on $G\alpha_{i1}$ subunit are shown in yellow.

BRET signal was detect between $G\alpha_{i1}$ protein subunits ($G\alpha_{i1\text{-}60}$-Venus, $G\alpha_{i1\text{-}91}$-Venus and $G\alpha_{i1\text{-}121}$-Venus) and $G\beta_1$-Rluc or $G\gamma_2$-Rluc subunits after 1h incubation of SR.

As shown in Fig. 28A, SR significantly increased BRET signal between $G\beta_1$-Rluc and $G\alpha_{i1\text{-}91}$Venus, and between $G\beta_1$-Rluc and $G\alpha_{i1\text{-}121}$-Venus. Similar results were obtained measuring the basal BRET signal between $G\alpha_{i1\text{-}91}$-Venus or $G\alpha_{i1\text{-}121}$-Venus and $G\gamma_2$-Rluc (Fig. 28B).

As previously observed using Rluc tag on D2 receptor, no effect was detected between $G\alpha_{i1\text{-}60}$-Venus and $G\beta_1$-Rluc or $G\gamma_2$-Rluc in the presence of SR (25 µM).

The BRET changes monitored when using $G\alpha_{i1\text{-}91}$-Venus and $G\alpha_{i1\text{-}121}$-Venus as BRET acceptors probably reflect a SR-promoted conformational rearrangement within Gαβγ complex that is differentially monitored depending on the acceptor and donor position.

The absence of change in the BRET signal using the $G\alpha_{i1\text{-}60}$Venus might be due to a possible interaction between SR and the linker 1 region, leading to a different movement of α helical.

These results confirm that SR induced conformational changes in the G protein heterotrimeric conformation independently from the receptor, suggesting that the Gα subunit might be the direct target of this compound, inducing rearrangement in the α-helical domain.

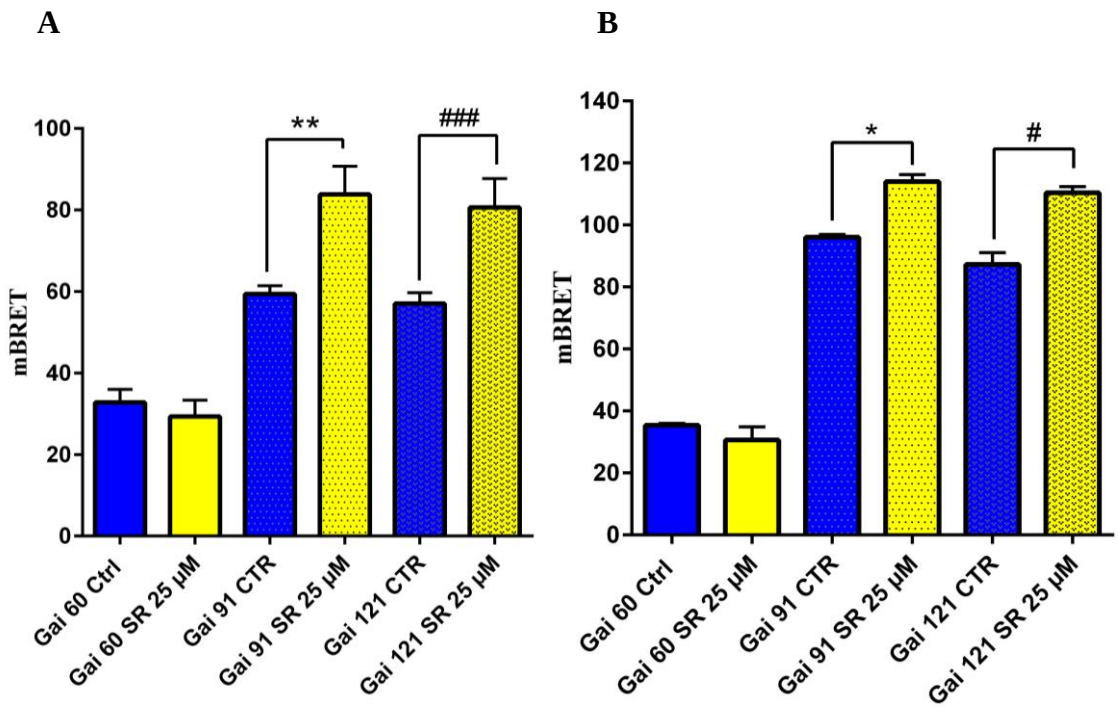

Figure 28. Effect of SR on $G\alpha_{i1}$ subunit and Gβγ rearrangement. Differences in BRET signals observed between specified $G\alpha_{i1}$ and Gβ subunits (A) and Gγ (B) in the presence and absence of 25 µM of SR. (B) Data are presented as a mean ± SEM of 5 experiments. **p<0.01 vs Gi91 CTR, $^{###}$p<0.001 vs Gai121 CTR, *p<0.05 vs Gai91 Ctr, $^{\#}$ p<0.05 vs Gai121 CTR, Bonferroni test.

3.3 Effects of SR on G protein subunits effectors

3.3.1 SR inhibits the agonist-mediated inhibition of Adenylate Cyclase activity

Recently, detection of the intracellular cAMP *in vivo* is become possible using BRET assay. Jiang et al. (2007) developed a sensor, known as CAMYEL (cAMP sensor using YFP-Epac-RLuc) that can be used to monitor cAMP intracellular formation in real time. Previous studies have employed this sensor to characterize distinct pathways, which modulate cAMP synthesis stimulated by Gs receptors.

Here, to identify whether SR induces effects on $G\alpha_{i/o}$ and/or $G\alpha_s$ protein pathway, CAMYEL sensor was transiently transfected together with $GABA_B$, dopamine D2, or dopamine D1 receptor. Changes in BRET ratio are used to continuously monitor intracellular cAMP in real time in living cells. First, forskolin application activates adenylate cyclase leading to a rapid elevation of cyclic cAMP that binds to CAMYEL. This leads to a conformational change resulting in a decrease of BRET signal.

The BRET signal was detected before and after $GABA_B$ receptor activation, induced by injection of GABA (100 μM). As expected GABA (100 μM) reverted the decrease of BRET signal induced by forskolin, indicating an inhibition of cAMP forskolin-induced. Importantly, SR at 50 μM decreased the GABA-induced BRET signal, attenuating the GABA inhibitory effect (Fig. 29A). Moreover, SR (25 and 50 μM) decreased significantly the tau of CAMYEL activation, which indicates a faster CAMYEL activation, and reduced ΔBRET. These results suggest that SR inhibited G proteins activation induced by $GABA_B$ receptors (Fig. 29, panels B and C).

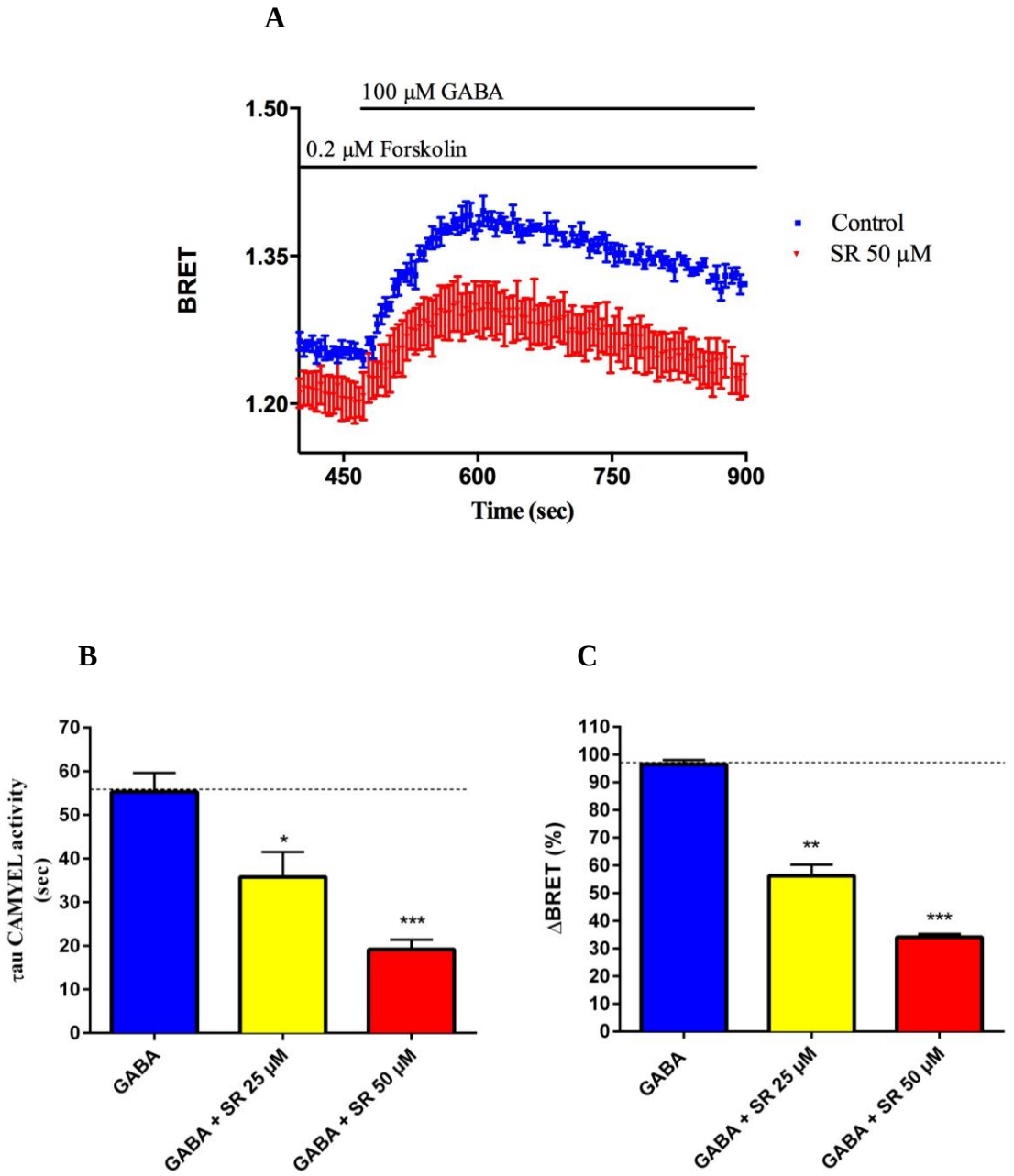

Figure 29. Effects of SR on CAMYEL activity in HEK293-GABA$_B$. (A) HEK293 cells transiently transfected with CAMYEL and GABA$_B$ receptor were incubated with SR (25 µM and 50 µM) for 1 h a 37°C. BRET measurements were performed after the addition of the substrate. Data represent the BRET ratio of YFP/Rluc for control and SR under GABA-stimulation conditions. The curves were fitted with One-phase association equation using Prism GraphPad software. (B) Bar graph of the amplitude-weighted mean time constant (tau CAMYEL activity) showed that SR increased CAMYEL activation, expressed as decrease of tau CAMYEL activity. Data are presented as a mean ± SEM of 5 experiments. *p<0.05 vs GABA, Bonferroni test. (C) Bar graph showed that

SR decreased the ΔBRET, calculated as the difference between the basal and the plateau of BRET signal. Data are presented as a mean ± SEM of 5 experiments. *p<0.05, **p<0.01, ***p<0.001vs GABA, Bonferroni test. SR: SR141716A.

As regard the D2 receptor, its agonist quinpirole stimulated the receptor thereby activating $G\alpha_{i/o}$ protein that inhibited the adenylate cyclase resulting in a decreased CAMYEL activity. After injection of quinpirole (10 µM), SR increased CAMYEL activation, expressed as decrease of tau CAMYEL activity, and decreased ΔBRET. Taken together these results showed that SR blocked the inhibitory effect of $G_{i/o}$-protein on cAMP production resulting in increase of CAMYEL activation (Fig. 30).

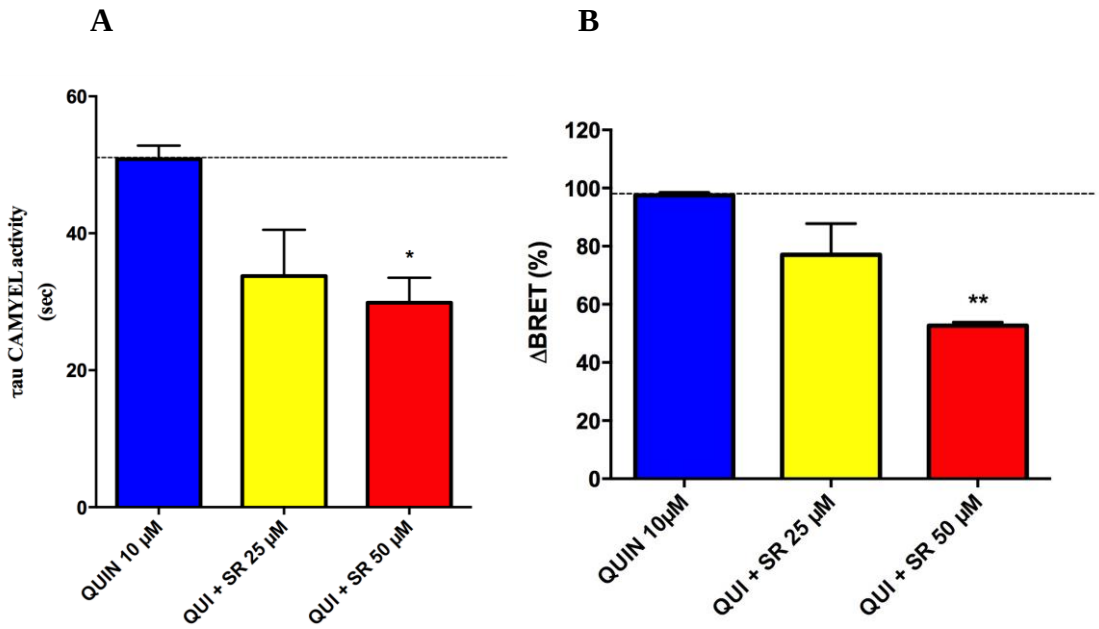

Figure 30. Effects of SR on CAMYEL activity in HEK293-D2. HEK293 cells transiently transfected with CAMYEL and D2 were incubated with SR (25 µM and 50 µM) for 1 h a 37°C. BRET measurements were performed after the addition of the substrate. (A) Bar graph of the amplitude-weighted mean time constant (tau CAMYEL activity) showed that SR increased CAMYEL activation, expressed as decrease of tau CAMYEL activity. Data are presented as a mean ± SEM of 5 experiments. *p<0.05 vs quinpirole, Bonferroni test. (B) Bar

graph showed that SR decreased the ΔBRET, calculated as the difference between the basal and the plateau of BRET signal. Data are presented as a mean ± SEM of 5 experiments. **p<0.001 vs quinpirole, Bonferroni test.

In the same way, we evaluated the effect of SR on G_s-coupled receptor stimulation. For this purpose, D1 receptor, which is coupled to G_s-protein, was transfected with CAMYEL, and the BRET signal was detected after dopamine injection.

As shown in Fig. 31, dopamine decreased the BRET signal through increase of cAMP and activation of CAMYEL sensor. In the presence of SR (50 µM), no effect was observed in the BRET signal, indicating that SR did not interact with $G\alpha_s$ subunit.

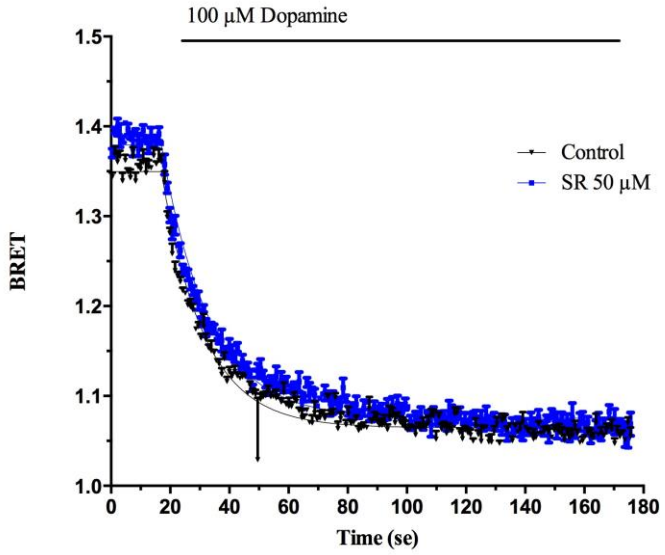

Figure 31. Effects of SR on CAMYEL activity in HEK293-D1. HEK293 cells transiently transfected with CAMYEL and D1 receptor were incubated with SR (50 µM) for 1 h a 37°C. BRET measurements were performed after the addition of the substrate. Data represent the BRET ratio of YFP/Rluc for control and SR under agonist-stimulation conditions. The curves were fitted with Plateau followed by one-phase decay equation using Prism GraphPad software. SR: SR141716A.

3.3.2 SR blocks GIRK channel activity in VTA slices

Whole cell voltage clamp recordings from midbrain dopamine neurons in acute rat brain slices *ex vivo* were performed to evaluate the effects of SR on baclofen and quinpirole-induced outward K^+ current. In order to establish whether SR acts independently from CB1 receptors, experiments were carried out using CB1-WT and -KO mice. As shown in Fig. 32A, baclofen application (10 μM) induced outward GIRK current activated by the $GABA_B$ receptor. However, when the slice was treated with SR (10 μM), baclofen induced current was completely blocked (Fig. 32B). Moreover, when D2 receptor was activated by quinpirole (1 μM), SR treatment (10 μM) blocked the D2-induced current as well (Fig. 32C).

Thereafter, to confirm that the blocking of $GABA_B$-mediated current is independent of CB1 receptor, CB1-KO mice were used. The CB1 receptor was not required for SR inhibition of $GABA_B$ induced current, since SR treatment blocked the $GABA_B$-induced GIRK current in CB1-KO mice similarly to the WT mice (Fig. 32D). These results demonstrate that by inhibiting G protein activation, SR blocked Gβγ effector systems, such as GIRK channel activation, and that this effect was not CB1 receptor mediated.

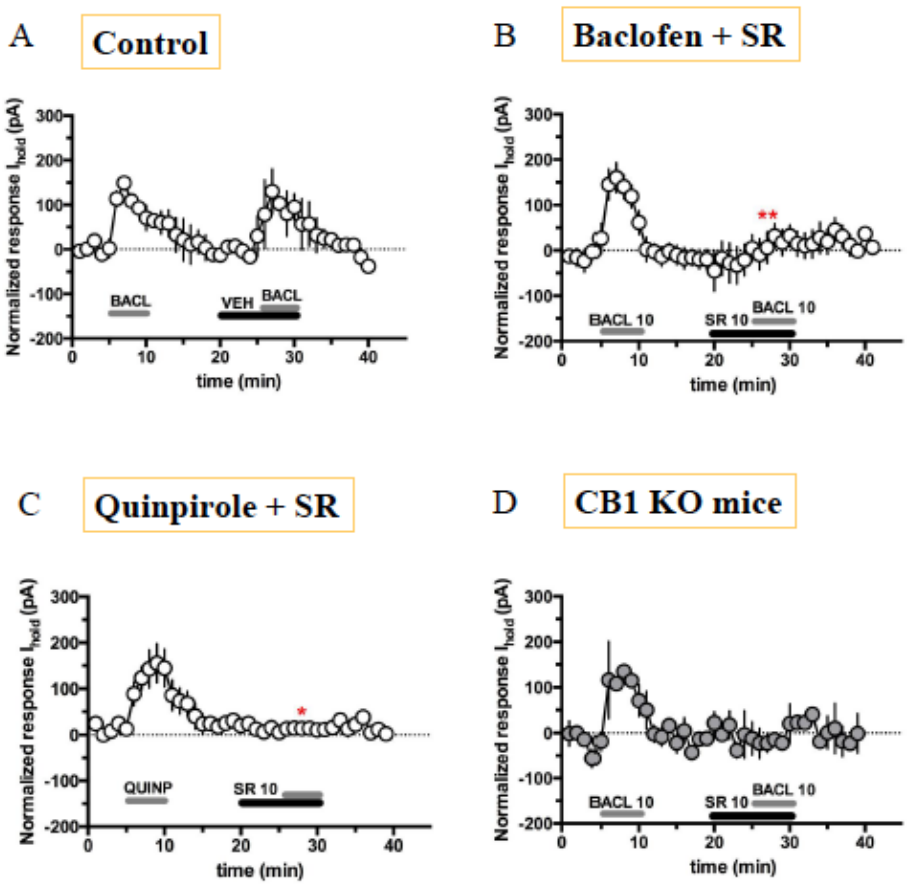

Figure 32. SR blocks baclofen- and quinpirole- induced outward current in dopamine neurons via a mechanism independent from CB1 receptor activation. Time course graphs illustrate the average effects of baclofen (10 µM, A-B-D), quinpirole (1 µM, C) and SR 10 µM (B-C-D) on holding current (Ihold) of dopamine cells. BACL: baclofen; QUINP: quinpirole; SR: SR141716A; VEH: vehicle.

3.3.3 SR decreases GIRK channel activity in the absence of GPCRs

In order to evaluate whether SR blocks GIRK activation by directly acting at the G protein, whole cell patch clamp recordings were performed in CHO cells transiently transfected with Kir 3.1/3.2. For this purpose, GIRKs were activated in a receptor-independent manner with the non-hydrolysable GTP-analog guanosine, 5'-O-(3-thiotriphosphate) (GTPγS), perfused

into the cell via the recording pipette (Fig. 33A). By exchanging for GDP at Gα, GTPγS liberates Gβγ and constitutively activates GIRKs. In the absence of SR, GTPγS induced inwardly rectifying K^+ currents that exhibited modest desensitization over the 10 min recording period (Fig. 33A). In contrast, in the presence of SR (10 μM) the currents were significantly smaller. As shown in Fig. 33B, SR at 10 μM decreases the amplitude of K^+ current and increases the rise time of GIRK channel. In agreement with the BRET experiments, these data suggest that SR directly affects $G\alpha_{i/o}$ proteins, stabilizing their heterotrimeric state and blocking the G protein signaling in living cells.

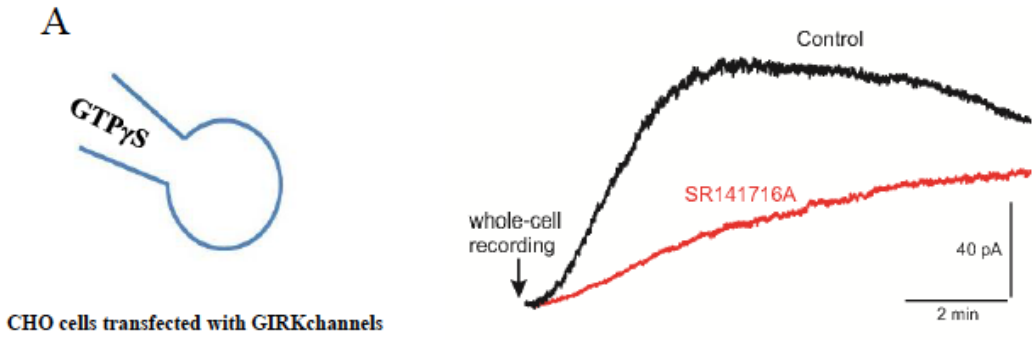

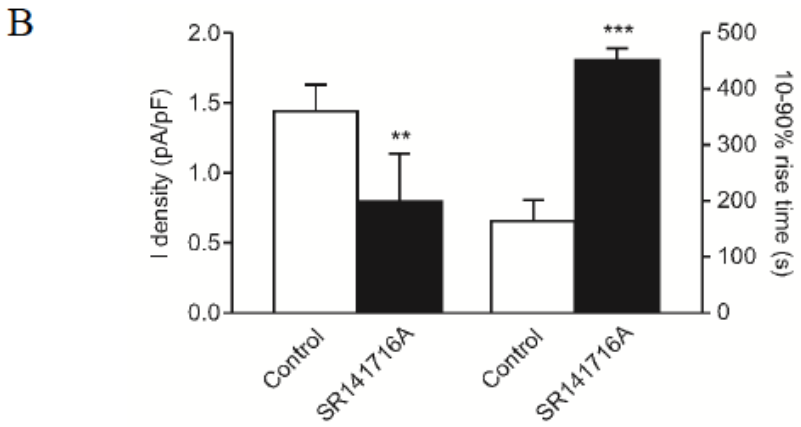

Figure 33. Effect of SR on GIRK activation in CHO cells. (A) Representative K^+ current activated by intracellular perfusion of GTPγS (0.6 mM) and recorded at -50 mV in transfected CHO cells expressing GIRK 1/2 channels. (B) Bar Graph summarizes the relative effects of SR on GTPγS-induced responses. Data are presented as a mean ± SEM of 4 experiments and Statistical significance was assessed using a paired Student's *t*-test (***$p<0.001$).

Chapter 4. Discussion

In this study, we investigated the molecular mechanisms of SR on G protein activity in native and recombinant systems by combining different experimental approaches, i.e GTPγS, BRET, and electrophysiological recordings.

The main finding is that SR, at micromolar concentrations, prevented GPCR-G protein signaling through a direct interaction with G proteins, mostly with αi/o subunits.

Specifically, we showed that SR (i) inhibited G protein basal activity in native and recombinant systems independently of the presence of GPCRs, (ii) attenuated G-protein activation produced by $GABA_B$ and D2 receptor agonists via the CB1 receptor-independent mechanism, (iii) stabilized the constitutive state of G-protein and (iv) induced a rearrangement of Gα and Gβγ subunits. Moreover, SR suppressed both $GABA_B$ and the D2 receptor-activated inwardly rectifying K^+ currents in VTA dopamine cells, and prevented a GTPγS-induced response on GIRK activation in CHO cells.

By using ligand-modulated [^{35}S]GTPγS binding, which allows both the investigation of drug actions directly at the level of the G-protein and the evaluation of spontaneous receptor activity by monitoring the levels of basal [^{35}S]GTPγS binding, we found that SR decreased basal [^{35}S]GTPγS binding to striatal and cortical membranes of rats and to cortical membranes of wild-type mice, CB1 receptor- and $GABA_B$ receptor-KO mice. Moreover, a SR-induced decrease of basal [^{35}S]GTPγS binding was not prevented by co-application of CB1, $GABA_B$ and D2 receptor antagonists. The efficacy and potency of SR in inhibiting G protein basal activity were similar in rat and mouse brain tissues obtained from WT animals or mice lacking either CB1 or $GABA_B$ receptors. Specifically, SR inhibited in a concentration-dependent manner the basal activity of [^{35}S]GTPγS binding with IC_{50} of 3.8 ± 0.45 μM,

12.56 ± 2.0 μM, 12.66 ± 2.1 μM and 3.9 ± 0.8 μM in the cortex of rats, wild-type mouse, CB1-KO and $GABA_B$-KO mice, respectively. The percentage of maximal inhibition (Imax) of basal activity ranged from -36 to -48% with respect to basal activity (considered as 100%) in all tissue preparations.

Our findings confirm and extend previous data showing that at high concentration (μM) SR behaves as an "inverse agonist" (see Pertwee 2005 for a review). The reduction of [^{35}S]GTPγS binding by SR has been previously described in rat, mouse and human tissues (Sim-Selley, 2003; Savinainen et al. 2003; Breivogel et al., 2001; Erdozain et al., 2012) as well as in heterologous expression systems (MacLennan, 1998) and in cultured rat brain (Breivogel et al., 2004).

Furthermore, our results support the evidence that SR effects on basal G protein activity are independent not only from CB1 receptors but also from other GPCRs, such as $GABA_B$ receptors, whose signaling is mediated (as for the CB1 receptor) mainly by the G protein subunit Gi/o.

Indeed, we showed that SR decreased G protein basal activity in cell lines containing a homogenous population of either $GABA_B$ (CHO-$GABA_B$) or D2 (CHO-D2) receptors, thereby excluding that receptor interactions, such as hetero-oligomerization or cross-talk, might influence the action of SR. Moreover, we demonstrated that the extent of the inhibitory effect on G-protein signaling was very similar in the CHO- $GABA_B$, CHO-D2 and the parental CHO-K1 cell membranes, which supports the possibility that SR might act in a receptor-independent manner. The degree of SR-induced decrease of basal G protein activity (approximately 25%) in both cells expressing GPCRs and non transfected CHO-K1 cells was lower than that observed in mouse and rat tissue membranes. One possible explanation may be represented by the lower amount of endogenous G_{i2} and G_{i3} protein subtypes present in

CHO cells (approximately 5 pmol/mg and 0.6 pmol/mg, respectively) (Raymond *et al*., 1993; Gettys *et al*., 1994) compared with native systems such as rat, mouse and human tissue membranes.

It has been previously reported that SR may act as an "inverse agonist" toward other GPCRs. For example, Cinar et al. (2009) demonstrated that in CHO stable cells transfected with MORs, the specific MOR agonist DAMGO stimulated [^{35}S]GTPγS binding that was inhibited by 10 μM SR. In addition, SR binds directly to MORs, albeit with low affinity, and modulates their signaling in mouse cortex and MOR-CHO membranes (Cinar and Szucs, 2009). Recently, it was shown that the CB1 receptor antagonist/inverse agonist AM251 and SR bind with mid-nanomolar concentration to human MORs and competitively antagonize morphine-induced G-protein activation in CHO-hMOR cell homogenates (Seely et al., 2012). The same authors also demonstrated a cross-inhibition of G-protein signaling between $GABA_B$ and CB1 receptors in hippocampal membranes (Cinar et al., 2008).

Recently, Erdozain et al. (2012) evaluated which G protein subunits are activated by CB1 receptors using an antibody-capture [^{35}S]GTPγS scintillation proximity assay (SPA), coupled with immunoprecipitation with a specific antibody for different Gα subunits. Thanks to this assay, which permits the determination of receptor-mediated activation of specific G-protein families, the authors showed that in *post-mortem* human brain cortical membranes WIN (10 μM) produced a significant stimulation of the GTPγS binding mediated by $G_{\alpha i1}$, $G_{\alpha i2}$, $G_{\alpha i3}$ and G_o, but not $G_{q/11}$, $G_{s/olf}$ or G_z, this stimulation being constantly blocked by the CB1 receptor neutral antagonist O-2050 and SR. Moreover, 10 μM SR inhibited SPA-[^{35}S]GTPγS binding when specific anti- $G_{i3,}$ G_o, and G_z antibodies were used, an effect not prevented by O-2050. Based on these premises, we evaluated whether SR affects the agonist-stimulated [^{35}S]GTPγS binding mediated by $GABA_B$ and D2 receptors, which share almost the same pool of G

inhibitory proteins, by using different tissue membrane preparations.

Our data revealed that SR, other than CB1, also modulates $GABA_B$ and D2 receptor signaling. SR attenuated the activation of [^{35}S]GTPγS binding to cortical and striatal membranes produced by the $GABA_B$ receptor agonist baclofen and the D2 receptor agonist quinpirole, an effect not blocked by the respective specific antagonists CGP54626 and sulpiride. Moreover, in our native system SR competitively antagonized G protein activation by the two agonists, baclofen and quinpirole. Specifically, co-incubation with SR (5 μM) resulted in a 2-fold reduction of the potency of baclofen to activate G protein with a concomitant significant reduction of its efficacy. Similarly, co-incubation of quinpirole with equal and lower concentrations of SR (1 and 5 μM) induced a greater reduction of potency (18 and 24 fold at 1 and 5 μM, respectively) and a significant reduction of efficacy of quinpirole-stimulated G protein activity. Moreover, SR at a micromolar concentrations inhibited the G protein activity induced by both submaximal and saturating concentrations of baclofen. Finally, by using a radioligand competition binding assay in cortical membranes, we showed that SR did not interact with the ortosteric site of $GABA_B$ receptor, confirming that its effects on baclofen-stimulation were $GABA_B$ receptor-independent.

Collectively, these findings indicate that SR effects on both basal and agonist-stimulated G protein activity are independent from all GCPRs receptor tested, suggesting that SR might act directly on G protein activity.

Indeed, SR is a highly hydrophobic molecule, thus able to cross the cell membrane and exert a multitude of effects directly on the G protein subunits. To investigate whether this compound might act directly on the G protein heterotrimer complex, we used a recently described BRET approach that allowed the direct monitoring of G protein activation (Ayoub et al., 2009; Gales et al., 2006).

First, by using BRET measurements between $G\alpha_o$-Rluc and $G\gamma_2$-Venus in CHO-$GABA_B$ transfected cells, we showed that SR increased the basal BRET signal between the $G\alpha_o$ and $G\gamma_2$ subunits significantly in a concentration-dependent manner. SR induced a strong effect on the G protein constitutive state by increasing the $G\alpha\beta\gamma$ heterotrimeric complex, independently from receptor activation.

These data are consistent with our [^{35}S]GTPγS results, which showed a decrease of basal G protein activity in a receptor-independent manner. Moreover, once the $GABA_B$ receptor is activated SR significantly reduces the GABA-induced changes in BRET signals between $G\alpha_o$-Rluc and $G\gamma_2$-Venus. These findings demonstrated that SR decreased the dissociation of G protein subunits (i.e $G_{\alpha o}$ and $G_{\beta\gamma}$) after $GABA_B$ receptor activation, promoting a preassembly within the $GABA_B$ receptor and G protein subunits.

In the last years, several studies have used agonist-promoted BRET changes as a readout of protein transition states, such as G protein subunit dissociation, while others have explained these changes as a molecular rearrangement within the $G\alpha\beta\gamma$ complex.

By using a crystal model it has been shown that structural differences observed between active and inactive conformers are relatively modest, and involve only switch I, II and III regions of the $G\alpha$ subunits, which are crucial in guanine nucleotide exchange (Noel et al., 1993).

However, by using multiple insertion sites for BRET donors and acceptors it was possible to monitor real-time ligand-promoted conformational changes between receptor and G protein and $G\alpha\beta\gamma$ subunits in living cells. Gales et al. (2006) have also shown that, in the absence of an agonist, a fraction of the adrenergic α_{2A} receptor exists in a pre-associated complex with G protein. Indeed, a basal BRET signal between receptor and $G\alpha\beta\gamma$ subunits was observed before agonist stimulation.

Accordingly, SR was found to increase the basal BRET signal within D2 receptors tagged with Rluc and $G\alpha_{i1}$ tagged with Venus in three different positions. Depending on the position of the probes, SR increased the BRET signal reflecting a pre-associated receptor-G-protein complex rather than effects on $G\alpha_{i1}$ subunit recruitment. Detection of different BRET signals between $G\alpha_{i1\text{-}91}$Venus, $G\alpha_{i1\text{-}121}$Venus and the D2 receptor indicated that SR induces a re-arrangement on α-helical domain, affecting the interactions between the receptor and the Gα subunits.

Finally, our findings demonstrated that SR directly interacts with the Gα subunit inducing conformational changes within the Gαβγ trimeric complex in a receptor-independent manner. This conclusion is supported by the increase in the BRET signal induced by SR and detected between $G\alpha_{i1\text{-}91}$Venus and $G\alpha_{i1\text{-}121}$Venus and $G\beta_1$ or $G\gamma_2$-Rluc fusion proteins.

In this study, the position of BRET donors and acceptors allowed us to monitor the relative movement between the $G\alpha_{i1}$ and both $G\gamma_2$ and $G\beta_1$ subunits. We found that SR increased the BRET signal for both $G\alpha_{i1\text{-}91}$Venus and $G\alpha_{i1\text{-}121}$Venus detected with $G\beta_1$-Rluc, and $G\gamma_2$-Rluc. No effects were observed in the BRET signal monitored between $G\alpha_{i1\text{-}60}$Venus and $G\beta_1$-Rluc, $G\gamma_2$-Rluc and D2-Rluc. These findings have lead us to speculate that the mutation in the linker 1 region in the $G\alpha_{i1\text{-}60}$Venus fusion protein might disrupt the SR binding site. SR induced changes in the BRET signal was detected for all fusion proteins rather than when $G\alpha_{i1\text{-}60}$Venus was used.

The linker 1 region acts as a hinge during the opening of the α-helical domain, allowing the necessary route for GDP to leave the GTPase domain. The absence of changes in the BRET signal detected using $G\alpha_{i1\text{-}60}$Venus, which is situated in the linker 1, in the presence of SR supports the hypothesis that SR might bind to Gα subunits by keeping the α helical domain in the inactive conformation and thus decreasing GDP/GTP exchange.

In addition, the "gear-shift" model (Cherfils and Chambre, 2003) proposes that receptor activation promotes the strength of interaction between the β propeller region of the Gβ subunit and the GTPase domain in the nucleotide-empty state. Our results suggest that SR blocks the displacement of the α-helical domain away from the GTPase region by inhibiting the dissociation between the Gα subunit and the Gβγ dimer. This hypothesis is consistent with the increase of the BRET signal monitored in the presence of SR between $G\beta_1$-Rluc or $G\gamma_2$-Rluc and both of $G\alpha_{i1}$-Venus (91 and 121 position).

Further, this suggestion reflects a common structural re-arrangement that might be characteristic of a G protein constitutive state. Indeed, crystal structures of the GTPase domain have revealed that only local changes are involved in the nucleotide binding (Noel et al., 1993).

The conformational change induced by SR on $G\alpha_{i1}$ and $G\alpha_o$ subunits might directly affect the molecular mechanism of G protein basal activity and its activation.

Next, we evaluated the effects of SR on adenylate cyclase activity, using BRET with the CAMYEL sensor, a recent technique developed to detect the level of cAMP in living cells. We investigated the inhibitory effects of SR on Gi and Gs protein pathways by measuring the BRET signal in cells transfected with CAMYEL and $GABA_B$, D2 or D1 receptors.

First, we showed that SR, which did not stimulate cAMP by itself, increases the level of cAMP after the injection of baclofen or quinpirole, suggesting that SR inhibited the $G\alpha_{i/o}$ pathway. Indeed, the Gα subunit is involved in regulating adenylate cyclase activity, while the activation of GPCRs affects intracellular cAMP levels.

Stimulation of receptors coupled with the $G\alpha_{i/o}$ subunit decreases cAMP and this effect is inhibited by SR. Conversely, stimulation of receptors coupled with the $G\alpha_s$ subunit increases cAMP. No effects are observed on cAMP levels regulated by the injection of dopamine in

cells expressing the D1 receptor.

Previous studies have found that SR increases Forskolin-stimulated cAMP in CHO-CB1 cells and in neuroblastoma cells (Bouaboula et al., 1997; Meschler et al., 2000), and enhances basal cAMP levels in rat and human frontal cortical and cerebellar membranes (Mato *et al*., 2002). These effects were explained as the antagonist/inverse agonist effects of SR on CB1 receptors.

In contrast, our results show that the effects of SR on cAMP regulation via the $G\alpha_{i/o}$ pathway are not linked to the CB1 receptor, since they were observed in HEK293 cells transfected with the $GABA_B$ or D2 receptor.

Furthermore, these effects are probably specific to $G\alpha_{i/o}$ subunits, since increased cAMP induced by D1 receptor stimulation was not affected in the presence of the highest concentration of SR.

Finally, using an electrophysiological approach, we showed that SR inhibited the G protein-mediated K^+ current induced by baclofen and quinpirole in dopamine neurons of CB1-WT and KO mice. SR also blocked the G protein-mediated K^+ current induced by GTPγS in CHO cells transfected with GIRK1/2.

The CB1 receptor regulates the activity of Ca^{2+} and K^+ channels. Previous studies showed that SR increased voltage-dependent Ca^{2+} current in CB1-expressing rat cultured neurons and cultured pelvic ganglion neurons (Pan et al., 1998), suggesting that SR affects Ca^{2+} activity by blocking the CB1 receptor in the "receptor-G protein-GDP" state.

Our results revealed that SR blocks GIRK channel activity independently of CB1 receptors in VTA dopamine cells. Particularly, whole cell patch clamp experiments showed that GIRK currents produced by baclofen or quinpirole were significantly reduced by SR. Moreover, a complete blockade of GIRK currents by SR (10 μM) in the VTA dopamine cell was also

reported in CB1-KO mice, thus suggesting that SR inhibits GIRK currents in a CB1 receptor-independent manner.

Finally, using a GPCR-free experimental setup, i.e. whole cell patch clamp experiments performed in CHO cells transfected with GIRK1/2 only, we showed that SR induces the inhibition of GIRK channel activity by acting directly on G protein. We found that SR inhibits GTPγS-mediated GIRK currents thus decreasing the current amplitude and increasing the rise time of the channel.

Taken together, these data suggest that SR interacts directly with G protein subunits and inhibits the Gβγ dissociation and its effectors system.

Our current hypothesis is that SR might bind to the G protein, stabilize the Gαβγ complex, and thus affect cAMP production and GIRK channel activity. Hence, several effector systems are regulated by $G_{i/o}$ protein-activation. In the presence of a micromolar concentration of SR we found a decrease in GDP/GTP exchange and K^+ current and an increase in intracellular levels of cAMP. These effects might all be correlated with a negative modulation induced by SR on the G-protein, both in its constitutive and activated form.

In conclusion, altogether our findings support the hypothesis that, at least at micromolar concentrations, SR might act directly on the G protein mostly with αi/o subunits.

Conclusions

This study provides the first demonstration that the commonly employed CB1 receptor antagonist SR, at micromolar concentration, inhibits G protein activity and blocks different signal pathways in a receptor-independent manner. As such, multiple effects on G protein signaling resulting from a high concentration of SR should be carefully interpreted.

GPCRs have a relevant function in various diseases, including metabolic, neurodegenerative and psychiatric disorders. They are also involved in cell proliferation and thus play a key role in tumor growth. Tumor cell proliferation is regulated by several neuropeptides that activate their receptors, stimulate $G\alpha_s$, $G\alpha_i$, $G\alpha_q$ and $G\alpha_{12}$ and regulate the nuclear expression of growth-promoting genes (Dorsam and Gutkind, 2007). Importantly, constitutive activation of a mutated form of GPCRs or G proteins is associated with endocrine tumors (Dorsam and Gutkind, 2007).

Recently, G protein inhibitors or antagonists, interacting with Gβγ subunits or stabilizing Gαβγ complex, have shown antitumor activity in animal models (Bonacci et al., 2006). Additional evidence that modulations of G protein signaling may represent a new therapeutic strategy for treating cancer come from Prévost et al. (2006). They found that a molecule, named BIM-46174, shows anticancer activity by inducing a conformational change on the G protein heterotrimeric complex thus blocking GPCR activation.

Previous studies showed that SR exerted anti-proliferative effects in human peripheral blood cells, blocking the G_1/S phase of the cell cycle without inducting cell death (Malfitano et al., 2008).

In this study, we found that SR inhibited basal and agonist-stimulated G protein activity, increased the Gαβγ heterotrimeric state, and induced a conformational rearrangement between

G protein subunits.

Our data highlight that SR can be a potential specific-inhibitor of heterotrimeric $G_{i/o}$ proteins. More importantly, SR might bind to linker 1 region on the $G\alpha_{i/o}$ subunit, thus representing a possible tool for developing new drugs for simultaneous $G_{i/o}$ protein inhibition.

Acknowledgements

A special thanks goes to the following people for their assistance and support during this project. First, I would like to thank my supervisor Dott.ssa Maria Paola Castelli for giving me the opportunity to undertake this PhD; she always trusted me, gave me the confidence I needed and the freedom to pursue my own ideas.

I would like to thank Prof. Gian Luigi Gessa, for his invaluable advices, unfailing support and encouragement in this work and for our numerous hours of productive discussions.

I would like to thank Prof. Bernhard Bettler, my supervisor at the University of Basel, who supported my project and gave me the opportunity to work in his lab.

I would also like to show my deepest gratitude to all the researchers I met during these 3 years, both in Italy and abroad, whose suggestions were very valuable for me and my work. In particular, I would like to thank Miriam Melis and Rostislav Turecek who have performed the electrophysiology experiments showed in this work.

Thank you to Celine Ullrich and Adi Raveh for teaching me the BRET technique and for sharing their expertise. A big thank you to Ramona Felix and Margarita Dinamarca and to all of Bettler Lab's members for their hospitality, kindness and moral support.

I am also most thankful to Liana Fattore and Fabrizio Sanna for helping me in the correction of my thesis.

Thank you to Camilla Madeddu, Mariella Martorelli and all of my special colleagues of the University of Cagliari for the great atmosphere at work and for their friendliness.

Also, I want to thank my friends in Italy for keeping my spirits up as well as many friends I have made in Switzerland, without whom life in Basel would have never been the same. Last,

but not least, I would like to thank my family back home for their long-distance support. The thought of them always has and always will make me feel at home, no matter where I go.

List of abbreviations

2-AG	2-arachinoyl-glycerol
2-AGE	2-arachidonyl-glyceryl ether
AD	adenylate cyclase
ADP	adenosine diphophate
AEA	N-arachinodil-ethanolamine
ATP	adenosine triphosphate
BRET	Bioluminescence resonance energy transfer
cAMP	cyclic-adenosine 3',5'-monophosphate
CAMYEL	cAMP sensor using YFP-Epac-Rluc
CB1	cannabinoid receptor type 1
CB2	cannabinoid receptor type 2
CHO	Chinese hamster ovary
CNS	central nervous system
DAMGO	Tyr-D-Ala-Gly-(NMe)Phe-Gly-ol Tyr-D-Ala-Gly-(NMe)Phe-Gly-ol
DOR	δ opioid receptor
EC	endocannabinoids
EC	extracellular loops
ECS	Endocannabinoid system
FAAH	Fatty Acid Amide Hydrolase
FDA	Food and Drug Administration
G protein	guanine-nucleotide binding protein
GDP	guanosine diphosphate
GEF	guanine nucleotide exchange factor
GIRK	G protein-activated rectifying K^+ channel
GPCR	G-protein-coupled receptor
GRK	G protein-coupled receptor kinase
GTP	guanosine thriphosphate
HU-210	11-hydroxy-Δ^8-THC-dimethy-pentyl

IC	intracellular domains
KO	knock out
LT	leukotrienes
LX	lipoxins
MAGL	monoacylglycerol lipase
MAPK	mitogen-activated protein kinase
MOR	μ opioid receptor
NADA	N-arachidonoyl-dopamine
PG	prostaglandins
PKA	cAMP-dependent protein kinase
PKC	protein kinase C
PLC	phospholipase C
RGS	regulator of G protein signalling
Rluc	Renilla luciferase
SR	SR141716A
THC	(-)-Δ^9-tethrahydrocannabinol
TM	transmembrane domains
TRPV1	Vanilloid 1 receptor
TX	thromboxanes
WIN	R-(+)-WIN55212
WT	wild type
YFP	yellow fluorescence protein

References

Alonso, R., Voutsinos, B., Fournier, M., Labie, C., Steinberg, R., Souilhac, J., Le Fur, G., and Soubrié, P. (1999). Blockade of cannabinoid receptors by SR141716 selectively increases Fos expression in rat mesocorticolimbic areas via reduced dopamine D2 function. *Neuroscience* 91:607-20

Ameri, A. (1999). The effects of cannabinoids on the brain. Progress in Neurobiology 58:315-48

Arnone, M., Maruani, J., Chaperon, F., Thiébot, M.H., Poncelet, M., Soubrié, P., Le Fur, G.(1997). Selective inhibition of sucrose and ethanol intake by SR 141716A, an antagonist of central cannabinoid (CB1) receptors. *Psychopharmacology* 132:104-106

Atwood, B.K., and Mackie, K. (2010). CB2: a cannabinoid receptor with an identity crisis. *British of Journal of Pharmacology* 160:467-79

Ayoub, M.A., Damian, M., Gespach, C., Ferrandis, E., Lavergne, O., De Wever, O., Banères, J.L., Pin, J.P., and Prévost, G.P.(2009). Inhibition of heterotrimeric G protein signaling by a small molecule acting on Galpha subunit. *The Journal of Biological Chemistry* 284:29136-45

Bénard, G., Massa, F., Puente, N., Lourenço, J., Bellocchio, L., Soria-Gómez, E., Matias, I., Delamarre, A., Metna-Laurent, M., Cannich, A., Hebert-Chatelain, E., Mulle, C., Ortega-Gutiérrez, S., Martín-Fontecha, M., Klugmann, M., Guggenhuber, S., Lutz, B., Gertsch, J., Chaouloff, F., López-Rodríguez, M.L., Grandes, P., Rossignol, R., and Marsicano, G. (2012). Mitochondrial CB1 receptors regulate neuronal energy metabolism. *Nature Neuroscience* 15:558-64

Bettler, B. and Tiao, J.Y. (2006). Molecular diversity, trafficking and subcellular localization of GABAB receptors. *Pharmacology & Therapeutics* 110:533-543

Bockaert, J., and Pin, J.P. (1999). Molecular tinkering of G protein-coupled receptors: an evolutionary success. *EMBO Journal* 18:1723-1729

Bonacci, T.M., Mathews , J.L., Yuan, C., Lehmann, D.M., Malik, S., Wu, D., Font, J.L., Bidlack, J.M. and Smrcka, A.V. (2006). Differential targeting of Gbetagamma-subunit signaling with small molecules. *Science* 312:443-6.

Bosier, B., Bellocchio, L., Metna-Laurent, M., Soria-Gomez, E., Matias, I., Hebert-Chatelain, E., Cannich, A., Maitre, M., Leste-Lasserre, T., Cardinal, P., Mendizabal-Zubiaga, J., Canduela, M.J., Reguero, L., Hermans, E., Grandes, P., Cota, D., and Marsicano, G. (2013). Astroglial CB1 cannabinoid receptors regulate leptin signaling in mouse brain astrocytes. *Molecular Metabolism* 2:393-404

Bouaboula, M., Perrachon, S., Milligan, L., Canat, X., Rinaldi-Carmona, M., Portier, M., Barth, F., Calandra, B., Pecceu, F., Lupker, J., Maffrand, J.P., Le Fur, G., and Casellas, P.

(1997). A selective inverse agonist for central cannabinoid receptor inhibits mitogen-activated protein kinase activation stimulated by insulin or insulin-like growth factor 1. Evidence for a new model of receptor/ligand interactions. *The Journal of Biological Chemistry* 272:22330-22339

Bramblett, R.D., Panu, A.M., Ballesteros, J.A., Reggio, P.H. (1995). Construction of a 3D model of thecannabinoids CB1 receptor: determination of the helix ends and helix orientation. *Life Science* 56:1971-1982

Breivogel, C.S., Griffin, G., Di Marzo, V., and Martin, B.R. (2001). Evidence for a new G protein-coupled cannabinoid receptor in mouse brain. *Molecular Pharmacology* 60:155-63

Breivogel, C.S., Walker, J.M., Huang, S.M., Roy, M.B., and Childers, S.R. (2004). Cannabinoid signaling in rat cerebellar granule cells: G-protein activation, inhibition of glutamate release and endogenous cannabinoids. *Neuropharmacology* 47:81-91

Cabrera-Vera, T.M., Vanhauwe, J., Thomas, T.O., Medkova, M., Preininger, A., Mazzoni, M.R., and Hamm, H.E. (2003). Insights into G Protein Structure, Function, and Regulation. *Endocrine Reviews* 24:765-781

Canals, M., and Milligan, G. (2008). Constitutive activity of the cannabinoid CB1 receptor regulates the function of co-expressed Mu opioid receptors. *The Journal of Biological Chemistry* 283:11424-34

Castelli, M.P., Casu, A., Casti, P., Lobina, C., Carai, M.A., Colombo, G., Solinas, M., Giunta, D., Mugnaini, C., Pasquini, S., Tafi, A., Brogi, S., Gessa, G.L., and Corelli, F. (2012). Characterization of COR627 and COR628, two novel positive allosteric modulators of the GABA(B) receptor. *Journal of Pharmacology and Experimental Therapeutics* 340:529-38

Ceruso, M.A., Periole, X., and Weistein, H. (2004). Molecular dynamics simulations of transduction: Interdomain and front to back communication in activation and nucleotide exchange. *Journal of Molecular Biology* 338:469-481

Cherfils, J., and Chabre, M. (2003). Activation of G-protein Galpha subunits by receptors through Galpha-Gbeta and Galpha-Ggamma interactions. *Trends in Biochemical Sciences* 28:13-7

Cinar, R., and Szucs, M. (2009). CB1 Receptor-Independent Actions of SR141716 on G-Protein Signaling: Co-application with the Opioid Agonist Tyr-D-Ala-Gly-(NMe)Phe-Gly-ol Unmasks Novel, Pertussis Toxin-Insensitive Opioid Signaling in Opioid Receptor-Chinese Hamster Ovary Cells. *Journal of Pharmacology and Experimental Therapeutics* 330:567-574

Cinar, R., Freund, T.F., Katona, I., Mackie, K., and Szucs, M. (2008). Reciprocal inhibition of G-protein signaling is induced by CB(1) cannabinoid and GABA(B) receptor interactions in rat hippocampal membranes. *Neurochemistry International* 52:1402-9

Colombo, G., Agabio, R., Diaz, G., Lobina, C., Reali, R., and Gessa, G.L. (1998). Appetite suppression and weight loss after the cannabinoid antagonist SR 141716. *Life Science* 63:PL113-7

Compton, D.R., Aceto, M.D., Lowe, J., and Martin B.R. (1996). In vivo characterization of a specific cannabinoid receptor antagonist (SR141716A): Inhibition of Δ9-tetrahydrocannabinol-induced responses and apparent agonist activity. *Journal of Pharmacology and Experimental* 227:586-594

Cota, D., Marsicano, G., Tschop, M., Grübler, Y., Flachskamm, C., Schubert, M., Auer, D., Yassouridis, A., Thöne-Reineke, C., Ortmann, S., Tomassoni, F., Cervino, C., Nisoli, E., Linthorst, A.C., Pasquali, R., Lutz, B., Stalla, G.K., and Pagotto, U. (2003). The endogenous cannabinoid system affects energy balance via central orexigenic drive and peripheral lipogenesis. *The Journal of Clinical Investigation* 112:423-431

Croci, T., Manara, L., Aureggi, G., Guagnini, F., Rinaldi-Carmona, M., Maffrand, J.P., Le Fur, G., Mukenge, S., and Ferla, G. (1998). In vitro functional evidence of neuronal cannabinoid CB1 receptors in human ileum. *British of Journal of Pharmacology* 125:1393-1395

Crunelle, C.L., Van De Giessen, E., Schulz, S., Vanderschuren, L.J., De Bruin, K., Van Den Brink, W., and Booij, J. (2013). Cannabinoid-1 receptor antagonist rimonabant (SR141716) increases striatal dopamine D2 receptor availability. *Addiction Biology* 18:908-11

Dascal, N. (2001). Ion-channel regulation by G proteins. *TRENDS in Endocrinology & Metabolism* 12:391-398

De Petrocellis, L., et al. (2004) The endocannabinoid system: a general view and latest additions. *British Journal of Pharmacology* 141:765-774

De Vry, J., and Jentzsch, K.R. (2004). Partial agonist-like profile of the cannabinoid receptor antagonist SR141716A in a food-reinforced operant paradigm. *Behavioural Pharmacology* 15:13-20

Di Marzo, V., and De Petrocellis, L. (2012). Why do cannabinoid receptors have more than one endogenous ligand? *Philosophical Transactions of the Royal Society B* 367:3216-3228

Di Marzo, V., De Petrocellis, L., Fezza, F., Ligresti, A., and Bisogno, T. (2002) Anandamide receptors. *Prostaglandins, Leukotrienes and Essential Fatty Acid*s 66:377-391

Di Marzo, V., Goparaju, S.K., Wang, L., Liu, J., Bátkai, S., Járai, Z., Fezza, F., Miura, G.I., Palmiter, R.D., Sugiura, T., and Kunos, G. (2001). Leptin-regulated endocannabinoids are involved in maintaining food intake. *Nature* 410:822-5

Di Marzo, V., Melck, D., Bisogno, T., and De Petrocellis, L. (1998). Endocannabinoids: endogenous cannabinoid receptor ligands with neuromodulatory action. *Trends Neuroscience* 21:521-528

Dorsam, R.T., and Gutkind, J.S. (2007). G-protein-coupled receptors and cancer. *Nature Reviews Cancer* 7:79-94

Duc, N.M., Kim, H.R., Chung, K.Y. (2015). Structural mechanism of G protein activation by G protein-coupled receptor. *European Journal of Pharmacology* 763:214-22

Erdozain, A.M., Diez-Alarcia, R., Meana, J.J., and Callado, L.F. (2012). The inverse agonist effect of rimonabant on G protein activation is not mediated by the cannabinoid CB1 receptor: Evidence from postmortem human brain. *Biochemical Pharmacology* 83:260–268

Felder, C.C., Joyce, K.E., Briley, E.M., Glass, M., Mackie, K.P., Fahey, K.J., Cullinan, G.J., Hunden, D.C., Johnson, D.W., Chaney, M.O., Koppel, G.A., and Brownstein, M. (1998). LY320135, a novel cannabinoid CB1 receptor antagonist, unmasks coupling of the CB1 receptor to stimulation of cAMP accumulation. *Journal of Pharmacology and Experimental Therapeutics* 284:291-7

Fernández-Ruiz, J., Pazos, M.R., García-Arencibia, M., Sagredo, O., and Ramos, J.A. (2008). Role of CB2 receptors in neuroprotective effects of cannabinoids. *Molecular and Cellular Endocrinology* 286:S91-6

Fonseca, F.R., Del Arco, I., Martín-Calderón, J.L., Gorriti, M.A., and Navarro, M. (1998). Role of the endogenous cannabinoid system in the regulation of motor activity. *Neurobiology of Disease* 5:483-501

Gales, C., Van Durm, J.J., Schaak, S., Pontier, S., Percherancier, Y., Audet, M., Paris, H., and Bouvier, M. (2006). Probing the activation-promoted structural rearrangements in preassembled receptor-G protein complexes. *Nature structural & molecular biology* 13:778-786

Gettys, T.W., Sheriff-Carter, K., Moomaw, J., Taylor, I.L., Raymond, J.R. (1994). Characterization and use of crude alpha-subunit preparations for quantitative immunoblotting of G proteins. *Analytical Biochemistry* 220:82-91

Gifford, A.N., Bruneus, M., Gatley, S.J., and Volkow, N.D. (2000). Cannabinoid receptor-mediated inhibition of acetylcholine release from hippocampal and cortical synaptosomes. *British of Journal of Pharmacology* 131:645-50

Glaser, S.T., Abumrad, N.A., Fatade, F., Kaczocha, M., Studholme, K.M., and Deutsch, DG. (2003). Evidence against the presence of an anandamide transporter. *Proc. Natl. Acad. Sci. USA* 100:4269-4274

Glass, M., and Felder, C.C. (1997). Concurrent stimulation of cannabinoid CB1 and dopamine D2 receptors augments cAMP accumulation in striatal neurons: evidence for a Gs linkage to the CB1 receptor. *The Journal of Neuroscience* 17:5327-33

Gomes, I., Jordan, B. A., Gupta, A., Trapaidze, N., Nagy, V. and Devi, L. A. (2000) Heterodimerization of μ and δ opioid receptors: a role in opiate synergy. *The Journal of Neuroscience* 20:RC110

Gong, J.P., Onaivi, E.S., Ishiguro, H., Liu, Q.R., Tagliaferro, P.A., Brusco, A., and Uhl, G.R. (2006). Cannabinoid CB2 receptors: immunohistochemical localization in rat brain. *Brain Research* 1071:10-23

Grace, C.R., Perrin, M.H., Di Gruccio, M.R., Miller, C.L., Rivier, J.E., Vale, W.W., and Riek, R. (2004). NMR structure and peptide hormone binding site of the first extracellular domain of a type B1 G protein-coupled receptor. *Proc. Natl. Acad. Sci. USA.* 101:12836-12841

Greasley, P.J., and Clapham J.C. (2006). Inverse agonism or neutral antagonism at G-protein coupled receptors: A medical chemistry challenge worth pursuing? *European Journal of Pharmacology* 553:1-9

Grimaldi, P., Orlando, P., Di Siena, S., Lolicato, F., Petrosino, S., Bisogno, T., Geremia, R., De Petrocellis, L., and Di Marzo, V. (2009). The endocannabinoid system and pivotal role of the CB2 receptor in mouse spermatogenesis. *Proc. Natl. Acad. Sci. USA* 106:11131-6

Guzmán, M. (2003). Cannabinoids: potential anticancer agents. Nature Reviews Cancer 3:745-55

Hasbi, A., Nguyen, T., Fan, T., Cheng, R., Rashid, A., Alijaniaram, M., Rasenick, M. M., O'Dowd, B. F. and George, S. R. (2007). Trafficking of preassembled opioid μ-δ heterooligomer-Gz signaling complexes to the plasma membrane: coregulation by agonists. *Biochemistry* 46:12997-13009

Hebert-Chatelain, E., Reguero, L., Puente, N., Lutz, B., Chaouloff, F., Rossignol, R., Piazza, P.V., Benard, G., Grandes, P., and Marsicano, G. (2014). Studying mitochondrial CB1 receptors: Yes we can. *Molecular Metabolism* 3:339

Heng, B.C. (2013). An overview of the diverse roles of G-protein coupled receptors (GPCRs) in the pathophysiology of various human diseases. *Biotechnology Advance* 31:1676-1694

Herkenham, M., Lynn, A.B., Little, M.D., Johnson, M.R., Melvin, L.S., de Costa, B.R, and Rice, K.C. (1990). Cannabinoid receptor localization in brain. Proc Natl Acad Sci U.S.A 87:1932-1936

Hermans, E. (2003). Biochemical and pharmacological control of the multiplicity of coupling at G-protein-coupled receptors. *Pharmacologic and Therapeutics* 99:25-44

Howlett, A.C, and Mukhopadhyay, S. (2002). Cellular signal transduction by anandamide and 2-arachidonoylglycerol. *Chemistry and Physics of Lipids* 108:53-70

Howlett, A.C., Barth, F., Bonner, T.I., Cabral, G., Casellas, P., Devane, W.A., Felder, C.C., Herkenham, M., Mackie, K., Martin, B.R., Mechoulam, R., and Pertwee, R.G. (2002). International Union of Pharmacology. XXVII. Classification of Cannabinoids receptors. *Pharmacological Reviews* 54:161-202

Howlett, A.C., Breivogel, C.S., Childers, S.R., Deadwyler, S.A., Hampson, R.E., and Porrino, L.J. (2004). Cannabinoid physiology and pharmacology: 30 years of progress. *Neuropharmacology* 47:345-358

Howlett, A.C., Wilken, G.H., Pigg, J.J., Houston, D.B., Lan, R., Liu, Q., and Makriyannis, A. (2000). Azido- and isothiocyanato-substituted aryl pyrazoles bind covalently to the CB1 cannabinoid receptor and impair signal transduction. *Journal of Neurochemistry* 74:2174-81

Jansen, K.L., Faull, R.L., Storey, P., and Leslie, R.A. (1993). Loss of cannabinoid receptors in the substantia nigra in Huntington's disease. *Neuroscience* 56:523-527

Jiang, L.I., Collins, J., Davis, R., Lin, K.M., DeCamp, D., Roach, T., Hsueh, R., Rebres, R.A., Ross, E.M., Taussig, R., Fraser, I., and Sternweis, P.C. (2007). Use of a cAMP BRET sensor to characterize a novel regulation of cAMP by the sphingosine 1-phosphate/G13 pathway. *The Journal of Biological Chemistry* 282:10576-84

Karnik, S.S., Gogonea, C., Patil, S., Saad, Y., and Takezako, T. (2003) Activation of G-protein-coupled receptors: a common molecular mechanism. *TRENDS in Endocrinology & Metabolism* 14:431-437

Katona, I., and Freund, T.F. (2012). Multiple Functions of Endocannabinoid Signaling in the Brain. *Annual Review of Neuroscience* 35:529-558

Katritch, V., Cherezov, V., and Stevens, R.C. (2012). Diversity and modulatory of G protein-coupled receptor structures. *Trends in Pharmacological Sciences* 33:17-27

Kenakin, T. (2002). Efficacy at G-protein-coupled receptors. *Nature Reviews* 1:103-110

Kim, S.H., Fraser, P.E., Westaway, D., St George-Hyslop, P.H., Ehrlich, M.E., and Gandy, S. (2010). Group II metabotropic glutamate receptor stimulation triggers production and release of Alzheimer's amyloid(beta)42 from isolated intact nerve terminals. *The Journal of Neuroscience* 30:3870-5

Kimple, A.J., Bosch, D.E., Giguère, P.M., Siderovski, D.P., (2011). Regulators of G-Protein Signaling and Their Gα Substrates: Promises and Challenges in Their Use as Drug Discovery Targets. *Pharmacological Reviews* 63:728-749

Landsman, R.S., Burkey, T.H., Consroe, P., Roeske, W.R., and Yamamura, H.I. (1997). SR 141716A is an inverse agonist at the human cannabinoid CB1 receptor. *European Journal of Pharmacology* 334:R1-R2

Lichtman, A.H., and Martin, B.R. (1996). Δ9-Tetrahydrocannabinol impairs spatial memory through a cannabinoid receptor mechanism. *Psychopharmacology* 126:125-131

Lichtman, A.H., Varvel, S.A., and Martin B.R. (2002). Endocannabinoids in cognition and dependence. *Prostaglandins, Leukotrienes and Essential Fatty Acids* 66:269-8

Luttrell, L. M. (2008). Reviews in Molecular Biology and Biotechnology: Transmembrane Signaling by G Protein-Coupled Receptors. *Molecular Biotechnology* 39:239-264

Maccarrone, M. (2008). CB2 receptors in reproduction. *British of Journal of Pharmacology* 153:189-980

Maccarrone, M., Dainese, E., and Oddi, S. (2010). Intracellular trafficking of anandamide: new concepts for signaling. *Trends in Biochemical Sciences* 35:601-608

Mackie, K. (2005) Distribution of cannabinoid receptors in the central and peripheral nervous system. *Handbook of Experimental Pharmacology* 168:299-325

MacLennan, S.J., Reynen, P.H., Kwan, J., and Boubaus, D.W. (1998) Evidence for inverse agonism of SR141716A at human recombinant cannabinoid CB1 and CB2 receptors. *British of Journal of Pharmacology* 124:619-622

Maldonado, R., Valverde, O., and Berrendero, F. (2006). Involvement of the endocannabinoid system in drug addiction. *Trends in Neurosciences* 29:225-232

Malfitano, A.M., Laezza, C., Pisanti, S., Gazzerro, P., and Bifulco, M. (2008). Rimonabant (SR141716) exerts anti-proliferative and immunomodulatory effects in human peripheral blood mononuclear cells. *British of Journal of Pharmacology* 153:1003-10

Mansbach, R.S., Rovetti, C.C., Winston, E.N., and Lowe, J.A., (1996). Effects of the cannabinoid CB1 receptor antagonist SR 141716A on the behavior of pigeons and rats. *Psychopharmacology* 124:315-322

Marsicano, G., Moosmann, B., Hermann, H., Lutz, B., and Behl, C. (2002). Neuroprotective properties of cannabinoids against oxidative stress: role of the cannabinoid receptor CB1. *Journal of Neurochemistry* 80:448-56

Massa, F., Marsicano, G., Hermann, H., Cannich, A., Monory, K., Cravatt, B.F., Ferri, G.L., Sibaev, A., Storr, M., Lutz, B. (2004). The endogenous cannabinoid system protects against colonic inflammation. *The Journal of Clinical Investigation* 113:1202-9

Mato, S., Pazos, A., and Valdizán, E.M. (2002). Cannabinoid receptor antagonism and inverse agonism in response to SR141716A on cAMP production in human and rat brain. *European Journal of Pharmacology* 443:43-6

May, L.T., Leach, K., Sexton, P.M., and Christopoulos, A. (2007). Allosteric modulation of G-protein coupled receptor. *Annual Review of Pharmacology and Toxicology* 47:1-51

Melis, M., and Pistis, M. (2007). Endocannabinoid signaling in midbrain dopamine neurons: more than physiology? *Current Neuropharmacology* 5:268-77

Melis, M., Pillolla, G., Bisogno, T., Minassi, A., Petrosino, S., Perra, S., Muntoni, A.L., Lutz, B., Gessa, G.L., Marsicano, G., Di Marzo, V., and Pistis, M. (2006). Protective activation of the endocannabinoid system during ischemia in dopamine neurons. *Neurobiology of Disease* 24:15-27

Meschler, J.P., Kraichely, D.M., Wilken, G.H., and Howlett, A.C. (2000). Inverse agonist properties of N-(piperidin-1-yl)-5-(4-chlorophenyl)-1-(2, 4-dichlorophenyl)-4-methyl-1H-pyrazole-3-carboxamide HCl (SR141716A) and 1-(2-chlorophenyl)-4-cyano-5-(4-methoxyphenyl)-1H-pyrazole-3-carboxyl ic acid phenylamide (CP-272871) for the CB(1) cannabinoid receptor. *Biochemical Pharmacology* 60:1315-23

Miller, L.J. and Kenakin, T. (2010). Seven Transmembrane Receptors as Shapeshifting Proteins: the impact of allosteric modulation and functional selectivity on New Drug Discovery. *Pharmacological Reviews* 62: 265-304

Milligan, G. (2003). Constitutive Activity and Inverse Agonists of G protein-Coupled Receptors: a Current Perspective. *Molecular Pharmacology* 64:1271-1276

Milligan, G. and Kosteins, E. (2006). Heterotrimeric G-proteins: a short history. British of *Journal of Pharmacology* 147:S46-S55

Mnpotra, J.S., Qiao,Z., Cai, J., Lynch, D.L., Grossfield, A., Leioatts, N., Hurst, D.P., Pitman, M.C., Song, Z.H., Reggio, P.H. (2014). Structural basis of G protein-coupled receptor-Gi protein interaction: formation of the cannabinoid CB2 receptor-Gi protein complex. *The Journal of Biological Chemistry* 289:20259-20272

More, S.V., and Choi, D. (2015). Promising cannabinoid-based therapies for Parkinson's disease: motor symptoms to neuroprotection. *Molecular Neurodegeneration* 10:17

Morozov, Y.M., Dominguez, M.H., Varela, L., Shanabrough, M., Koch, M., Horvath, T.L., and Rakic, P. (2013). Antibodies to cannabinoid type 1 receptor co-react with stomatin-like protein 2 in mouse brain mitochondria. *European Journal of Neuroscience* 38:2341-2348

Mukhopadhyay, S., Shim, J.Y., Assi, A.A., Norford, D., and Howlett, A.C. (2002). CB(1) cannabinoid receptor-G protein association: a possible mechanism for differential signalling. *Chemistry and Physics of Lipids* 121:91-109

Nakamura-Palacios, E.M., Moerschbaecher, J.M., and Barker, L.A. (1999). The Pharmacology of SR 141716A: A Review. *CNS Drug Reviews* 5:43-58

Newman-Tancredi, A., Cussac, D., Audinot, V., Pasteau, V., Gavaudan, S., and Millan, M.J. (1999). G protein activation by human dopamine D3 receptors in high-expressing Chinese hamster ovary cells: A guanosine-5'-O-(3-[35S]thio)- triphosphate binding and antibody study. *Molecular Pharmacology* 55:564-74

Noel, J.P., Hamm, H.E., and Sigler, P.B. (1993). The 2.2 A crystal structure of transducin-alpha complexed with GTP gamma S. *Nature* 366:654-63

Ofek, O., Karsak, M., Leclerc, N., Fogel, M., Frenkel, B., Wright, K., Tam, J., Attar-Namdar, M., Kram, V., Shohami, E., Mechoulam, R., Zimmer, A., and Bab, I. (2006). Peripheral cannabinoid receptor, CB2, regulates bone mass. *Proc. Natl. Acad. Sci. USA* 103:696-701

Oldham, W. M., and Hamm, H.E. (2007). How do receptors activate G proteins? *Advances in Protein Chemistry* 74:67-93

Oldham, W. M., and Hamm, H.E. (2008). Heterotrimeric G protein activation by G-protein-coupled receptors. *Nature Reviews* 9:60-71

Pan, X., Ikeda, S.R., and Lewis, D.L. (1998). SR 141716A acts as an inverse agonist to increase neuronal voltage-dependent Ca^{2+} currents by reversal of tonic CB1 cannabinoid receptor activity. *Molecular Pharmacology* 54:1064-72

Parsons, L.H. and Hurd, L.Y.(2015). Endocannabinoid signalling in reward and addiction. *Nature Reviews Neuroscience* 16:579-594

Pertwee, R.G. (1997). Pharmacology of cannabinoid CB1 and CB2 receptors. *Pharmacology & Therapeutics* 74:129-180

Pertwee, R.G. (2006). The pharmacology of cannabinoid receptors and their ligands: an overview. *International Journal of Obesity* 30:S13-8

Pertwee, R.G. (2015) Endocannabinoids and Their Pharmacological Actions. *Handbook of Experimental Pharmacology, Chapter Endocannabinoids* pp:1-37

Pertwee, R.G., and Ross, R.A. (2002). Cannabinoid receptors and their ligands. *Prostaglandins, Leukotrienes and Essential Fatty Acids* 66:101-121

Pertwee, R.G., Gibson, T.M., Stevenson, L.A., Ross, R.A., Banner, W.K., Saha, B., Razdan, R.K., and Martin, B.R. (2000). O-1057, a potent water-soluble cannabinoid receptor agonist with antinociceptive properties. *British of Journal of Pharmacology* 129:1577-1584

Pertwee, R.G., Thomas, A., Stevenson, L.A., Maor, Y., and Mechoulam, R. (2005). Evidence that (–)-7-hydroxy-40-dimethylheptyl-cannabidiol activates a non-CB1, non-CB2, non-TRPV1 target in the mouse vas deferens. *Neuropharmacology* 48:1139-1146

Pickel, V.M., Chan, J., Kearn, C.S., and Mackie, K. (2006). Targeting dopamine D2 and cannabinoid-1 (CB1) receptors in rat nucleus accumbens. *Journal of Comparative Neurology* 495:299-313

Pinard, A., Seddik, R., and Bettler, B. (2010). GABAB receptors: physiological functions and mechanisms of diversity. *Advances in Pharmacology* 58:231-55

Pinna, A., Bonaventura, J., Farré, D., Sánchez, M., Simola, N., Mallol, J., Lluís, C., Costa, G., Baqi, Y., Müller, C.E., Cortés, A., McCormick, P., Canela, E.I., Martínez-Pinilla, E., Lanciego, J.L., Casadó, V., Armentero, M.T., and Franco, R. (2014). L-DOPA disrupts adenosine A(2A)-cannabinoid CB(1)-dopamine D(2) receptor heteromer cross-talk in the striatum of hemiparkinsonian rats: biochemical and behavioral studies. *Experimental Neurology* 253:180-91

Prévost, G.P., Lonchampt, M.O., Holbeck, S., Attoub, S., Zaharevitz, D., Alley, M., Wright, J., Brezak, M.C., Coulomb, H., Savola, A., Huchet, M., Chaumeron, S., Nguyen, Q.D., Forgez, P., Bruyneel, E., Bracke, M., Ferrandis, E., Roubert, P., Demarquay, D., Gespach, C., and Kasprzyk, P.G. (2006). Anticancer activity of BIM-46174, a new inhibitor of the heterotrimeric Galpha/Gbetagamma protein complex. *Cancer Research* 66(18):9227-34

Raymond, J.R., Olsen, C.L., and Gettys, T.W. (1993). Cell-specific physical and functional coupling of human 5-HT1A receptors to inhibitory G protein alpha-subunits and lack of coupling to Gs alpha. *Biochemistry* 32:11064-11073

Richardson, J.D., Aanonsen, L., and Hargreaves, K.M. (1997). SR141716A, a cannabinoid receptor antagonist, produces hyperalgesia in untreated mice. *European Journal of Pharmacology* 319:R3-R4

Rinaldi-Carmona, M., Barth, F., Héaulme, M., Shire, D., Calandra, B., Congy, C., Martinez, S., Maruani, J., Néliat, G., and Caput, D. (1994). SR141716A, a potent and selective antagonist of the brain cannabinoid receptor. *FEBS Letter* 350:240-4

Rinaldi-Carmona, M., Calandra, B., Shire, D., Bouaboula, M., Oustric, D., Barth, F., Casellas, P., Ferrara, P., and Le Fur, G. (1996). Characterization of two cloned human CB1 cannabinoid receptor isoforms. *Journal of Pharmacology and Experimental Therapeutics* 278:871-878

Rios, C., Gomes, I. and Devi, L. A. (2006). μ-Opioid and CB1 cannabinoid receptor interactions: reciprocal inhibition of receptor signaling and neuritogenesis. *British of Journal of Pharmacology* 148:387-395

Roche, R., Hoareau, L., Bes-Houtmann, S., Gonthier, M.P., Laborde, C., Baron, J.F., Haffaf, Y., Cesari, M., and Festy, F. (2006). Presence of the cannabinoid receptors, CB1 and CB2, in human omental and subcutaneous adipocytes. *Histochemistry and Cell Biology* 126:177-187

Rodríguez, J.J., Mackie, K., and Pickel V.M. (2001). Ultrastructural localization of the CB1 cannabinoid receptor in m-opioid receptor patches of the rat caudate putamen nucleus. *The Journal of Neuroscience* 21:823

Rodriguez, J.J., Mackie, K., and Pickel, V.M. (2001). Ultrastructural localization of the CB1 cannabinoid receptor in mu-opioid receptor patches of the rat Caudate putamen nucleus. *The Journal of Neuroscience* 21:823-33

Romero, J., Lastres-Becker, I., de Miguel, R., Berrendero, F., Ramos, J.A., and Fernández-Ruiz, J. (2002). The endogenous cannabinoid system and the basal ganglia. biochemical, pharmacological, and therapeutic aspects. *Pharmacology & Therapeutics* 95:137-52

Rozenfeld, R., and Devi, L.A. (2011). Exploring a role for heteromerization in GPCR signaling specificity. *Biochemical Journal* 433:11-18

Rubino, T., Patrini, G., Massi, P., Fuzio, D., Viganò, D., Giagnoni, G., and Parolaro, D. (1998). Cannabinoid-precipitated withdrawal: A time-course study of the behavioral aspect

and its correlation with cannabinoid receptors and G protein expression. *Journal of Pharmacology and Experimental* 285:813-819

Savinainen, J.R., Saario, S.M., Niemi, R., Järvinen, T., and Laitinen J.T. (2003). An optimized approach to study endocannabinoid signaling: evidence against constitutive activity of rat brain adenosine A1 and cannabinoid CB1 receptors. *British of Journal of Pharmacology* 140:1451-9

Schlicker, E., and Kathmann, M. (2001). Modulation of transmitter release via presynaptic cannabinoid receptors. *Trends in Pharmacological Sciences* 22:565-72

Schlicker, E., Timm, J., and Göthert, M. (1996). Cannabinoid receptor-mediated inhibition of dopamine release in the retina. *Naunyn-Schmiedeberg's Archives of Pharmacology* 354:791.795

Schuler, V., Lüscher, C., Blanchet, C., Klix, N., Sansig, G., Klebs, K., Schmutz, M., Heid, J., Gentry, C., Urban, L., Fox, A., Spooren, W., Jaton, A.L., Vigouret, J., Pozza, M., Kelly, P.H., Mosbacher, J., Froestl, W., Käslin, E., Korn, R., Bischoff, S., Kaupmann, K., van der Putten H., and Bettler, B. Epilepsy, hyperalgesia, impaired memory, and loss of pre- and postsynaptic GABA(B) responses in mice lacking GABA(B(1)). *Neuron* 31:47-58

Schwenk, J., Metz, M., Zolles, G., Turecek, R., Fritzius, T., Bildl, W., Tarusawa, E., Kulik, A., Unger, A., Ivankova, K., Seddik, R., Tiao, J.Y., Rajalu, M., Trojanova, J., Rohde, V., Gassmann, M., Schulte, U., Fakler, B., Bettler, B. (2010). Native GABA(B) receptors are heteromultimers with a family of auxiliary subunits. *Nature* 65:231-5

Seely, K.A., Brents, L.K., Franks, L.N., Rajasekaran, M., Zimmerman, S.M., Fantegrossi, W.E., and Prather, P.L. (2012). AM-251 and rimonabant act as direct antagonists at mu-opioid receptors: implications for opioid/cannabinoid interaction studies. *Neuropharmacology* 63:905-915

Seifer, R., and Wenzel-Seifert, K. (2002). Constitutive activity of G-protein-coupled receptors: cause of disease and common property of wild-type receptors. *Naunyn-Schmiedeberg's Arch Pharmacology* 366:381-416

Sim-Selley, L.J. (2003). Regulation of cannabinoid CB1 receptors in the central nervous system by chronic cannabinoids. *Critical Reviews in Neurobiology* 15:91-119

Sim-Selley, L.J., Brunk, L.K., Selley, D.E. (2001). Inhibitory effects of SR141716A on G-protein activation in rat brain. *European Journal of Pharmacology* 414:135-43

So, C. H., Verma, V., O'Dowd, B. F. and George, S. R. (2007). Desensitization of the dopamine D1 and D2 receptor hetero-oligomer mediated calcium signal by agonist occupancy of either receptor. *Molecular Pharmacology* 72:450-462

Souilhac, J., Poncelet, M., Rinaldi-Carmona, M., Fur, G.L., and Soubrié, P. (1995). Intrastriatal injection of cannabinoid receptor agonists induced turning behavior in mice. *Pharmacology Biochemistry and Behavior* 51:3-7

Stella, N. (2009). Endocannabinoid signaling in microglial cells. *Neuropharmacology* 56:244-53

Stella, N. (2010). Cannabinoid and cannabinoid-like receptors in microglia, astrocytes and astrocytomas. *Glia* 58:1017-1030

Sugiura, T., Kobayashi, Y., Oka, S., and Waku, K. (2002). Biosynthesis and degradation of anandamide and 2-arachidonoyl-glycerol and their possible physiological significance. *Prostaglandins, Leukotrienes and Essential Fatty Acids* 66:173-192

Svíženská, I., Dubový, P., and Šulcová, A. (2008) Cannabinoid receptors 1 and 2 (CB1 and CB2), their distribution, ligands and functional involvement in nervous system structures-A short review. *Pharmacology, Biochemistry and Behavior* 90:501–511

Szabo, B., and Schlicker, E. (2005). Effects of cannabinoids on neurotransmission. *Handbook of experimental pharmacology* 168:327-65

Szabo, B., Nordheim, U., and Niederhoffer, N. (2001). Effects of cannabinoids on sympathetic and parasympathetic neuroeffector transmission in the rabbit heart. *Journal of Pharmacology and Experimental Therapeutics* 297:819-826

Szefel, J., Kruszewski, W.J. and Sobczak, E. (2015). Factors Influencing the Eicosanoids Synthesis In Vivo. *BioMed Research International* 2015:690-692
Terranova, J.P., Storme, J.J., Lafon, N., Péŕio, A., Rinaldi-Carmona, M., Le Fur, G., and Soubrié, P. (1996). Improvement of memory in rodents by the selective CB1 cannabinoid receptor antagonist, SR 141716. *Psychopharmacology* 126:165-172

Urwyler, S., Mosbacher, J., Lingenhoehl, K., Heid, J., Hofstetter, K., Froestl, W., Bettler, B., and Kaupmann, K. (2001). Positive allosteric modulation of native and recombinant gamma-aminobutyric acid(B) receptors by 2,6-Di-tert-butyl-4-(3-hydroxy-2,2-dimethyl-propyl)-phenol (CGP7930) and its aldehyde analog CGP13501. *Molecular Pharmacology* 60:963-71

Van Dop, C., Yamanaka, G., Steinberg, F., Sekura, R.D., Manclark, C.R., Stryer, L., Bourne, H. (1984). ADP-ribosylation of transducin by pertussis toxin blocks the light-stimulated hydrolysis of GTP and cGMP in retinal photoreceptors. *The Journal of Biological Chemistry* 259:23-26

Vanhauwe, J.F., Fraeyman, N., Francken, B.J., Luyten, W.H., and Leysen J.E. (1999). Comparison of the ligand binding and signaling properties of human dopamine D(2) and D(3) receptors in Chinese hamster ovary cells. *Journal of Pharmacology and Experimental Therapeutics* 290:908-16

Vanhauwe, J.F., Fraeyman, N., Francken, B.J., Luyten, W.H., Leysen, J.E. (1999). Comparison of the ligand binding and signaling properties of human dopamine D(2) and D(3) receptors in Chinese hamster ovary cells. *Journal of Pharmacology and Experimental Therapeutics* 290:908-16

Vásquez, C., and Lewis, D.L. (1999). The CB1 cannabinoid receptor can sequester G-proteins, making them unavailable to couple to other receptors. *The Journal of Neuroscience* 9:9271-80

Verty, A.N., Boon, W.M., Mallet, P.E., McGregor, I.S., and Oldfield, B.J. (2009). Involvement of hypothalamic peptides in the anorectic action of the CB receptor antagonist rimonabant (SR 141716). *The European journal of neuroscience* 29:2207-2216

Verty, A.N., McFarlane, J.R., McGregor, I.S., and Mallet, P.E. (2004). Evidence for an interaction between CB1 cannabinoid and oxytocin receptors in food and water intake. *Neuropharmacology* 47:593-603

Vivian, J.A., Kishioka, S., and Woods, J.H. (1997). Behavioral effects of the cannabinoid antagonist SR 141716A in rhesus monkeys. *27th Annual Meeting Society for Neuroscience* 23:1869

Wall, M.A., Coleman, D.E., Lee, E., Iniguez-Lluhi, J.A., Posner, B.A., Gilman, G.A., Sprang, S.R. (1995). The structure of the G protein heterotrimer Giα1β1γ2. Cell 83:1047-1058
Walter, L., Franklin, A., Witting, A., Moller, T., and Stella, N. (2002). Astrocytes in culture produce anandamide and other acylethanolamides. *The Journal of Biological Chemistry* 23:20869-20876

Ward, S.J., Lefever, T.W., Rawls, S.M., Whiteside, G.T., and Walker, E.A. (2009). Age-dependent effects of the cannabinoid CB1 antagonist SR141716A on food intake, body weight change, and pruritus in rats. *Psychopharmacology* 206:155-65

Warner, D.R., Weng, G., Yu, S., Matalon, R., Weinstein, L.S. (1998). A novel mutation in the switch 3 regions of Gαs in a patient with albright hereditary osteodystrophy impairs GDP binding and receptor activation. *The Journal of Biological Chemistry* 273:23976-23983

Welch, S.P., Huffman, J.W., and Lowe, J. (1998). Differential blockade of the antinociceptive effects of centrally administered cannabinoids by SR 141716A. *Journal of Pharmacology and Experimental* 286:1301-1308

Wess, J. (1998). Molecular basis of receptor/G-protein-coupling selectivity. *Pharmacologic and Theraupetics* 80:231-264

White, J.H., Wise, A., Main, M.J., Green, A., Fraser, N.J., Disney, G.H., Barnes, A.A., Emson, P., Foord, S.M., and Marshall, F.H. (1998). Heterodimerization is required for the formation of a functional GABA(B) receptor. *Nature* 396:679-682

Wiley, J.L., Lowe, J.A., Balster, R.L., and Martin, B.R. (1995). Antagonism of the discriminative stimulus effects of Δ9-tetrahydrocannabinol in rats and rhesus monkeys. *Journal of Pharmacology and Experimental* 275:1-6

Wyrosky, R., McGonigle, P., and Van Bockstaele, E.J. (2015). Drug discovery strategies that focus on the endocannabinoid signalling system in psychiatric disease. *Expert Opinion on Drug Discovery 10:17-36*

Zador, F., Lenart, N., Csibrany, B., Santha, M., Molnar, M., Tuka, B., Samavati, R., Klivenyi, P., Vecsei, L., Marton, A., et al. (2015). Low dosage of rimonabant leads to anxiolytic-like behavior via inhibiting expression levels and G-protein activity of kappa opioid receptors in a cannabinoid receptor independent manner. *Neuropharmacology* 89:298-307

Zoratti, C., Kipmen-Korgun, D., Osibow, K., Malli, R., and Graier, W.F. (2003). Anandamide initiates Ca2+ signaling via CB2 receptor linked to phospholipase C in calf pulmonary endothelial cells. *British of Journal of Pharmacology* 140:1351-62